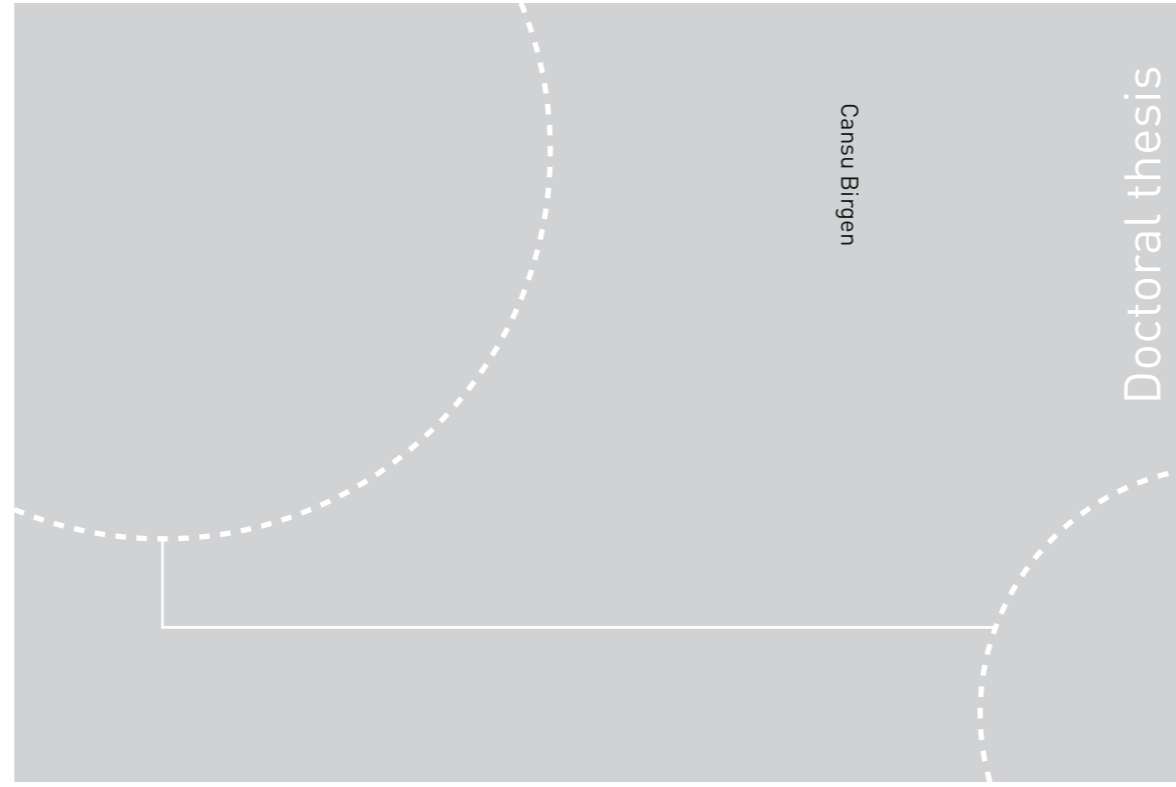


ISBN 978-82-326-4354-7 (printed ver.)
ISBN 978-82-326-4355-4 (electronic ver.)
ISSN 1503-8181



Doctoral theses at NTNU, 2019:378

Cansu Birgen

Experimental and Modeling Studies of Fermentative Butanol Production from Lignocellulosic Sugars

 **NTNU**
Norwegian University of
Science and Technology

Doctoral theses at NTNU, 2019:378

 NTNU

NTNU
Norwegian University of Science and Technology
Thesis for the Degree of
Philosophiae Doctor
Faculty of Natural Sciences
Department of Chemical Engineering

 **NTNU**
Norwegian University of
Science and Technology

Cansu Birgen

Experimental and Modeling Studies of Fermentative Butanol Production from Lignocellulosic Sugars

Thesis for the Degree of Philosophiae Doctor

Trondheim, December 2019

Norwegian University of Science and Technology
Faculty of Natural Sciences
Department of Chemical Engineering



Norwegian University of
Science and Technology

NTNU
Norwegian University of Science and Technology

Thesis for the Degree of Philosophiae Doctor

Faculty of Natural Sciences
Department of Chemical Engineering

© Cansu Birgen

ISBN 978-82-326-4354-7 (printed ver.)
ISBN 978-82-326-4355-4 (electronic ver.)
ISSN 1503-8181

Doctoral theses at NTNU, 2019:378

Printed by NTNU Grafisk senter

To people who resist oppression.

Preface

This thesis is submitted in partial fulfillment of the requirements for the degree of Philosophiae Doctor (Ph.D.) at the Norwegian University of Science and Technology (NTNU) in Trondheim, Norway.

The PhD work has been carried out at the Department of Chemical Engineering, between July 2015 and January 2019, with Prof. Dr. Heinz A. Preisig as the main supervisor from Department of Chemical Engineering in Norwegian University of Science and Technology. Dr. Alexander Wentzel has been the co-supervisor from the Biotechnology and Nanomedicine Department at SINTEF Industry in Trondheim, Norway.

This work has been funded by the project “Efficient Production of Butyl-Butyrate from Lignocellulose derived Sugars (EcoLodge),” supported by the Research Council of Norway, grant no. 246821/E20.

Acknowledgments

I would like to thank my supervisor, Prof. Dr. Heinz A. Preisig for being generous and giving me the opportunity to pursue my PhD in the field that I most wanted, and stimulating my intellect with his valuable insights in a variety of topics. I sincerely thank my co-supervisor Dr. Alexander Wentzel for his time, support, kindness, and constructive feedback, and helping me shape my research with his great knowledge and experience shared with great efficiency, precision and accuracy. I would like to express my gratitude for Sidsel Markussen for supervising me during the experiments and guiding me with her deep knowledge and expertise.

I wish to thank Department of Chemical Engineering for their help throughout my graduate study. I wish to thank Biotechnology and Nanomedicine Department in SINTEF Industry for providing me a very welcoming and supportive work environment in their laboratories. I would like to thank Randi Aune for sharing her knowledge in fermentation, Kathinka Lystad and Kari Hjelen for their guidance during HPLC analysis, Kristin Fløgstad Degnes and Håvard Sletta for their supervision and collaboration in conducting fermentation experiments and dissemination of research results, Olaf Trygve Berglihn and Bernd Wittgens for discussions about process and modelling.

I would like thank Sezen Aksu who always accompanied, guided, consolidated and brighten me with her songs in my entire life. I am blessed to be surrounded by so many great people. Trondheim became my home thanks to my dear friends Dilan, Seniz, Emrah, Utkucan, Mustafa, Derya, Deniz, Maria, Burcu, Tufan, Damla, Serkan, Batu, Lise, Mads, Guray, Tuna, Heidi and Elke. Dear colleagues from Process Systems group, Tobias, Adriana, Julian, Dinesh, Sigve, Adriæn, Eka and Tamal. My dear fellow improvisers Sophia, Marius, Stella, Thomas, Helen, Andrea, Krzysztof, Agnieszka, Kris-

toffer, Martin, Bogdan, Roel and Laura who made me better at listening, accepting, story telling and collaborating, which helped me in my research and improved my soft skills in addition to the sheer joy of doing impro together. I also would like thank my life-long friends Duygu, Çağla, Gökçen, Zeynep and Ezgi with whom I shared great moments, and went through every phase of life since my childhood.

I am privileged to have a wonderful family - my mom, dad, brother, aunts, uncles, cousins and my lovely niece. I am grateful for their generosity, respect, support and love throughout my life. They have always filled me with joy, happiness, enthusiasm, and inspired me to be ambitious and courageous.

I would like to thank my one and only, Emre. It is the greatest joy of my life to learn, explore, grow and evolve together with you. Thank you for standing by my side as my love, family, friend, ally, comrade and companion.

Cansu Birgen
Trondheim, Norway
December 2019

Abstract

The primary focus of the work performed and summarized in this thesis was to understand and improve anaerobic fermentation of lignocellulosic sugars for butanol production by *Clostridia*. Experimental studies form the basis for systematic data collection for modeling. The secondary focus of the thesis was to develop a model for fermentative butanol production from lignocellulosic sugars. The tertiary focus was to investigate all fermentation variables and performance indicators with exploration of the interdependencies. This thesis accommodated these focuses.

First, fermentation variables including typical operating conditions and performance indicators were identified by collecting literature data. Exploratory data analysis of the variables provided a holistic overview of the process to demonstrate their significance and interconnectedness.

Initial fermentation experiments were done with different lignocellulosic sugar ratios at different scales i.e. serum flasks and microbioreactors. Results showed that sugar ratio had a profound impact on the fermentation kinetics, and serum flask setup was more beneficial in terms of stability of operation and sample collection.

Next, the effect of different pre-growth conditions on fermentation performance was explored by using different sugar ratios. Culture pre-grown on xylose as the sole sugar shows a better performance than culture pre-grown on a mixture of glucose and xylose in bench-scale bioreactors, and this strategy was used in the next experiments.

A model for *Clostridial* growth on mixtures of lignocellulosic sugars was developed first, which included the noncompetitive inhibition between them. By using this growth model, fermentative butanol production from lignocellulosic sugars was modelled. The model was validated with extra experimental data, and a sensitivity analysis was performed to gain better understanding of the model parameters.

Contents

Preface	v
Acknowledgments	vii
Abstract	ix
Contents	xi
List of Tables	xv
List of Figures	xvii
List of Abbreviations, Glossary & Nomenclature	xxi
1 Introduction	1
1.1 Motivation	1
1.1.1 Need for a Holistic Approach	1
1.1.2 Scalability Issues	2
1.1.3 Co-utilization of Lignocellulosic Sugars	2
1.1.4 Need for Simple Models	2
1.2 Scope	3
1.3 Basic Definitions	3
1.4 Thesis Overview	4
1.5 Contributions	6
1.5.1 Publications Contained in the Thesis	6
1.5.2 Other Publications As First Author	7
1.5.3 Co-authored Publications	7

2	Literature Review	9
2.1	Butanol as a Promising Renewable Chemical	9
2.1.1	A Brief History of Fermentative Butanol Production	12
2.1.2	Challenges and Possible Solutions	13
2.2	Fermentative Butanol Production from Lignocellulosic Biomass	15
2.2.1	<i>Clostridial species</i>	15
2.2.2	Pretreatment	16
2.2.3	Detoxification	18
2.2.4	Fermentation	20
2.2.5	Strain Development	20
2.2.6	Process Integration and Intensification	21
2.3	Fermentative Butanol Production from Mixed Sugars	22
2.4	Modeling Fermentative Butanol Production	23
2.4.1	Structural Models	23
2.4.2	Dynamic Models for Batch Fermentation	24
2.4.3	Dynamic Models for Continuous Fermentation	26
2.4.4	Models for Fermentation with <i>in situ</i> Product Removal	27
2.4.5	Unstructured Models	28
2.4.5.1	Microbial Growth Models	28
2.4.5.2	Microbial Growth Models with Influence of Inhibitors	31
2.4.5.3	Binary Substrate Growth Models	33
2.4.5.4	Substrate Utilization Models	34
2.4.5.5	Product Formation Models	36
3	Exploratory Data Analysis of Fermentation Variables	39
3.1	Introduction	39
3.2	Methods	39
3.3	Results and Discussion	40
3.3.1	Substrate Properties	41
3.3.2	Product Mixture Properties	42
3.3.3	Performance Indicators	43
3.3.4	Correlations between Fermentation Variables	45
3.4	Conclusions	48
4	Butanol Production from Lignocellulosic Sugars in Microbioreactors	51
4.1	Introduction	51
4.2	Materials and Methods	52
4.2.1	Microorganism and Medium	52
4.2.2	Fermentations	52

4.3	Results and Discussion	53
4.3.1	Evaluation of Growth in BioLector Microbioreactor Fermentations	53
4.3.2	Comparison of Fermentations Performed in Microbioreactors and Serum Flasks	58
4.4	Conclusions	61
5	Effect of Pre-growth Conditions on Fermentation	63
5.1	Introduction	63
5.2	Materials and Methods	64
5.2.1	Microorganism and Medium	64
5.2.2	Fermentations	64
5.3	Results and Discussion	64
5.3.1	Progress of Fermentations	64
5.3.2	Kinetic Coefficients	67
5.4	Conclusions	70
6	Modelling The Binary Substrate Growth	71
6.1	Introduction	71
6.2	Materials and Methods	72
6.2.1	Microorganism and Medium	72
6.2.2	Fermentations	72
6.2.3	Design of Experiments	72
6.2.4	Model Fitting	73
6.3	Results and Discussion	73
6.3.1	Characterization of the Growth on Mixtures of Glucose and Xylose	73
6.3.2	Modelling the Growth on Mixtures of Glucose and Xylose	78
6.4	Conclusions	83
7	Modelling Fermentative Butanol Production from Glucose and Xylose	85
7.1	Introduction	85
7.2	Materials and Methods	86
7.2.1	Microorganism and Medium	86
7.2.2	Fermentations	86
7.3	Model Development	87
7.3.1	Parameter Estimation	89
7.4	Results and Discussion	89
7.4.1	Parameter Estimates	89

7.4.2 Comparison of Model Predictions and Experimental Observations	92
7.4.3 Sensitivity Analysis on Model Parameters	96
7.5 Conclusions	98
8 Concluding Remarks and Future Work	101
8.1 Concluding Remarks	101
8.2 Recommendations for Future Work	103
8.2.1 Experimental Work	104
8.2.2 Modeling Work	106
Appendices	109
A Correlations	111
B Materials and Methods	115
B.1 Bacterial Strain	115
B.2 Media	115
B.3 Analytical Methods	117
B.4 Growth Conditions	118
B.5 Exploratory Data Analysis	119
B.6 Analysis of Variance	121
B.7 Determination of Kinetic Coefficients and Fermentation Variables	122
B.8 Design of Experiments	124
B.9 Regression	124
B.10 Parameter Estimation	126
B.11 Index of Model Accuracy	127
B.12 Sensitivity Analysis	128
References	129

List of Tables

2.1	Butanol isomers and their applications areas.	10
2.2	Properties of gasoline, diesel, methanol, ethanol and butanol.	11
2.3	Main challenges and solutions for fermentative butanol production.	14
2.4	Models developed for microbial growth on single substrate for pure cultures.	30
2.5	Models developed for microbial growth on single substrate for pure cultures with effects of substrate inhibitions.	31
2.6	Models developed for microbial growth on single substrate for pure cultures with effects of product inhibitions.	32
2.7	Binary substrate growth models.	34
4.1	p values obtained from ANOVA for fermentations done in BioLector	60
4.2	p values obtained from ANOVA for fermentations done in serum flasks.	61
5.1	Kinetic coefficients for fermenter 1 and fermenter 2.	67
5.2	Comparison of results with previous studies.	69
6.1	Real and coded values of circumscribed central composite design for 2 factors.	72
6.2	Experimental values of circumscribed central composite design and responses.	74
6.3	Model coefficients and corresponding statistical values.	77
6.4	Fit results for binary substrate growth models.	78

6.5	Parameters of the noncompetitive binary substrate growth model.	81
6.6	Correlation matrix of noncompetitive binary substrate growth model.	81
7.1	Parameter estimation results.	90
7.2	Average squared correlation coefficients (r^2) between predicted and observed values.	95
A.1	Kendall's correlation coefficients for correlations between 22 fermentation variables.	113
B.1	Typical composition of Reinforced <i>Clostridial</i> Medium, CM0149.	116
B.2	Medium components used in fermentation and flask test experiments.	117
B.3	Model parameters, their bounds and initial points used for initialization.	127

List of Figures

2.1	A representative schematic diagram of fermentative butanol production from lignocellulosic biomass.	15
2.2	Common <i>Clostridium</i> strains used in fermentative butanol production from lignocellulosic biomass.	16
2.3	Common lignocellulosic feedstocks used in fermentative butanol production from lignocellulosic biomass.	17
2.4	Common pretreatment methods used in fermentative butanol production from lignocellulosic biomass.	18
2.5	Common detoxification methods used in fermentative butanol production from lignocellulosic biomass.	19
2.6	A representative growth curve of microorganisms (top) and the respective growth rate curve (bottom).	28
2.7	Representative curves of substrate utilization, cell mass growth and product formation at different production types, where X is the cell mass concentration, S is the substrate concentration and P is the product concentration.	36
3.1	Concentrations of substrate components present in the lignocellulosic hydrolysates.	40
3.2	Substrate concentrations of a) lignocellulosic hydrolysate, b) lignocellulosic hydrolysate with additional glucose, and c) mixed sugar fermentations.	41
3.3	Product concentrations of a) lignocellulosic hydrolysate, b) lignocellulosic hydrolysate with additional glucose, and c) mixed sugar fermentations.	43

3.4	Performance indicator values of a) lignocellulosic hydrolysate, b) lignocellulosic hydrolysate with additional glucose, and c) mixed sugar fermentations.	44
3.5	Correlations of all fermentation variables	46
4.1	Experiment design of fermentations performed in serum flasks (top) and microbioreactors with a schematic representation of a single well (bottom).	54
4.2	Cell mass versus time plots of fermentations done in BioLector using 5 and 10 g/l total sugar and varied glucose (G) to xylose (X) ratios.	55
4.3	pH plots of fermentations done in BioLector using 5 and 10 g/l total sugar and varied glucose (G) to xylose (X) ratios.	56
4.4	Growth rate (h^{-1}) values during exponential growth for all 12 experiments done in the BioLector setup.	57
4.5	Butanol concentration and butanol yield values of fermentations done in BioLector and serum flasks with 5 and 10 g/l total sugar.	58
5.1	Glucose and xylose a), and butanol and cell mass b) profiles for fermenter 1 with xylose as the initial sugar.	65
5.2	Glucose and xylose a), and butanol and cell mass b) profiles for fermenter 2 with glucose as the initial sugar.	66
6.1	Normal probability distribution of residuals.	75
6.2	Response surface of glucose and xylose concentrations versus growth rates.	75
6.3	Contour plot of glucose and xylose concentrations versus growth rates.	76
6.4	Normalized values of model coefficients versus growth rate.	77
6.5	Noncompetitive binary substrate growth model predictions and experimental observations.	79
6.6	Residuals of noncompetitive binary substrate growth model predictions and experimental observations.	80
6.7	Effects of parameters of the noncompetitive binary substrate growth model on the growth rate (h^{-1}).	82
7.1	Comparison of model predictions and experimental observations with the data from Fond et al. (1986) for a) xylose pre-grown culture, FondX, and b) glucose and xylose pre-grown culture, FondGX.	92

7.2	Comparison of model predictions and our experimental observations for xylose pre-grown, and glucose and xylose pre-grown cultures.	94
7.3	Sensitivity analysis on model parameters for a) and e) cell mass, b) and f) glucose, c) and g) xylose, and d) and h) butanol concentrations.	97
B.1	BioLector setup, round-well plate, and a single well showing the sensors for dissolved oxygen (DO), pH, cell mass and fluorescence.	119
B.2	A geometrical representation of the CCC design with two factors.	124

List of Abbreviations, Glossary & Nomenclature

Abbreviations

ABE	Acetone-butanol-ethanol
ANOVA	Analysis of variance
CCC	Circumscribed Central Composite
CCR	Carbon Catabolite Repression
EDA	Exploratory Data Analysis
RSM	Response Surface Methodology

Glossary

ABE	ABE solvents concentration
ABE_y	ABE solvents yield on total substrate
Ac	Acetone concentration
$Acids$	Total acids concentration
B	Butanol concentration
B_{acc}	Accumulated butanol concentration
B_{max}	Maximum butanol concentration at which growth stops
$BuOH$	Butanol concentration
$BuOH_r$	Butanol ratio in solvent mixture
$BuOH_y$	Butanol yield on total substrate
$EtOH$	Ethanol concentration

HAc	Acetic acid concentration
HAc_i	Initial acetic acid concentration
HBu	Butyric acid concentration
i_B	Butanol inhibition constant to growth
k_d	Specific death rate
K_I	Substrate inhibition constant
K_{sG}	Substrate affinity constant for glucose
K_{sX}	Substrate affinity constant for xylose
S	Substrate concentration
S_i	Initial substrate concentration
S_u	Utilized amount of substrate
S_{ur}	Percental utilization of substrate
SG	Glucose concentration
SG_i	Initial glucose concentration
SG_u	Utilized amount of glucose
SG_{acc}	Accumulated glucose consumption
SG_{ir}	Initial glucose ratio in substrate
SG_{ur}	Percental utilization of glucose
SX	Xylose concentration
SX_i	Initial xylose concentration
SX_u	Utilized amount of xylose
SX_{acc}	Accumulated xylose consumption
SX_{ir}	Initial xylose ratio in substrate
SX_{ur}	Percental utilization of xylose
X	Cell mass concentration
$Y_{B/SG}$	Butanol yield on glucose
$Y_{B/SX}$	Butanol yield on xylose
$Y_{B/XG}$	Butanol yield on cell mass utilizing glucose
$Y_{B/XX}$	Butanol yield on cell mass utilizing xylose
$Y_{X/SG}$	Cell mass yield on glucose
$Y_{X/SX}$	Cell mass yield on xylose

Nomenclature

μ	Experimental specific growth rate
μ_g	Specific growth rate
μ_{maxG}	Maximum specific growth rate on glucose
μ_{maxX}	Maximum specific growth rate on xylose
μ_{net}	Net growth rate
μ_{SG}	Specific growth rate on glucose
μ_{SX}	Specific growth rate on xylose

Chapter 1

Introduction

In this chapter, the motivation and the scope for this PhD work are stated, and contents are put into perspective. Thesis overview together with contributions and publications are presented.

1.1 Motivation

Production of chemicals via biological routes from renewable feedstock has been gaining interest as substitutes or complements to chemicals produced via petro-chemical routes to address environmental issues and sustainability concerns. Butanol is a promising green chemical, which can be produced from renewable sources by fermentation using microorganisms, and used as a biofuel, or a building block for synthesis of other high value green chemicals. One of the main objectives of research and development in the bioprocess industry producing butanol is to establish economically viable and sustainable operation by improving product yield, selectivity and conversion efficiency. Historically, the most common measures to achieve these have been strain development, and optimization of the fermentation medium and operating conditions such as temperature, pH and feeding rate. However, recent advancements in the field have addressed more specific research needs, which are categorized and explained in the following sections.

1.1.1 Need for a Holistic Approach

Fermentation is a complex process, which involves numerous reactions, metabolic products, genes, enzymes, metabolic switching mechanisms with interconnections between them and dependence on environmental/operating

conditions. Recent advances in biotechnology have created opportunities to understand this vastly complex process. However, there is room for discovery and understanding of undetected and unidentified characteristics. Therefore, it is crucial to have a holistic view of all fermentation variables as well as to map out interdependencies between them so that fermentation process design can be improved with this additional information.

1.1.2 Scalability Issues

Most of the experimental work for research and development takes place in scales smaller than industrial scale of fermentation applications to save time, energy and material cost. Typically, fermentation process design starts in milliliter scale i.e. serum or shake flasks to test as many operating conditions as possible within the scope of the research. Then, fermentations are done in lab-scale bioreactors (1-10 liters) under the pre-selected conditions. Finally, the design is fine-tuned in pilot scale bioreactors before moving towards an industrial scale application. This work flow requires benchmarking to gain insight into scalability and to have a smoother design process when changing scales of application.

1.1.3 Co-utilization of Lignocellulosic Sugars

Fermentation substrate has the greatest share in all costs of fermentative butanol production processes accounting for 66% of all [1]. To tackle this problem, many feedstock alternatives have been studied [2] and lignocellulosic biomass is among them because, it is the most abundant renewable biomass resource, and it circumvents the direct fuel-versus-food competition compared to e.g. corn and sugar cane in biofuel production. Hydrolysis of lignocellulosic biomass yields a mixture of pentoses and hexoses, which are fermented to butanol and by-products by the microorganisms. Full exploitation of all sugars bound in lignocellulosic biomass is necessary to decrease the substrate costs. However, mixed sugar fermentation studies are limited, and there is need for better understanding of this process.

1.1.4 Need for Simple Models

A wide variety of model structures has been proposed to describe fermentative butanol production. They serve different purposes, consequently require and produce different kinds of information/data. The most detailed models can provide the largest information volume; however, their industrial applications can be limited due to high complexity level. In addition,

the majority of models is only valid under certain process conditions and regimes. Therefore, it is important to develop models, which are simple to use, easy to interpret and applicable in wider operating conditions.

1.2 Scope

In the work underlying this thesis, the focus was to gain understanding of lignocellulosic sugar fermentation for butanol production and to propose a feeding strategy for achieving co-utilization of sugars. The scope also covers model development to describe the main characteristics of the process. The modeling studies involve the growth model and the butanol production model establishments together with sensitivity analysis of the model parameters and model validation with extra experimental data. The scope of this thesis also includes analysis and investigation of all fermentation variables, definition and calculation of performance indicators, and exploration of interconnectedness between all variables and indicators. Hence, the thesis work includes and connects both experiments and modeling/simulation.

1.3 Basic Definitions

Basic definitions of the most common terms used in this thesis are provided below for communication purposes and precision.

Process is a natural, progressively continuing operation or development marked by a series of gradual changes that succeed one another in a relatively fixed way and lead toward a particular results or end.

Fermentation is the anaerobic process of chemical breakdown of a substance by bacteria, yeasts, or other microorganisms. In the thesis, conversion of sugars to butanol is called as fermentative butanol production.

Fermentation variable is an element, feature, or factor that can vary or change in a fermentation process. Operating conditions are input variables, which can be changed by the user. In this thesis, sugar concentrations, compositions or ratios are the input variables, and independent variables are measured/observed concentrations of sugars, products and cell mass. In this thesis, fermentation performance indicators such as substrate utilization and product yield are also referred to as fermentation variables.

Biomass in this thesis refers to the biological feedstock converted to products by microorganisms. The term “biomass” is used interchangeably with “cell mass” in literature; however, they are hereby defined separately.

Substrate is defined as the surface or material on or from which an organism lives, grows, or obtains its nourishment. In the context of this thesis, lignocellulosic biomass and sugars, glucose and xylose, and other sugars are all referred to as substrate.

Coefficient is a factor that measures a particular property under certain conditions such as temperature, volume or a particular experimental setup. In the context of this thesis, kinetic coefficients are calculated using experimental data and employed as performance indicators of fermentation. Butanol yield, substrate utilization and growth rate are the mostly used coefficients in this thesis.

Model is broadly defined as something that mimics the behaviour of something else. In this thesis, a model is used to refer to a set of mathematical equations, which describes the changes in fermentation variables in terms of input-output relationships.

Parameter is a quantity whose value is selected for the particular circumstances and in relation to which other variable quantities may be expressed. In this thesis, parameters are estimated using experimental data, which are included in the models for cell mass growth and butanol production.

1.4 Thesis Overview

The thesis summarizes the content of 6 separate scientific articles on experimental and modeling studies of fermentative butanol production from lignocellulosic sugars. The chapter sequence has been organized to reflect the knowledge flow starting from overview of the process, and focusing on a specific problem, and then experimental and modeling studies targeted to the particular problem.

Chapter 2 provides a literature review on fermentative butanol production processes with its main challenges and possible solutions to overcome those. Properties and main application areas of butanol as a renewable chemical and biofuel are explained together with a history of the process. Different types of models describing fermentative butanol production are reviewed with corresponding application areas of those models with a focus on unstructured models.

Chapter 3 starts with identification and definition of fermentation variables, which includes typical operating conditions as well as indicators of the process performance. Exploratory data analysis of the fermentation

variables provides a holistic overview of the process to illustrate their significance and interconnectedness. Insights and results from the data analysis were used in design of the experiments in the following chapters.

Chapter 4 presents experimental results of fermentative butanol production from lignocellulosic sugars and at different sugar ratios and performed at different scales i.e. in serum flasks and microbioreactors. Comparative analysis of the fermentation kinetics showed that the sugar ratio has a profound impact on the cell mass growth, consequently on butanol production. Experiments were done in serum flasks and bench-scale fermenters in the subsequent chapters due to ease in offline data collection and analysis, and robust operation.

Chapter 5 explores the effect of pre-growth conditions on fermentation performance. Fed-batch fermenters inoculated with cultures pre-grown on xylose and glucose were fed with different mixtures of the two sugars. The fermenter started with the culture pre-grown on xylose as the sole sugar showed a better performance. Consequently, this strategy was used in the following chapters.

Chapter 6 consists of two steps for modeling the growth on mixtures of glucose and xylose. First, response surface methodology was followed by performing designed experiments and then fitting the experimental observations to a quadratic and interactive model. The statistical test showed that the interaction between the sugars was significant, thus an interactive growth model structure should be chosen. Secondly, binary substrate growth models with different types of interactions were fitted with experimental data, and the model with noncompetitive inhibition gave the best fit. Growth model was chosen and used in the following chapter.

Chapter 7 focuses on modeling work for fermentative butanol production to describe the process as well as to illustrate the effect of different pre-growth conditions. Modeling approach and assumptions were presented together with the model equations. The proposed model described the cell mass growth, glucose and xylose utilizations and butanol formation reflecting the major characteristics of the process i.e. substrate and butanol inhibitions. Model validation was done by employing 4 extra experimental datasets as well as literature data. Sensitivity analysis on model parameters was done to gain better insight into the process.

Chapter 8 concludes this thesis with a summary of its contents, and provides suggestions and guidelines for possible future research.

Appendix presents the materials and methods used in the thesis. Mi-

croorganism, medium components and compositions, growth conditions and experimental techniques, analytical methods, statistical methods, calculation of fermentation coefficients and estimation of model parameters, model accuracy measures and sensitivity analysis are given.

1.5 Contributions

1.5.1 Publications Contained in the Thesis

The research results obtained in the course of the PhD project are published in the following journal transactions.

- Paper I. **C. Birgen**, S. Markussen, A. Wentzel, H. A. Preisig and B. Wittgens, “Modeling the Growth of *Clostridium beijerinckii* NCIMB 8052 on Lignocellulosic Sugars,” *Chemical Engineering Transactions*, vol. 65, pp. 289 – 294, June 2018.
- Paper II. **C. Birgen**, S. Markussen, A. Wentzel and H. A. Preisig, “The Effect of Feeding Strategy on Butanol Production by *Clostridium beijerinckii* NCIMB 8052 Using Glucose and Xylose,” *Chemical Engineering Transactions*, vol. 65, pp. 283 – 288, June 2018.
- Paper III. **C. Birgen**, S. Markussen, A. Wentzel and H. A. Preisig, “Response Surface Methodology for Understanding Glucose and Xylose Utilization by *Clostridium beijerinckii* NCIMB 8052,” *Chemical Engineering Transactions*, vol. 65, pp. 61 – 66, June 2018.
- Paper IV. **C. Birgen**, Berglihn O. T., H. A. Preisig, and A. Wentzel, “Kinetic Study of Butanol Production from Mixtures of Glucose and Xylose and Investigation of Different Pre-growth Strategies,” *Biochemical Engineering Journal*, vol. 147, pp. 110-117, July 2019.
- Paper V. **C. Birgen**, H. A. Preisig, P. Dürre, and A. Wentzel, “Butanol Production from Lignocellulosic Biomass: Revisiting Fermentation Performance Indicators with Exploratory Data Analysis,” *Biotechnology for Biofuels*, 12(1), 167.
- Paper VI. **C. Birgen**, K. F. Degnes, S. Markussen, A. Wentzel, and H. Sletta, “Butanol Production from Lignocellulosic Sugars

by *Clostridium beijerinckii* in Microbioreactors,” *The 30th European Symposium on Computer Aided Process Engineering*. [submitted]

1.5.2 Other Publications As First Author

Papers related to the project, but not incorporated in this thesis:

- Paper VII. **C. Birgen**, H. A. Preisig, A. Wentzel, S. Markussen, B. Wittgens, U. Sarkar, S. Saha and S. Baksi, “Anaerobic Bio-reactor Modeling,” *Computer-aided chemical engineering*, vol. 38, 2016, pp. 557 – 582.
- Paper VIII. **C. Birgen**, S. Markussen, H. A. Preisig, B. Wittgens, A. Wentzel, U. Sarkar, A. Ganguly, S. Saha and S. Baksi, “Understanding Effect of Sugar Composition on Growth Kinetics: Fermentation of Glucose and Xylose by *Clostridium acetobutylicum* ATCC 824,” *25th European biomass conference and exhibition proceedings*, 2017, pp. 1042 – 1046.
- Paper IX. **C. Birgen**, H. A. Preisig, A. Wentzel, S. Markussen and B. Wittgens, “Attainable Region for Biobutanol Production,” *Computer-aided chemical engineering*, vol. 40, 2017, pp. 2893 – 2898.
- Paper X. **C. Birgen** and H. A. Preisig, “Dynamic Modeling of Butanol Production from Lignocellulosic Sugars,” *Computer-aided chemical engineering*, vol. 43, 2018, pp. 1547 – 1552.

1.5.3 Co-authored Publications

The author has also contributed to the following papers during her PhD period as co-author:

- Paper XI. S. Saha, U. Sarkar, **C. Birgen**, H. A. Preisig, A. Wentzel, S. Markussen, B. Wittgens, A. Ganguly, S. Baksi, “Alkaline Peroxide Pretreatment of Lignocellulose Material (*Crotalaria juncea*) and Reaction Mechanism Thereof,” *24th European Biomass Conference and Exhibition*, Amsterdam, 2016.
- Paper XII. S. Baksi, S. Saha, **C. Birgen**, U. Sarkar, H. A. Preisig, S. Markussen, B. Wittgens and A. Wentzel, “Valorization of Lignocellulosic Waste (*Crotalaria juncea*) Using Alkaline Peroxide

Pretreatment under Different Process Conditions: An Optimization Study on Separation of Lignin, Cellulose, and Hemicellulose,” *Journal of Natural Fibers*, pp. 1 – 15, February 2018.

- Paper XIII. S. Baksi, A. K. Ball, U. Sarkar, D. Banerjee, A. Wentzel, H. A. Preisig, J. C. Kuniyal, **C. Birgen**, S. Saha, B. Wittgens, and S. Markussen, “Efficacy of a novel sequential enzymatic hydrolysis of lignocellulosic biomass and inhibition characteristics of monosugars,” *International journal of biological macromolecules*, vol. 129, pp. 634 – 644, May 2019.
- Paper XIV. S. Baksi, U. Sarkar, S. Saha, A. K. Ball, J. C. Kuniyal, A. Wentzel, **C. Birgen**, H. A. Preisig, B. Wittgens, and S. Markussen, “Studies on delignification and inhibitory enzyme kinetics of alkaline peroxide pre-treated pine and deodar saw dust,” *Chemical Engineering and Processing-Process Intensification*, pp. 107607, August 2019.

Chapter 2

Literature Review

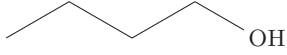
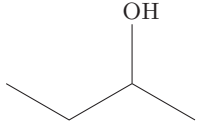
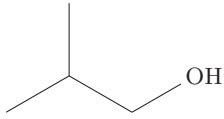
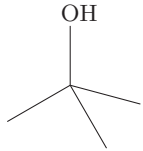
This chapter provides a literature review on fermentative butanol production from lignocellulosic biomass and sugars together with its main challenges and possible solutions to overcome those. Properties and common application areas of butanol and its isomers as green chemicals and biofuels are explained with a history of the fermentative production process. This chapter also summarizes different types of models describing the process with their applications, focusing on unstructured models as they are used in this thesis. Contents of this chapter were partly covered in Paper V.

2.1 Butanol as a Promising Renewable Chemical

Chemicals and fuels from renewable resources have gained global interest due to raising global warming and climate change concerns, volatility of oil price and supply, and legal restrictions on the use of nonrenewable resources [3]. Butanol has a 4-carbon structure and its isomers can present straight-chain or branched structures. Different structures and positions of the $-OH$ and the carbon chain lead to different properties and used for classification of the butanol isomers [4]. An overview of butanol isomers and their application areas can be seen in Table 2.1 [5, 6].

Common application areas of butanol isomers are similar, and the application as a solvent is predominant as well as the use as a gasoline additive. Throughout the thesis, n-butanol is referred to as butanol for simplicity reasons. The physical properties of butanol in comparison with other biofuels, gasoline and diesel can be found in Table 2.2 [5, 7].

Table 2.1: Butanol isomers and their applications areas.

Isomer	Formula	Application areas
1-butanol (n-butanol)		<ul style="list-style-type: none"> • Solvent (paint industry) • Plasticizer (plastics industry) • Hydraulic brake fluid • Cosmetics • Gasoline additive and alternative
2-butanol		<ul style="list-style-type: none"> • Solvent (several industries) • Domestic cleaning agent • Industrial cleaner • Paint remover • Perfumes and artificial flavours
iso-butanol		<ul style="list-style-type: none"> • Solvent and additive (paint industry) • Industrial cleaner • Paint remover • Ink ingredient • Gasoline additive
tert -butanol		<ul style="list-style-type: none"> • Solvent • Industrial cleaner and paint remover • Intermediate for MTBE, ETBE, TBHP • Denaturant for ethanol • Gasoline additive and octane booster

As Table 2.2 shows, butanol has several advantages compared to the more established biofuels ethanol and methanol: a longer carbon chain length, higher volatility, polarity, combustion value, octane rating and lower corrosive effects [8]. Moreover, diesel engines can run on pure butanol or diesel blends without any modifications [9]. In addition, butanol is a valuable 4-carbon feedstock for chemical synthesis, which can be used for production of esters, ethers, acetates, and plasticizers [3]. Therefore, butanol is a promising biofuel alternative as well as a renewable chemical.

Table 2.2: Properties of gasoline, diesel, methanol, ethanol and butanol.

	Gasoline	Diesel	Methanol	Ethanol	Butanol
Molecular formula	C ₄ – C ₁₂	C ₁₂ – C ₂₅	CH ₃ OH	C ₂ H ₅ OH	C ₄ H ₉ OH
Molecular weight	111.19	198.4	32.04	46.06	74.11
Cetane number	0-10	40-55	3	8	25
Octane number	80-99	20-30	111	108	96
Research octane number	88-98	0	109	109	98
Motor octane number	80-88	0	89	90	85
Oxygen content (% weight)	-	-	50	34.8	21.6
Density (g/ml) at 20 °C	0.72-0.78	0.82-0.86	0.796	0.79	0.808
Autoignition temperature (°C)	300	210	470	434	385
Flash point (°C) at closed cup	-45 to -38	65-88	12	8	35
Lower heating value (MJ/kg)	42.7	42.5	19.9	26.8	33.1
Boiling point (°C)	25-215	180-370	64.5	78.4	117.7
Stoichiometric ratio (air to fuel)	14.7	14.3	6.49	9.02	11.21
Latent heating (kJ/kg) at 25 °C	380-500	270	1109	904	582
Flammability limits (% volume)	0.6-8	1.5-7.6	6.0-36.5	4.3-19	1.4-11.2
Saturation pressure (kPa) at 38 °C	31.01	1.86	31.69	13.8	2.27
Viscosity (mm ² /s) at 40 °C	0.4-0.8 (20 °C)	1.9-4.1	0.59	1.08	2.63
Energy density (MJ/l)	32	35.86	16	19.6	29.2

There are two major butanol production processes: i) fermentative production from biomass, referred to as biobutanol and from fossil fuels referred to as petro-butanol; however, butanol produced from both sources have the same chemical properties. The majority of butanol produced today is via petrochemical reaction; the propylene hydroformylation, also known as oxo route [10, 11]. Consequently, petro-butanol production is closely linked to the propylene market, thus the price of crude oil [12]. Therefore, butanol production via the petrochemical route is not favorable due to environmental concerns as discussed above, and creating a greater interest in bio-based butanol production via fermentation. Details of the fermentative butanol production are discussed in the section below.

2.1.1 A Brief History of Fermentative Butanol Production

Fermentative butanol production under anaerobic conditions is typically referred to as a part of ‘ABE fermentation’, since acetone, butanol and ethanol are usually produced simultaneously. ABE fermentation is exclusively performed by solventogenic *Clostridia*. Their fermentation metabolism is typically characterized by two phases, exhibiting a distinct shift in the product spectrum. During the acidogenesis phase, the main (liquid) products are acetic acid and butyric acid, while the solvents, i.e. butanol, acetone and ethanol, are produced during the solventogenic phase [13].

Louis Pasteur was the first to report about fermentative butanol production in 1862 [14]. The first production utilizing the Weizmann process began only in 1913, aiming to produce acetone for rubber synthesis [15]. Later in 1916, the first industrial-scale ABE fermentation began operation due to a high demand for acetone during World War I, and was able to produce 3000 tons of acetone and 6000 tons of butanol within the next two years. After the armistice in November 1918, most of the plants were shut down [16].

The Weizmann process, which was operated in batch mode at 37 °C using cooked maize mash was commonly applied with a production of up to 150000 liters [16]. The process became more economical in 1936 with use of molasses and other industrial sugars and a decreased operating temperature of 31 °C [17]. In 1945, two-thirds of the butanol and one-tenth of the acetone in the U.S. were produced by ABE fermentation processes. However, their share in the total output declined rapidly during the 1950s mainly due to the acute competition with the expanding petrochemical industry and decreasing feedstock availability [18].

ABE fermentation became popular again in the 1970s after the oil crisis. Initial attempts to improve fermentation performance focused on optimization of operating conditions such as medium composition, nutrient limitation and feeding profiles, pH control, cell density and gas transfer considerations [15]. It has been gaining increasing interest owing to the advancements in Metabolic Flux Analysis (1984), Metabolic Engineering (1992), Gene Knock-out by Homologous Recombination (1994), and Complete Genome Sequencing (2001) [16], holding promise of improved production yields and productivities for more economic microbial production processes. There are several excellent reviews covering the historical development of ABE fermentation in detail [15, 16, 19–21].

2.1.2 Challenges and Possible Solutions

There are several challenges such as high substrate cost, solvent toxicity, low cell density and by-product formation that need to be addressed for sustainable and economical fermentative butanol production. Main issues and possible solutions discussed in review articles are summarized in Table 2.3 providing a comprehensive view in terms of their frequency of appearance.

Great efforts have been made to find cheap/free feedstock and cost efficient processing methods to overcome the high substrate cost, which constitutes 66% of all costs [1]. To tackle this problem, many feedstock alternatives have been proposed [22–29] and lignocellulosic biomass is the one proposed the most because, it is the most abundant renewable biomass resource, and it circumvents the direct fuel-versus-food competition due to the use of e.g. corn and sugar cane in biofuel production.

Low solvent tolerance limits the butanol titer to maximum 2% [30], which causes high downstream processing cost; therefore two major approaches were followed to address this problem: i) develop strains with higher butanol tolerance [24, 31–33] and ii) alleviate the inhibitory effects of butanol by *in situ* product removal [33, 34]. There is a variety of separation techniques for removing butanol from the fermentation broth, and their advantages and disadvantages were discussed in detail as a guideline for process design [22, 35]. Other process level measures to enhance fermentative butanol production include operating at different modes such as chemostat and fed-batch as well as cell recycle and immobilization together with novel technologies such as membrane reactors. It is essential to highlight the role of metabolic engineering for optimizing butanol production by strain improvement as presented in Table 2.3. Research efforts are still ongoing employing different methods at both metabolic and process levels.

Table 2.3: Main challenges and solutions for fermentative butanol production.

Challenge	Solution
High substrate cost	<ul style="list-style-type: none"> • Lignocellulosic biomass [1, 2, 5, 8, 22, 24, 26–28, 31, 36–38] • Starch based waste [1, 36, 37] • Syngas [1, 2, 25, 31, 36] • Macroalgae [2, 29, 36] • Crude glycerol [2, 25, 36, 38] • Protein waste [2], • Whey permeate [5, 24, 37], • Economical feedstock processing methods [22, 27, 37] • Medium optimization [27, 39] • Inulin [38]
Low butanol selectivity	<ul style="list-style-type: none"> • Metabolic engineering for disruption of the pathway for acetone [2, 5, 8, 22, 24, 26, 28, 32, 40] • Homo-butanol fermentation via chemical mutagenesis and metabolic engineering [1, 2, 25, 31] • Conversion of acetone into isopropanol [2, 26, 28] • Decoupling sporulation from solventogenesis [2, 5, 22, 24, 26, 31, 32, 39, 40]
Low butanol titer	<ul style="list-style-type: none"> • Metabolic engineering and mutagenesis for higher butanol tolerance [1, 2, 5, 24–26, 28, 31–33, 39, 40] • <i>In situ</i> product removal [2, 5, 8, 22, 24, 26–28, 31, 32, 35, 36, 39] • Introducing butanol pathways in other hosts [1, 2, 5, 22, 25, 26, 28, 31–33, 40] • Re-enforcing hot channel for butanol formation [24]
Low butanol yield	<ul style="list-style-type: none"> • Co-utilization of sugars without Carbon Catabolite Repression [2, 24, 38] • Extending the substrate utilization range [5, 28, 31]
Low butanol productivity	<ul style="list-style-type: none"> • Co-utilization of sugars without Carbon Catabolite Repression [2, 22, 37, 39] • Fed-batch fermentation [5, 22, 24, 27, 36] • Chemostat/continuous culturing [5, 8, 22, 24, 26–28, 36] • Immobilized cell chemostat [5, 22, 24, 26–28, 36] • Cell recycle chemostat [5, 22, 24, 26–28, 36] • Multi stage chemostat [22, 24, 26, 27]
Low O ₂ tolerance	<ul style="list-style-type: none"> • Co-culturing to maintain anaerobic conditions [8] • Random mutagenesis and selection [26, 31] • Metabolic engineering [32, 41]
Culture degeneration	<ul style="list-style-type: none"> • Prevention of excessive acidification of the culture [31]
Phage contamination	<ul style="list-style-type: none"> • Good factory hygiene, strains immune to specific phages [31, 32]

2.2 Fermentative Butanol Production from Lignocellulosic Biomass

A typical conversion process from lignocellulosic biomass to butanol involves three major steps: pretreatment, detoxification and fermentation as shown in Figure 2.1.

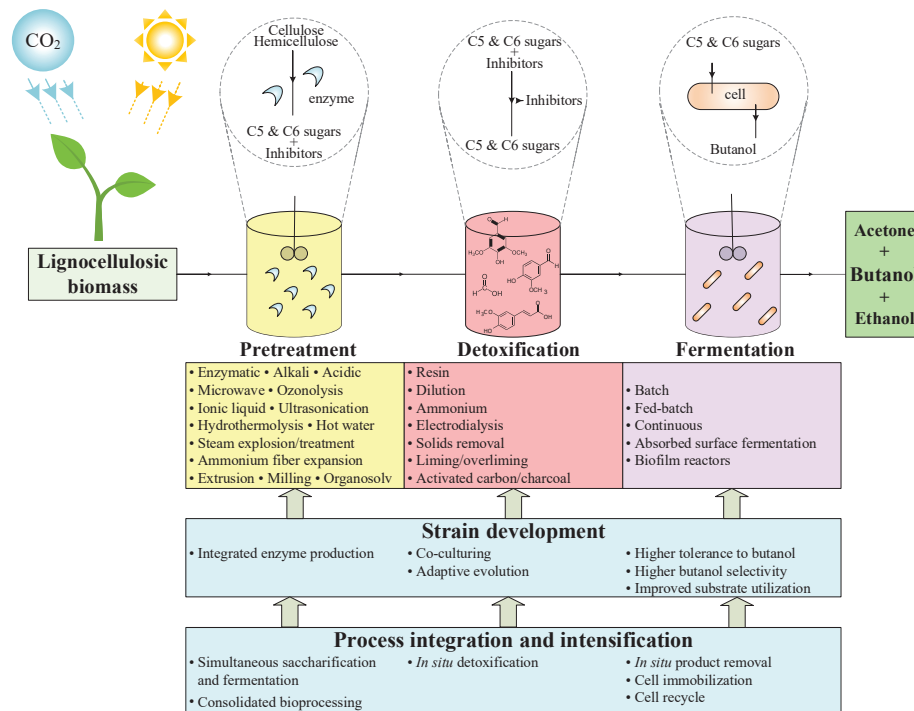


Figure 2.1: A representative schematic diagram of fermentative butanol production from lignocellulosic biomass.

Details of the fermentative butanol production from lignocellulosic biomass are explained in the following sections.

2.2.1 *Clostridial species*

Clostridial species are typically used in fermentative butanol production. *Clostridia* are rod-shaped, spore-forming Gram-positive bacteria and typically strict anaerobes [42]. *Clostridia* are saccharolytic butyric acid-producing bacteria under certain conditions to ferment saccharides

i.e. mono- (pentoses, hexoses), di- and polysaccharides, cellulosic-based materials and other biomass feed stocks. Many strains have the ability to secrete profuse enzymes that catalyze conversion of polysaccharides into monosaccharides [22]. Throughout the years, many *Clostridial species* have been isolated and characterized that differ in their substrate preferences, fermentation product profiles and other relevant properties [13]. Popular butanol producers include *C. acetobutylicum*, *C. beijerinckii*, *C. saccharoperbutylacetonicum*, *C. saccharoacetobutylicum*, *C. aurantibutyricum*, *C. pasteurianum*, *C. sporogenes*, *C. cadaveris*, and *C. tetanomorphum*. Commonly used strains are shown in Figure 2.2.

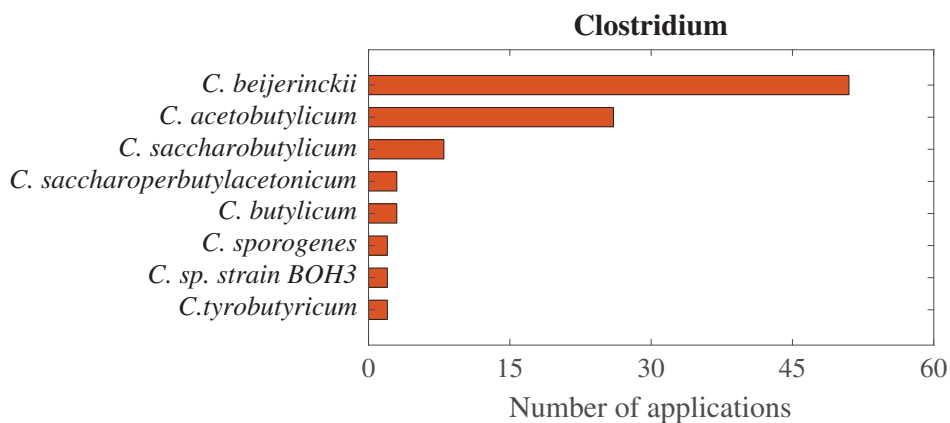


Figure 2.2: Common *Clostridium* strains used in fermentative butanol production from lignocellulosic biomass.

Strain selection depends on i) type of substrates, ii) nutrient requirement, iii) tolerance of butanol, iv) desired yield and concentration, v) resistance to bacteriophage and antibiotics [22].

2.2.2 Pretreatment

Lignocellulosic biomass is a favorable feedstock and proposed widely for a more economical butanol production as discussed above. Its main constituents are cellulose, hemicellulose and lignin [43]. The opening of the lignocellulosic biomass structure and the release of sugar content from hemicellulose and cellulose with other cross-linked units and the residual non-hydrolyzed raw feedstock is called pretreatment [44]. Commonly used lignocellulosic feedstocks are shown in Figure 2.3.

Conversion of biomass into its main constituents is referred to in liter-

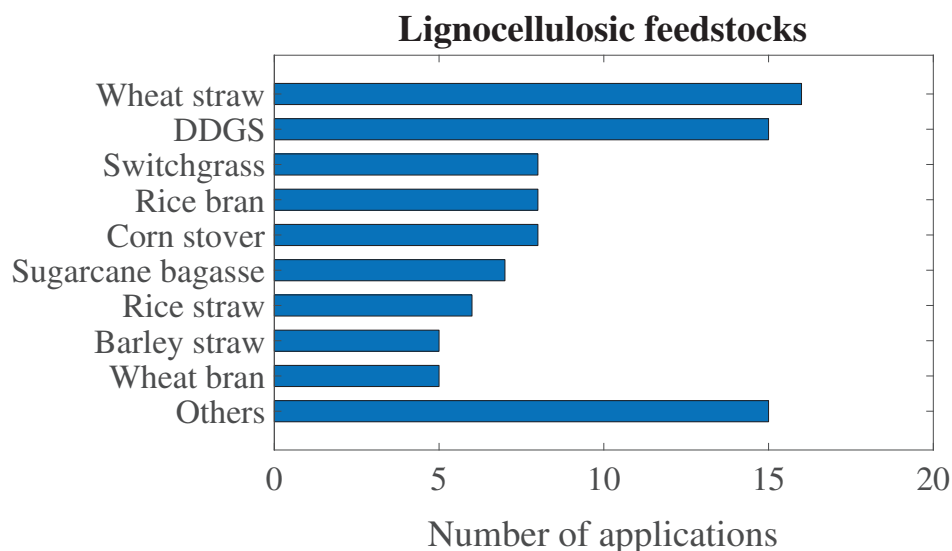


Figure 2.3: Common lignocellulosic feedstocks used in fermentative butanol production from lignocellulosic biomass.

ature as fractionation, which is sometimes used interchangeably with pretreatment i.e., pretreatment is mentioned as a way of achieving biomass fractionation, or the term fractionation is used as (part of) a pretreatment method [26, 45, 46]. In the thesis, for simplicity reasons all steps involved in the conversion of the feedstock to sugars are named as pretreatment, though enzymatic hydrolysis of the polysaccharide fractions is often referred to as a step that is distinct from other pretreatment measures. Commonly used pretreatment methods are shown in Figure 2.4.

Predominance of enzymatic hydrolysis in the pretreatment methods in Figure 2.4 shows its widespread application to produce fermentable sugars from lignocellulosic biomass. Milling/grinding, extrusion, microwave and ultra-sonication are common physical pretreatment methods that open up the physical structure of lignocellulosic biomass [47–53]. Physico-chemical methods such as steam explosion, steam treatment, hydrothermolysis, ammonium fiber expansion, hot water treatment cause both the structure to unravel and to release sugar monomers and dimers [52, 54–58]. Major chemical pretreatment methods are alkali, acidic, ozonolysis, ionic liquid and organosolv treatments [48, 51–77].

Enzymatic hydrolysis using suitable enzyme mixtures degrades polysaccharides such as cellulose and xylan to fermentable C6 and C5 sugar

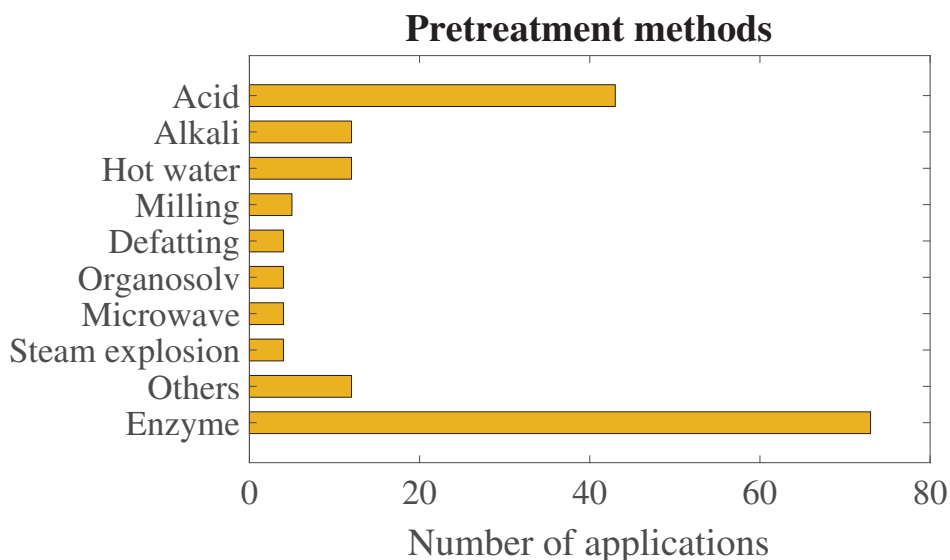


Figure 2.4: Common pretreatment methods used in fermentative butanol production from lignocellulosic biomass.

monomers, respectively [78]. Typically, combinations of several of the above-mentioned pretreatment methods are employed depending on the feedstock. Operating conditions of pretreatment are crucial since a small change in the operating parameters can cause great differences in reduced sugar composition and concentration as well as inhibitory compounds, consequently effecting the cost of substrate [27]. Therefore, it is crucial to examine the feasibility of any pretreatment method with respect to the generation of inhibitors, energy consumption, operating cost, and sugar yield.

2.2.3 Detoxification

Compounds that are inhibitory to microorganisms and enzymes are often generated during pretreatment [78]. Cellulose and hemicellulose should ideally only yield sugar monomers such as glucose, xylose, and mannose. However, harshness of some pretreatment conditions converts those sugars and other lignocellulosic components into furfural, 5-hydroxymethyl furfural (HMF), formic acid, acetic acid, levulinic acid and salts, which can be inhibitory [27, 79]. Partial decomposition of lignin generates inhibitory (poly)phenolic aromatic compounds such as p-coumaric acid, ferulic acid, syringe aldehyde, vanillic acid and vanillin [27]. Contrary to ethanol-producing microorganisms, furfural, HMF or acetic acid are not inhibitory

to *Clostridial* butanol producers, rather they are stimulatory [80]. Another common compound generated during pretreatment of lignocellulosic biomass is formic acid. It is found to be inhibitory to *C. acetobutylicum* at 0.5 g/l [81] and 0.074 g/l (1 mM) inside the cell wall [82] due to acid crash [83]. Therefore, it is a necessity to remove inhibitors for a successful fermentation. For this purpose, several detoxification methods such as electro dialysis [70], liming/overliming [55, 57, 60, 67, 71, 84], activated carbon/charcoal [56, 58, 75, 77], dilution [48, 70], resin [63, 70] treatments are applied. Even though it is not specifically mentioned as a detoxification method, solid/sediment removal by filtration or centrifugation is also commonly applied to alleviate the inhibitory effects of the solids and undissolved lignin in the lignocellulosic hydrolysates [51, 63, 67, 70, 72]. Commonly used detoxification methods are shown in Figure 2.5.

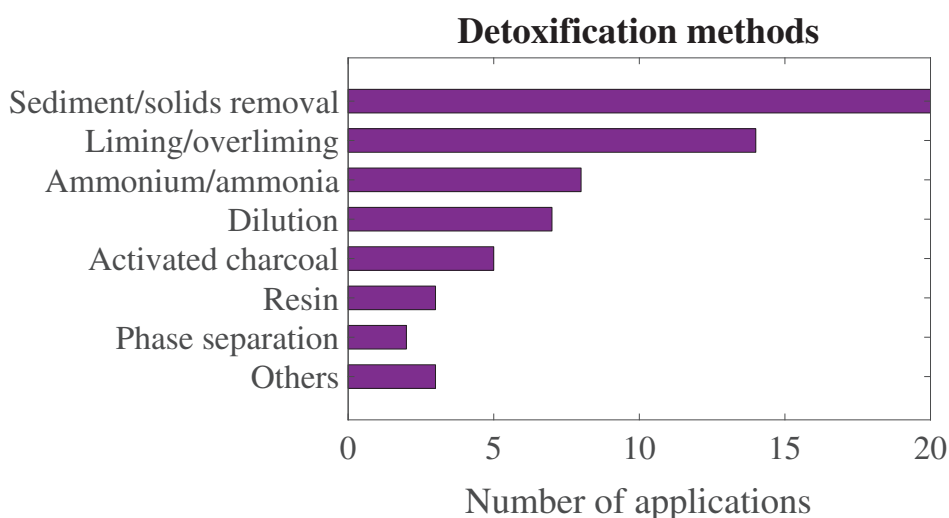


Figure 2.5: Common detoxification methods used in fermentative butanol production from lignocellulosic biomass.

It is important to note that the enzymes used in the hydrolysis step can be inhibited by the compounds mentioned above as well as their sugar yields, which can impose a limit to high substrate concentration [78]. Alternative lines of research currently target new pretreatment methods that are less prone of inhibitor formation (like organosolv or other low-temperature methods) and thus ideally do not require detoxification prior to fermentation, as well as increasing the inhibitor tolerance of fermentation strains e.g. by means of adaptive evolution.

2.2.4 Fermentation

ABE fermentation is biphasic; first acetic acid and butyric acid are produced in the acidogenesis phase, then the acids are re-assimilated to yield solvents, acetone, butanol and ethanol [85]. Batch fermentation is the most studied mode due to simple operation, good reproducibility and control, and low risk of contamination [42]. Low cell density can result in low productivity, and absorbed substrate fermentation [86] and biofilm reactors [87] have been applied to overcome this problem in batch processes. Fed-batch mode is beneficial to tackle substrate inhibition by gradually adding the substrate, thus keeping the substrate concentration below toxic levels [88]. However, fed-batch fermentation should still be accompanied by *in situ* product removal to alleviate product inhibition [68, 89, 90]. Continuous fermentation (chemostat) has advantages over batch and fed-batch modes in terms of better butanol yield and productivity [88]. Multi-stage [91], immobilized cell [92, 93], cell recycling and bleeding [94, 95] techniques have been applied to improve chemostat performance.

2.2.5 Strain Development

Strain development refers to any modifications in a strain done by random mutagenesis and selection, like in adaptive laboratory evolution, or directed, rational and/or Systems biology guided genetic modification employing metabolic engineering and synthetic biology to improve fermentation performance by means of increased tolerance to toxic components, butanol selectivity, improved substrate utilization and range.

In general, detoxification methods shown in Figure 2.5 are used for removal of inhibitors present in the substrate and/or feedstock as described in Section 2.2.3. Co-culturing with other species to eliminate toxic components such as oxygen in case of anaerobic fermentation is an alternative method. Random mutagenesis and selection and metabolic engineering have been applied for the same purpose. Inhibition due to butanol accumulation is one of the greatest challenges. Therefore, metabolic engineering and mutagenesis have been targeting this specific problem.

A typical fermentative butanol production yields acetone and ethanol as well, which decreases the selectivity of the product of interest. Metabolic engineering for disruption of acetone producing pathways [96], homo-butanol fermentation via chemical mutagenesis and metabolic engineering and conversion of acetone into isopropanol are among the strategies developed to address this issue.

Efficient utilization of the substrate is crucial to achieve a high butanol yield, thus better fermentation performance [2, 24, 38]. Disrupting the genes responsible for Carbon Catabolite Repression and overexpression of genes responsible for xylose transport and catalytic enzymes (D-xylose isomerase, xylulokinase, and enzymes of PPP) are commonly followed approaches [75, 77, 97, 98].

It is important to mention the recent efforts on CRISPR-Cas9 genome engineering systems to improve butanol production by fermentation. Most of the research focuses on production by *Escherichia coli* [99]. However, *Clostridial* butanol production improvements have been achieved by using this technique as well [100].

In summary, the increasing numbers of publications in recent years employing strain engineering techniques and approaches to address key bottlenecks in *Clostridial* butanol production hold promise to finally solving these in the future.

2.2.6 Process Integration and Intensification

Process integration and intensification techniques are applied to obtain cost-effective fermentation processes. Important process intensification approaches include a) simultaneous saccharification and (co-)fermentation (SSF or SSCF) in which hydrolysis of polysaccharides present in (pre-treated) biomass is performed by externally produced and added hydrolytic enzyme mixes *in situ* with the simultaneous fermentation of the liberated sugars by a strain (or in the case of SSCF several strains with complementary sugar substrate spectrum) producing the product of choice, e.g. butanol [52, 101], and b) consolidated bioprocessing (CBP) in which the saccharolytic enzymes are produced within the sugar fermenting culture e.g. by the target product producing strain itself or in co-culture with a partner strain specialized in enzyme production and secretion [102].

Gas stripping, pervaporation, adsorption, liquid-liquid extraction, pervaporation (membrane extraction), reverse osmosis and membrane distillation are *in situ* product removal methods used to alleviate inhibitory effects of butanol [22, 35]. Fermentation with integrated gas stripping has widely been studied mostly in fed-batch mode, which showed improved butanol productivity [68, 89].

Cell immobilization and cell recycle are mostly integrated to fermenters operated in continuous mode to improve butanol productivity by preventing the loss of cell mass with the bleeding stream out from the fermenter.

Process integration and intensification measures therefore play crucial roles in optimizing butanol fermentation processes for improved performance and economic competitiveness.

2.3 Fermentative Butanol Production from Mixed Sugars

There has been a great scientific interest in the utilization of different sugars in mixed form for the production of biofuels, since pre-processed lignocellulosic biomass feedstock usually contains a mixture of pentoses (C5) such as xylose and arabinose, and hexoses (C6) such as glucose and mannose. Therefore, efficient utilization of C5 and C6 sugars is a prerequisite for a successful fermentation process with optimized carbon utilization. In this section, the studies focusing on *Clostridial* mixed sugar fermentations producing butanol are reviewed.

Mixed sugar fermentation studies date back to early 1980s, in which researchers investigated the influence of different pentose and hexose sugars and their mixtures at different ratios on the fermentation kinetics [103]. Some *Clostridia* have shown to readily consume sugar mixtures; however, they do so with poor efficiency [104]. Even though both strains can utilize glucose and xylose, *C. beijerinckii* has a large gene cluster containing most of the genes involved in xylose metabolism and regulation, while in *C. acetobutylicum* the xylose-related genes are dispersed over several different chromosomal locations [105]. Moreover, *C. beijerinckii* has more sets of xylose metabolic pathway genes than *C. acetobutylicum* [106].

Cells' efficiency of simultaneously using sugars in mixed form decreases due to a phenomenon called Carbon Catabolite Repression (CCR). Consequently, utilization of pentose sugars is reduced or prevented entirely in the presence of a preferred sugar such as glucose [97]. Furthermore, CCR can cause sequential utilization of sugars (diauxic growth for binary substrate growth) and a lag phase, which increases the residence time, thus operating costs. There have been attempts to improve product titers by using immobilized cultures [107], optimizing the culture pH and glucose to xylose ratio [108] and adding nutritional supplements [109] for fermentative butanol production from mixed sugars. In addition, genomic information [106,110,111] and transcriptome analysis results [112–117] of lignocellulosic sugar metabolisms and respective repression mechanisms are available in the literature.

There is an ongoing research on metabolic engineering to develop

Clostridial strains capable of simultaneously fermenting hexose and pentose for butanol production [75, 97, 98, 118, 119]. Even though Lee et al., (2016) [2] stated metabolic engineering is necessary for simultaneous utilization of sugars, researchers have developed different feeding and pre-growth strategies achieving co-utilization without any strain manipulation [60, 120–125]. However, in the mixed sugar fermentation study of Zhang et al. (2016), transcriptional studies suggested that glucose inhibition on xylose metabolism-related genes was still present despite the simultaneous utilization of glucose and xylose [126]. Therefore, more research on the subject is necessary to investigate this phenomenon further.

2.4 Modeling Fermentative Butanol Production

Mathematical modeling has been a crucial part of the ABE fermentation research. Experimental studies of fermentation processes are typically time consuming due to slow kinetics, which results in a high operating cost together with the cost of the consumables. Fermentation performance is often defined in terms of product yield, selectivity and productivity. Those depend significantly on the operating conditions such as temperature, pH, substrate concentrations, presence of inhibitors, mode of operation, and the type of the strain. Therefore, finding the most suitable operating conditions would require a great number of experiments with different permutation combinations of those. To tackle this experimental work load, bioprocess designers usually do an initial screening of the alternatives and come up with a combination of best operating conditions suited for their purpose. Fermentation models are useful tools serving this objective.

Model simulations can provide insight into the main characteristics of the fermentation processes as well as the influence of different operating conditions and their interconnectedness. The purpose of modeling should be identified clearly, thus the level of detail and type of the information included in the models should be in accordance with that. In the sections below, different types of models developed for fermentative butanol production were categorized according to previous classifications done in the field [13, 127] and presented with a historical perspective.

2.4.1 Structural Models

The first structural model to describe fermentative butanol production dates back to 1984, done by Papoutsakis [128]. The model made a steady state assumption for metabolic activity and balanced the elemental

compositions of the substrates, cell mass and extracellular products using stoichiometric relations; therefore, it is often referred to as 'stoichiometric model' [128]. Desai and coworkers extended the original stoichiometric model in 1999 by adding a non-linear constraint that relates the experimentally observed ratio of butyrate and acetate uptake to the ratio of their intracellular concentrations [129].

The metabolic networks assumed to develop the models mentioned above were manually constructed based on the biochemical and genetic information available at the time. However, there was a rise of the database-driven network reconstruction in the early 2000s initiated by major improvements in sequencing technologies allowing for an ever increasing number of organisms to be completely sequenced. Consequently, genomes of *C. acetobutylicum* ATCC 824 and *C. beijerinckii* NCIMB 8052 were published in 2001 and 2011, respectively and served as a basis of development of genome-scale (metabolic) models [106,130]. In 2008, the first two genome-scale metabolic models of *C. acetobutylicum* were established simultaneously by Senger and Papoutsakis (2008) and Lee et al. (2008) [131–133]. McAnulty et al. (2012) constructed a new and comprehensive model (*iCAC490*) [134] using previous genome-scale models as a starting point and utilizing recent fluxomics data [135,136]. A second generation genome-scale model of *C. acetobutylicum* was developed by Dash et al. (2014) with 800 genes, 1500 reactions and 1200 metabolites, thus three times larger than the first-generation models [137]. The model was further improved by Yoo et al. (2015) covering 20% more genes [138]. For *C. beijerinckii*, the first genome-scale metabolic model was developed by Milne et al. (2011) comprising of 925 genes, 938 reactions, 881 metabolites and 67 membrane transporters [139].

2.4.2 Dynamic Models for Batch Fermentation

The structural models based on fermentation equations or other stoichiometric models are essentially steady-state models; therefore, they do not provide any time variant or temporal information on formation of different metabolites. Consequently, applicability of these models for design and optimization of bioprocesses is rather limited. Dynamic models, which can be used to tackle this problem are presented in the paragraphs below.

Two dynamic models describing batch fermentation for butanol production by a modified *C. acetobutylicum* ATCC 824 were published in 1986 by Volesky and coworkers. Their initial model, termed process-oriented, comprised a set of differential equations describing product formation, acid re-assimilation and sugar utilization [140]. The model did not consider in-

tracellular metabolites and incorporated butanol effects by means of inhibition of acid production and cellular decay. Subsequently, they developed a ‘physiological state model’, which distinguished between intra- and extracellular concentrations of metabolites [141]. The intracellular product concentrations were linked to their extracellular counterparts described by their initial model in terms of diffusion along concentration gradients [140]. In 1990, they developed a model taking pH effects into account using their previous models [142]. The model features a general inhibition term and a pH-dependence term for intracellular conversion of undissociated acids into solvents to extend its applicability to a wide range of culture growth and pH conditions.

Inhibition of the ABE fermentation by its products is an important aspect affecting the performance. A careful investigation of possible causes and mechanisms, leading to inhibition is necessary for a successful process design. This issue was addressed by Yang and Tsao (1994) with a study using statistical analysis of cell mass growth kinetics under the synergistic inhibition of multiple products and byproducts [143]. The model employed the Monod equation to express growth kinetics under inhibition of acetate, butyrate or butanol described by the parabolic function. The mechanism of inhibition is rather complex; therefore, a deterministic model for this process would be quite difficult. Nevertheless, the semi-empirical approach presented in this model can be useful for analysis of the inhibition phenomena and identification of governing factors.

A group of scientists from Japan developed kinetic models for ABE fermentation based on the metabolic pathways of *C. acetobutylicum* ATCC 824, which reveal dynamic behavior of main metabolites and give information about metabolic pathways with the maximum influence on butanol formation. Their first model was developed using Michaelis–Menten kinetics for all the 19 reactions and represented by a set of 16 differential equations for 16 metabolites for fermentation of glucose [144]. The model could predict the dynamics of the substrate, intermediates, and target metabolites. In 2008, they extended their first model for fermentation of xylose as the substrate by replacing the metabolic steps of the Embden–Meyerhof–Parnas (EMP) pathway used in the glucose model with the pentose phosphate (PP) pathway [145]. Although these models are most comprehensive, the major drawback in its application for various processes is that estimation of a complete set of kinetic parameters is extremely difficult. In addition, they do not consider ATP- and NADH-balances. The effects of pH and butanol inhibition, the metabolic regulatory effects of transcriptional control and

the information of some key metabolites such as butyryl phosphate are not considered either. As a result, Li et al. (2011) proposed a new model by improving the models of Shinto et al. (2007, 2008) [146]. This model incorporated butyryl phosphate, whose initial peak marks the onset of solvent production, described net effects of complex ABE regulations according to endogenous enzyme activity variations, and introduced time-dependent enzyme activity coefficients (EAC) for every time interval [146]. In a more recent study, Raganati et al. (2015) adapted the model introduced in Shinto et al. (2008) for investigating the effects of different sugars on batch fermentations by *C. acetobutylicum* [147]. In this updated model, a formally unbounded butanol inhibition of cell mass growth was replaced with a finite ‘critical’ butanol concentration that constrained butanol-inhibited glucose uptake and self-inhibitory butanol formation as well.

2.4.3 Dynamic Models for Continuous Fermentation

The first model for fermentative butanol production was published in 1983 by the research group at Technical University of Delft (the Netherlands) for continuous operation by immobilized *C. beijerinckii* [148]. In 1986, the model was extended with a butanol inhibition term and cell mass distribution in the immobilization matrix [149, 150]. In the same year, Volesky and coworkers reported a model for production in a cell retention fermentor employing membrane filters [151] by adapting their earlier models describing batch fermentation [140, 141]. Their model demonstrated the effectiveness of cell retention while the cell mass is retained within the fermentation system to achieve higher dilution rates, thus higher productivity [151].

Another model for continuous production was developed by Jarzebski et al. (1992) [152]. This kinetic and physiological model described solvent formation at acidic extracellular pH and acid production at more neutral pH assuming solventogenesis is triggered by attaining a given threshold concentration of intracellular butyrate and the undissociated form of butyric acid passes freely through the cell membrane [152]. Haus et al. (2011) focused on pH effects on continuous fermentation as well, and their model studied the observed pH-induced changes in gene expression on the two steady states, i.e. at pH 5.7 and pH 4.5 [153]. Thorn et al. (2013) extended their model by taking pH-dependent sporulation into account with the assumption of acid-forming cells sporulating in response to the sudden drop in culture pH and resulting in metabolically inactive cells [154]. Even though this model could explain the differences between acidogenic and solventogenic cells, it

could not predict the experimentally observed transition dynamics between the two metabolic steady states [13]. Therefore, a new model was suggested by Millat et al. (2013) which considered two subpopulations with distinct metabolic activity and assumed that acidogenic cells stop growing when the pH falls below 5.2 to 5.1 while, simultaneously, the solvent-forming cells increase in numbers to establish a solventogenic culture [155, 156].

2.4.4 Models for Fermentation with *in situ* Product Removal

As mentioned in the sections above, accumulation of products in the fermentation broth causes inhibition. Therefore, *in situ* product removal using different techniques such as pervaporation, liquid–liquid extraction, gas stripping, and extractive distillation helps to alleviate inhibitory effects of products. There has been several attempts to model fermentation processes with simultaneous product recovery, which are presented below.

Wankat and coworkers modeled simultaneous fermentation and separation in a packed column with an immobilized cell trickle bed reactor and integrated gas stripping [157–159]. Their system consisted of an enricher, and a stripper, stacked over one another. They used Monod type production for butanol with product inhibition on the cell mass growth and assumed an equilibrium stage with steady state and isothermal operation, and surface reaction with no diffusion limitation in an immobilization matrix for model development. By using this model, they studied effects of gas to water mole ratio in the enriched and stripper streams, total gas flow rate, product inhibition kinetics, operating temperature and pressure and inlet glucose concentration.

Park and Geng (1996) proposed a model for fed-batch fermentation with simultaneous pervaporation as well. Their system consisted of a fermenter and a pervaporation module mounted inside the fermenter [160]. They again applied Monod growth kinetics with inhibitions, and the complete model comprised eight ordinary differential equations describing the change of medium volume, and concentrations of cell mass, butyric acid, butanol, acetic acid, ethanol, acetone and glucose over time. Product formations were defined with yield coefficients (g product/g glucose) related to the cell growth.

Shukla et al. (1989) suggested a model for a hollow fiber fermentor-extractor. It was a tubular fermenter filled with hydrophobic microporous hollow fibers with immobilized cells, and the extraction solvent passing

through the fibers [161]. The model consists of eleven equations in which the model of Mulchandani and Volesky (1986) was coupled to simple mass balance equations for simultaneous solvent extraction [151]. The model assumes that there is no mass transfer resistance in radial direction in the fermenter and steady state conditions exist.

Oleyl alcohol is a commonly used extractant for solvent recovery from the broth in ABE fermentation. The extracted solvent is recovered by distilling the solvents from the extractant under vacuum conditions by maintaining boiling point at mild temperature. Based on this, Shi et al. (2005) developed a model for a flash extractive fermentation system and assessed its performance by means of productivity, energy requirement, and product purity [162]. Mariano et al. (2009) proposed a model for a flash fermentation process as well and studied the optimization of a continuous flash fermentation process for butanol production [163], and used the model of Mulchandani and Volesky (1986) for description of the fermentation process.

2.4.5 Unstructured Models

Unstructured models are a generic class of models describing microbial processes in terms of the growth of microorganisms, the utilization of substrates and the formation of products. They are explained below.

2.4.5.1 Microbial Growth Models

The life cycle of microorganisms is characterized by different phases. A representative growth curve and the respective growth rate curve can be seen in Figure 2.6.

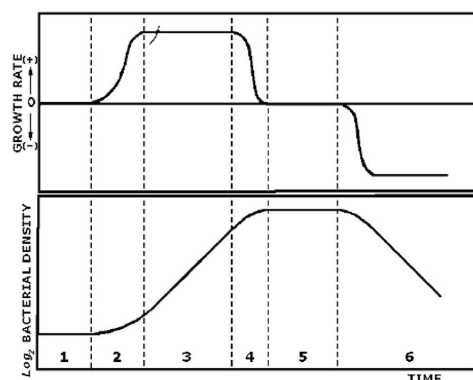


Figure 2.6: A representative growth curve of microorganisms (top) and the respective growth rate curve (bottom) [164].

The actual shapes of the curves shown in Figure 2.6 depend on several factors such as environmental conditions, substrate properties, type of the microorganism, physiology of the inoculum [165]. Lag phase (1) occurs due to adaptation of the culture to a new environment, and once the cells are adapted, acceleration phase (2) is observed. The growth is most apparent during the exponential or logarithmic growth phase (3). This phase is typically followed by retardation or deceleration phase (4) and then stationary phase (5) due to exhaustion of nutrients and substrates, and accumulation of toxic metabolites [166]. Finally, the phase of decline or death is observed during which the number of viable cells decrease at a death rate of k_d (h^{-1}). The mass of dead cells is assumed to decay into carbohydrates, lipids, proteins and nucleic acids, and this process is called disintegration or lysis. Consequently, the change in cell mass concentration can be expressed as in Equation 2.1.

$$\frac{dX}{dt} = \mu X - k_d X \quad (2.1)$$

where X is the cell mass concentration (g/l), k_d is the death rate (h^{-1}), μ is the specific growth rate (h^{-1}). The specific growth rate (μ) cannot be infinite due to the limited availability of nutrients, substrate concentration, S (g/l) and other ambient conditions such as inhibitors, I (g/l), pH value and temperature T , as shown in Equation 2.2.

$$\mu = \mu(S, I, pH, T), \quad \mu \neq \infty \quad (2.2)$$

The Michaelis-Menten model describing the dependency of enzyme activity on the substrate concentration was the basis for the kinetics of microbial growth, since it can be seen as an autocatalytic reaction as well. In the light of this connection, Monod identified the non-linear relation between specific growth rate and limited substrate concentration, and suggested that the specific growth rate is inversely proportional to substrate concentration [165]. Therefore, the specific growth rate increases fast at low substrate concentrations and slowly at high substrate concentration, until a saturation is reached according to Equation 2.3.

$$\mu = \frac{\mu_{max} S}{K_s + S} \quad (2.3)$$

This limit is the maximum specific growth rate, μ_{max} . The substrate affinity constant K_s shows the relation of microorganism to the limiting substrate. The specific growth rate is approximately linear when $S < K_s$. K_s is always greater than zero, therefore $S/(S + K_s)$ is always less than 1,

consequently the specific growth rate, μ is less than μ_{max} . The growth can only start when the substrate concentration is at a certain value due to the maintenance energy requirement. If the substrate is not the limiting factor due to a high enough concentration, the maximum specific growth rate can be reached.

The maximum specific growth rate can be treated as an intrinsic property, since it is unique for every microorganism [167]. The Monod model applications for pure cultures and simple substrates showed very high accuracy [168]. There has been many attempts to extend the Monod model for better description of the systems with different characteristics. The most common ones are summarized in Table 2.4.

Table 2.4: Models developed for microbial growth on single substrate for pure cultures.

Author	Model	Reference
Monod	$\mu = \frac{\mu_{max} S}{K_s + S}$	[169]
Moser	$\mu = \frac{\mu_{max} S^n}{K_s + S^n}$	[170]
Contois	$\mu = \frac{\mu_{max} S}{K_c X + S}$	[171]
Tessier	$\mu = \mu_{max} (1 - e^{-K S})$	[172]

The Moser model was developed by upgrading the Monod model with a constant, n to include the effects of microorganism's adaptation to stationary process by mutation [170]. Contois equation takes cell mass concentration into account as well. This model has a saturation constant, K_c proportional to the cell mass concentration to describe the growth of cultures with high cell mass density [171]. The Tessier model has two constants as the previously mentioned growth models and characterizes the growth by using an exponential function [172].

Different growth models can have better prediction capacities for different cultures. Therefore, it is essential to have insight into available models and make the model selection accordingly. The above mentioned models apply to pure cultures and single substrate limited growth conditions. However, the growth is often hindered by inhibitors. The growth models considering the effects of inhibitors are discussed in the section below.

2.4.5.2 Microbial Growth Models with Influence of Inhibitors

The growth can be hindered in presence of a high substrate concentration. To illustrate, when the substrate concentration in a growth medium is increased, a maximum specific growth rate will be observed at a particular concentration, above which the specific growth rate will decrease [165]. The reasons can be a high osmotic pressure of the medium or a specific toxicity of the substrate [173]. Consequently, chemical potential of the substrates, intermediates and products, and functional activity of the cells can change, permeability of the cells can alter, enzyme activities can be manipulated as well in connection with genetic engineering and altering gene expression.

Microbial growth can also be hindered by certain product concentrations. Inhibition paths of substrates and products are based on similar effects and closely linked. The growth model with influence of substrate and product inhibitions can be seen in Tables 2.5 and 2.6, respectively.

Table 2.5: Models developed for microbial growth on single substrate for pure cultures with effects of substrate inhibitions.

Author	Model	Reference
Edwards	$\mu = \frac{\mu_{max} S}{(K_s + S)} e^{-S/K_I}$	[173]
Edwards	$\mu = \mu_{max} (e^{-S/K_I} - e^{-S/K_S})$	[173]
Webb	$\mu = \frac{\mu_{max} S (1 + \beta S/K_I)}{(K_s + S + S^2/K_I)}$	[174]
Andrews	$\mu = \frac{\mu_{max} S}{(K_s + S + S^2/K_I)}$	[175]
Haldane	$\mu = \frac{\mu_{max} S}{(K_s + S)(1 + S/K_I)}$	[176]
Tseng & Wayman	$\mu = \frac{\mu_{max} S}{(K_s + S)} - K_I(S - S^*)$	[177]
Luong	$\mu = \frac{\mu_{max} S}{(K_s + S) (1 - S/S_{max})^\alpha}$	[178]

Edwards (1970) proposed two models employing the substrate inhibition term in exponential form (S/K_I); one of which had the same structure

as the Monod model, while the other one described the substrate dependency of growth in exponential form as well [173]. Webb (1963) derived a model from enzyme kinetics with an integrated allosteric effect with β as reaction rate [174]. Similarly, Andrews (1968) suggested a model based on enzyme kinetics assuming that β was equal to zero [175], and Haldane's model (1930) also assumed that $K_I \gg K_s$ [176]. The model developed by Tseng and Wayman (1975) accounted for the fact that there is a threshold substrate concentration, S^* below which there is no growth inhibition, and the growth decreases linearly with respect to the concentration difference $(S - S^*)$ when $S > S^*$ [177]. Luong (1987) suggested a model including a maximum substrate concentration, S_{max} above which the growth stops entirely [178]. This model was reported to have better prediction capacity compared to the previous growth models with substrate inhibition terms, in addition, it had the advantage of estimating the value of S_{max} .

Table 2.6: Models developed for microbial growth on single substrate for pure cultures with effects of product inhibitions.

Author	Model	Reference
Hinshelwood	$\mu = \frac{\mu_{max} S}{(K_s + S)} - K_P P$	[179]
Holzberg	$\mu = \frac{\mu_{max} S}{(K_s + S)} K_{P1} (P - K_{P2})$	[180]
Aiba	$\mu = \frac{\mu_{max} S}{(K_s + S)} e^{-K_P P}$	[181]
Bazua & Wilke	$\mu = \frac{\mu_{max} S}{(K_s + S)} - \frac{K_{P1} P}{(K_{P2} - P_{max})}$	[182]
Han & Levenspiel	$\mu = \frac{\mu_{max} S}{(K_s + S)} (1 - P/P_{max})^n$	[183]
Luong	$\mu = \frac{\mu_{max} S}{(K_s + S)} (1 - (P/P_{max})^n)$	[184]
Egamberdiev & Ierusalimsky	$\mu = \frac{\mu_{max} S}{(K_s + S)(1 + P/K_P)}$	[185]
Competitive inhibition	$\mu = \frac{\mu_{max} S}{K_s(1 + P/K_P) + S}$	[166]

The first model accounting for product inhibition was a simple linear kinetics model proposed by Hinshelwood (1946) [179]. Holzberg's model (1967) suggested that the growth inhibition was prominent when the product concentration was higher than a threshold level [180]. Since the growth inhibition due to alcohols is noncompetitive in nature [186], Egamberdiev and Ireusalimsky (1968) described the specific growth rate as a hyperbolic function of product concentration [185]. Exponential relationship between the specific growth rate and product concentration was recognized in the model of Aiba (1968) [181].

For the first time, Bazua and Wilke's model (1975) included a maximum product concentration, P_{max} at which the growth entirely stopped, and its accuracy was better for describing the experimental observations [182]. In an attempt to generalize the product inhibition kinetics, Han and Levenspiel (1988) proposed a nonlinear kinetic model containing P_{max} and n to quantify the extent of inhibition [183]. Luong (1985) proposed a modification of Han and Levenspiel's model for improved flexibility [184]. Even though the inhibitory effects of alcohols on the growth are in noncompetitive form, inhibitory effects of other metabolites produced during fermentative butanol production can be in different forms. Therefore, competitive inhibition was given as a common form as well [166], which can describe butyric and acetic acids inhibitions [143].

2.4.5.3 Binary Substrate Growth Models

Fermentation substrates obtained from natural feedstock such as lignocellulosic biomass are typically mixtures of different components i.e. hexoses and pentoses as explained in the section above. Even though models for mixed substrate growth are available, the majority of the models were developed for single substrate growth. Therefore, it is essential to understand mixture effects and develop a kinetic model which can predict the cell mass growth for successful design of lignocellulosic fermentation processes. The models developed for binary substrate systems are summarized in Table 2.7.

McGee et al. (1972) developed a model describing growth for a heterogeneous substrate, which serves different purposes e.g. carbon and nitrogen mixtures [187]. The model was classified as interactive and based on the assumption that the growth rate can be affected by more than one substrate simultaneously [188].

Segel (1975) proposed a model for a noncompetitive inhibition between the substrates based on enzyme kinetics when both substrates simultaneously bound to an enzyme [189]. Furthermore, uncompetitive inhibition

model was suggested to characterize the interaction between the substrates. It differs from the noncompetitive substrate inhibition in which one of the substrates can only bind to the enzyme-substrate complex, not the free enzyme.

Table 2.7: Binary substrate growth models.

Type	Model	Ref.
Noncompetitive	$\mu = \frac{\mu_{maxG} SG}{(K_{sG} + SG) \left(1 + \frac{SX}{K_{sX}}\right)} + \frac{\mu_{maxX} SX}{(K_{sX} + SX) \left(1 + \frac{SG}{K_{sG}}\right)}$	[189]
Uncompetitive	$\mu = \frac{\mu_{maxG} SG}{K_{sG} + SG \left(1 + \frac{SX}{K_{sX}}\right)} + \frac{\mu_{maxX} SX}{K_{sX} + SX \left(1 + \frac{SG}{K_{sG}}\right)}$	[189]
Interactive	$\mu = \frac{\mu_{maxG} SG SX}{(K_{sG} + SG)(K_{sX} + SX)}$	[188]
Noninteractive	$\mu = \frac{\mu_{maxG} SG}{K_{sG} + SG} + \frac{\mu_{maxX} SX}{K_{sX} + SX}$	[190]
Competitive	$\mu = \frac{\mu_{maxG} SG}{K_{sG} + SG + SX \left(\frac{K_{sG}}{K_{sX}}\right)} + \frac{\mu_{maxX} SX}{K_{sX} + SX + SG \left(\frac{K_{sX}}{K_{sG}}\right)}$	[191]

Yoon et al. (1977) developed a kinetic model for the homologous substrate meaning that they serve for the same purpose e.g. as the carbon source [187] incorporating purely competitive kinetics [191]. The model shows that each substrate exhibits a competitive inhibition effect on the utilization of the other substrate. Competitive interaction kinetics can be used for describing both simultaneous and sequential substrate utilization for mixed substrates.

The model proposed by Bell (1980) assumed that there was no interaction between the substrates; therefore, parameters estimated in single substrate experiments were used to obtain the sum kinetic model [190].

2.4.5.4 Substrate Utilization Models

Substrate utilization (consumption or degradation) can be expressed in terms of specific growth rate as explained in previous sections. Microorganisms utilize substrate to synthesize new cell material and to supply maintenance and growth energy, and products are formed as a consequence [165].

- Synthesizing new cell material $((\frac{dS}{dt})_X)$.
- Production of products such as butanol $((\frac{dS}{dt})_P)$.
- Supply of maintenance and growth energy $((\frac{dS}{dt})_E)$.

Total substrate utilization is the sum of these three as shown in Equation 2.4.

$$\frac{dS}{dt} = \left(\frac{dS}{dt}\right)_X + \left(\frac{dS}{dt}\right)_P + \left(\frac{dS}{dt}\right)_E \quad (2.4)$$

Utilization of the substrate for cell material synthesis is described by using a stoichiometric relationship between them. This approach requires a molecular formula for the cell mass even though it is well known that the chemical constitution of the formed cell mass is not constant and varies within microorganisms group, growth phase and the utilized substrate. In this thesis, a typical molecular formula of bacteria, $CH_{1.666}N_{0.20}O_{0.27}$ was used in calculations [166]. Equation 2.5 shows the expression of substrate utilization for cell material synthesis.

$$\left(\frac{dS}{dt}\right)_X = -\frac{1}{Y_{X/S}} \left(\frac{dX}{dt}\right) \quad (2.5)$$

where $\left(\frac{dX}{dt}\right)$ is the cell mass change over time as given in Equation 2.1, and $Y_{X/S}$ is the cell mass yield on substrate (g cell mass/g substrate).

Microorganisms require energy for the synthesis of cell ingredients, which are consumed continuously, or for osmotic activities to sustain the concentration gradient between cell interior and exterior [165, 166]. Supply of maintenance and growth energy can be described separately or combined. When combined, substrate utilization for maintenance energy can be defined as in Equation 2.6.

$$\left(\frac{dS}{dt}\right)_E = -m_s \left(\frac{dX}{dt}\right) \quad (2.6)$$

where m_s (g substrate/g cell mass) is the maintenance energy constant.

The substrate utilization for product formation can be determined by Equation 2.7.

$$\left(\frac{dS}{dt}\right)_P = -\frac{1}{Y_{P/S}} \left(\frac{dX}{dt}\right) \quad (2.7)$$

where $Y_{P/S}$ is the product yield on substrate (g product/g substrate). Similar to the cell mass yield coefficient, $Y_{P/S}$ is calculated using the stoichiometric relationship between the substrate and the product of interest, which is butanol in this thesis.

2.4.5.5 Product Formation Models

There are three types of microbial product formation models with respect to the relation with the cell mass and specific growth rate. They are growth-associated (Type I), mixed-growth-associated (Type II) and nongrowth-associated (Type III) production types as illustrated in Figure 2.7 [166].

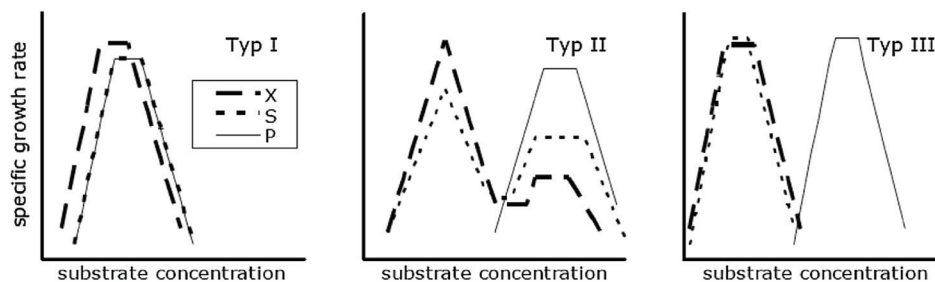


Figure 2.7: Representative curves of substrate utilization, cell mass growth and product formation at different production types, where X is the cell mass concentration, S is the substrate concentration and P is the product concentration [192].

Growth-associated products are produced simultaneously with cell mass growth as a result of primary energy metabolism. Therefore, the specific rate of product formation is proportional with the specific cell mass growth rate as given in Equation 2.8.

$$\frac{dP}{dt} = Y_{P/X} \left(\frac{dX}{dt} \right) \quad (2.8)$$

where $Y_{P/X}$ is the product yield on cell mass (g product/g cell mass). Typically alcohol fermentations exhibit this type of product formation (Type I), including fermentative butanol production.

Mixed-growth-associated product formation takes place during stationary phase when the specific growth rate of cell mass is zero (shown in Figure 2.6). This type of production (Type II) results from energy metabolism indirectly, and the specific rate of product formation is constant as given in

Equation 2.9.

$$\frac{dP}{dt} = Y_{P/X_1}X + Y_{P/X_2}\left(\frac{dX}{dt}\right) \quad (2.9)$$

where Y_{P/X_1} is the product yield on cell mass for the nongrowth-associated term and Y_{P/X_2} is for growth-associated term. The products are formed at side or secondary reactions or following interactions of direct metabolic products.

Nongrowth-associated (Type III) production takes place during the slow growth and stationary phases as Equation 2.10 shows.

$$\frac{dP}{dt} = Y_{P/X_1}X \quad (2.10)$$

Since the butanol production from fermentation follows Type I (growth-associated), Equation 2.8 was adapted and used in the thesis.

Chapter 3

Exploratory Data Analysis of Fermentation Variables

Contents of this chapter were covered in Paper V.

3.1 Introduction

Understanding the variables in fermentative butanol production and their interconnectedness is lacking to a great extent, since many studies narrow their focus on a particular problem and evaluate their solution in the same narrow window. A comprehensive dataset was developed by extracting information from original research articles on *Clostridial* fermentative production of butanol from lignocellulosic biomass and mixed sugars the last three decades and an exploratory data analysis was performed to derive current trends and dependencies.

3.2 Methods

77 lignocellulosic hydrolysate, 19 lignocellulosic hydrolysate with additional glucose, and 79 mixed sugars fermentations are in the dataset, covering 175 fermentations in total. The dataset contains initial and final concentrations of all sugars and other components found in the substrate mixtures, all products in the fermentation broth, fermentation time, types of *Clostridial* strain, feedstock, pretreatment, and detoxification methods for all 175 fermentations. As far as reported data were directly derived from the article texts and tables, otherwise WebPlotDigitizer tool [193] was used for mining the information from the plots.

Exploratory data analysis (EDA) is a statistical approach to analyze datasets for summarizing their main characteristics, which was promoted by John Tukey to encourage statisticians for in depth data exploration [194]. Boxplot is used as a visual tool for EDA, which is a graphical method for illustration of numerical data groups through their quartiles that is the middle number between the smallest number and the median of the dataset. The lines extending vertically from the boxes called whiskers indicate the variability outside the upper and lower quartiles. In Figures 3.2, 3.3 and 3.4, boxplots are represented as rectangles with a vertical line showing the mean value, whiskers shown as dashed lines, and outliers are individual plus signs. Detailed features of the boxplots can be found in Section B.5.1 in the Appendix. Kendall's correlation coefficient was used to determine the correlations between variables since it is able predict nonlinear relationships [195] and robust in presence of outliers in data [196]. The coefficient has a value between +1 and -1, where +1 is total positive correlation, 0 is no correlation, and -1 is total negative correlation. Further explanation about the correlation coefficient can be found in Section B.5.2 in the Appendix.

3.3 Results and Discussion

Clostridial strain type, feedstock type, pretreatment method, and detoxification method are summarized in Figures 2.2, 2.3, 2.4 and 2.5.

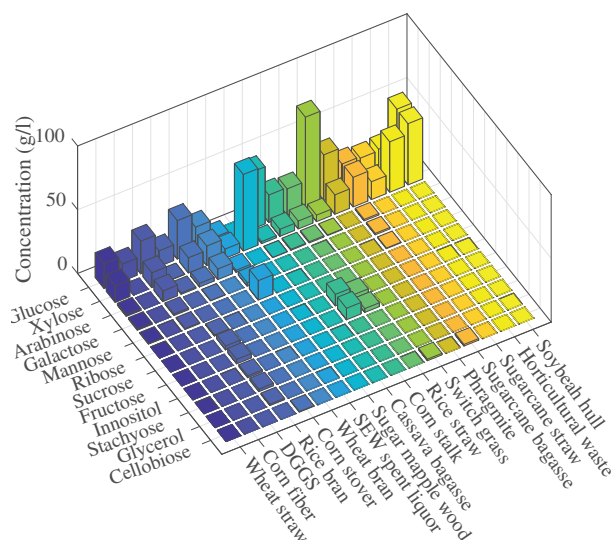


Figure 3.1: Concentrations of substrate components present in the lignocellulosic hydrolysates.

The substrate components present in the lignocellulosic hydrolysates are shown in Figure 3.1 with respect to their concentrations and the feedstock type. Detailed explanations of the dataset features are presented in terms of boxplots and correlation coefficients in the following sections.

3.3.1 Substrate Properties

In lignocellulosic substrate fermentation, the hydrolysate represents the sole source of carbon; however, microorganisms need other nutrients such as nitrogen, phosphorous, sulfur, vitamins and minerals for growth and production. Typically, P2 stock solution and yeast extract are added externally, which increases the substrate cost [28, 48, 51–77, 84]. To tackle this problem, there have been attempts to provide the essential nutrients from complex waste materials such as wastewater sludge [64]. Optimization of medium components to minimize the substrate cost is important to consider when designing a fermentation process [27]. In Figure 3.2, initial concentrations of total substrates and their common constituents glucose, xylose, arabinose, galactose, mannose and cellobiose are shown for lignocellulosic hydrolysate, lignocellulosic hydrolysate with glucose, and mixed sugar fermentations. It is important to note that the dataset could only include what was reported in the papers; there is therefore a possibility of unreported, unidentified and undetected components in the hydrolysates affecting results.

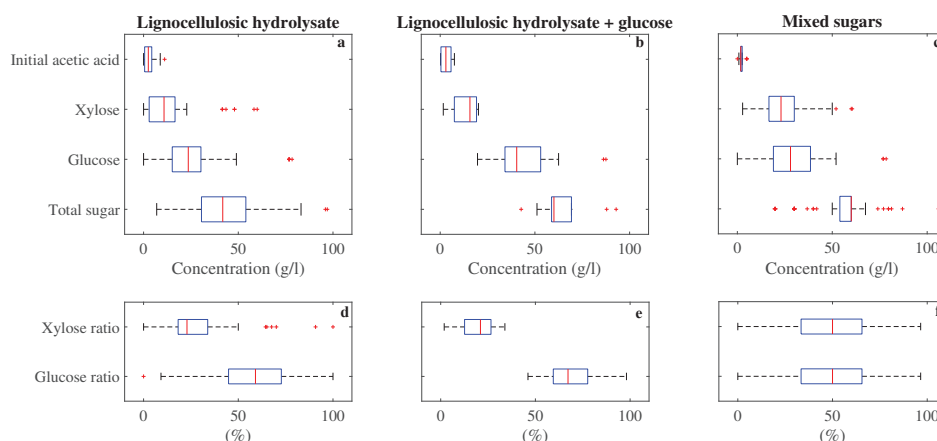


Figure 3.2: Substrate properties of a,d) lignocellulosic hydrolysate, b,e) lignocellulosic hydrolysate with additional glucose, and c,f) mixed sugar fermentations.

For lignocellulosic hydrolysates, the medians of total sugars, glucose, xylose and arabinose concentrations were 41.8, 23.6, 10.8 and 1.02 g/l, respectively.

ively. Outliers worth to mention include soybean hull hydrolysis yielding 49 g/l glucose and 48 g/l xylose [77], switchgrass yielding 77 g/l glucose with total sugar of 82 g/l [56], horticultural waste with 6 g/l glucose and 58 g/l xylose [75], and sugarcane bagasse containing 15 g/l glucose and 44 g/l xylose [52]. The deviation from the general trend could be due to the feedstock properties as well as the specific pretreatment methods. Addition of glucose to the hydrolysate is a common practice to increase the total sugar concentration in the fermentation medium. Therefore, the total and individual sugar concentrations were higher for lignocellulosic hydrolysates with glucose. The medians of total sugar, glucose, xylose and arabinose concentrations were 60.05, 40.4, 15.7 and 2.8 g/l, respectively. The amount of glucose added to the wheat straw hydrolysate was increased incrementally until the substrate inhibitory level [51], which resulted in outliers together with the glucose added cassava bagasse hydrolysate [68]. Mixed sugar fermentations are frequent among published lignocellulosic biomass fermentation studies. Researchers mimic the composition of hydrolysates with synthetic sugars to test the effect of impurities and inhibitors. Mixed sugar concentrations are more disperse with the medians of total sugar, glucose, xylose and arabinose concentrations of 60, 28, 23 and 0 g/l, respectively.

3.3.2 Product Mixture Properties

Maximization of butanol titer is an all-time objective as discussed previously. In addition, the product mixture properties can provide information about the state of the fermentation. Therefore, the composition and concentrations of the product mixtures were shown in Figure 3.3.

For lignocellulosic hydrolysate fermentations, the medians of total ABE solvents, acetone, butanol and ethanol concentrations are 9.33, 2.5, 6.95 and 0.4 g/l, respectively, while median total acid, butyric acid and acetic acid concentrations are 4.4, 1.94 and 2.26 g/l. The highest reported value of the product of interest, butanol was 14.5 g/l produced by *C. beijerinckii* P260 [84] shown as an outlier in Figure 3.3. High total acid concentrations of 14.1 and 15.1 g/l were reported for switchgrass hydrolysate fermentations by *C. acetobutylicum* 824, and those were reduced to 5.38 and 4.8 g/l after detoxification of the substrate with more than 100% increase in the total ABE solvent concentrations [56]. Total acid concentrations of 16.1 and 28.8 g/l were reported for soybean hull as the feedstock and engineered *C. tyrobutyricum* strains [77]. High acetone concentration in the product mixture is not desirable since it is corrosive to plastic piping and increases downstream costs. Therefore, wheat straw hydrolysate fermentation by *C. beijerinckii*

with 11.9 g/l acetone [51] and, switchgrass and phragmite hydrolysate fermentations by *C. saccharobutylicum* with 9.13 and 9.15 g/l acetone [62], respectively, are worth to mention.

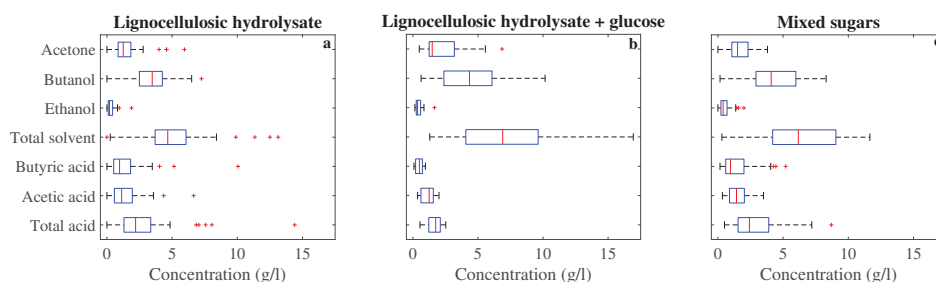


Figure 3.3: Product concentrations of a) lignocellulosic hydrolysate, b) lignocellulosic hydrolysate with additional glucose, and c) mixed sugar fermentations.

For lignocellulosic hydrolysate with glucose fermentations, the medians of total ABE solvents, acetone, butanol and ethanol concentrations are 13.81, 2.97, 8.69 and 0.71 g/l, which are 48%, 19%, 25% and 78% higher than fermentations of lignocellulosic hydrolysates only as reported above. Medians of total acid, butyric acid and acetic acid concentrations are 3.5, 1.0 and 2.5 g/l. Additional glucose resulted in an increase in ABE solvents, and a decrease in total acids indicating that the fermentations were closer to completion. Fermentation of wheat straw hydrolysate with added glucose by *C. beijerinckii* yielded a high acetone concentration of 13.7 g/l [45].

For mixed sugar fermentations, the medians of total ABE solvents, acetone, butanol and ethanol concentrations are 12.33, 3.01, 8.17 and 0.8 g/l, respectively, while those of total acid, butyric acid and acetic acid concentrations are 4.83, 1.93 and 2.85 g/l. Even though the initial total substrate concentrations of lignocellulosic hydrolysate with glucose and mixed sugar fermentations were almost the same, the latter had 12% lower ABE solvents, and 38% higher total acids. Reasons can be the difference in individual sugar concentrations and the stimulatory effects of compounds present in the hydrolysates [80].

3.3.3 Performance Indicators

Percental (%) utilizations of total sugar, glucose, xylose and arabinose, butanol and solvent yields in % (g product/g total sugar consumed \times 100%) and the butanol ratio in % in ABE solvents (g butanol/g ABE solvents \times 100%) were selected as the performance indicators, which

are shown in Figure 3.4. Even though solvent/butanol productivity is another important measure, reported values were difficult to compare due to the presence of lag phases and low data density, making it difficult to determine the exact termination time of fermentation.

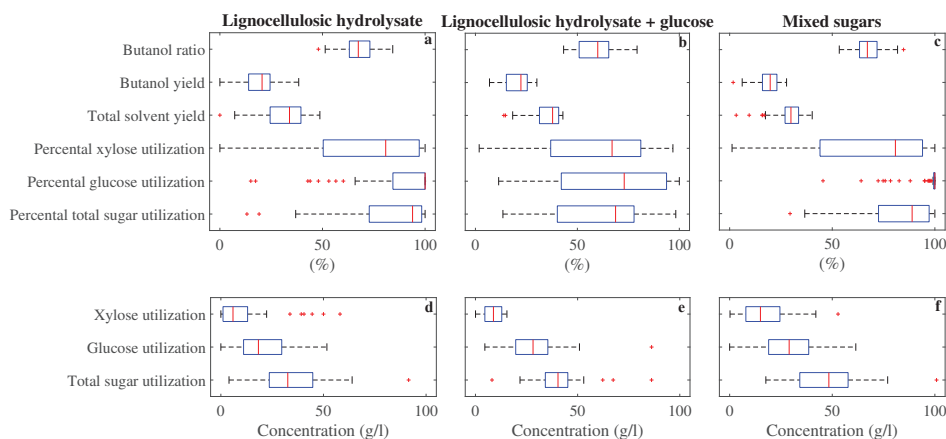


Figure 3.4: Performance indicator values of a,d) lignocellulosic hydrolysate, b,e) lignocellulosic hydrolysate with additional glucose, and c,f) mixed sugar fermentations.

For lignocellulosic hydrolysate fermentations, the medians of total sugar, glucose, xylose and arabinose utilizations (%) are 94, 100, 80.8 and 100, respectively, which indicates a rather inefficient use of xylose. Lowest glucose utilizations shown as outliers in Figure 3.4 are 49% for rice straw hydrolysate fermentation by non-acetone forming *C. sporogenes* [63] and 16% for switchgrass hydrolysate fermentation by *C. acetobutylicum* 824 that increased to 60% after detoxification [56]. In a similar manner, 14% glucose utilization during wheat straw hydrolysate fermentation by *C. beijerinckii* 6422 increased to 76% after detoxification [54]. Solvent and butanol yields are important measures of cells' efficiency to convert substrate to useful products, and a higher butanol ratio is desirable to minimize downstream processing costs. The medians of total ABE solvent yield, butanol yield and butanol ratio were 34%, 25.6% and 67.5%. The highest butanol yield with 38.4% was achieved for rice bran hydrolysate fermentation by *C. beijerinckii* 8052 [65], which represents 94% of the maximum theoretical butanol yield from glucose, 0.41 (g/g) [197]. The highest butanol ratio in ABE solvents was 84.2% achieved in the same fermentation [65]. It is interesting to note that the butanol ratio was only 64% in the fermentation by non-acetone forming *C. sporogenes* [63], which can still be favorable, since the ethanol and butanol blend is already a valuable and useful product mix.

For lignocellulosic hydrolysate fermentations with added glucose, the medians of total sugar, glucose, xylose and arabinose utilizations were 68.7%, 73%, 67% and 65%, respectively, which are lower than in fermentations of the hydrolysates without added glucose. The reason can be that the substrate concentrations reached inhibitory levels with the added glucose and consequently sugar utilizations became inefficient. Median values of total ABE solvent yield, butanol yield and butanol ratio were 37.8%, 22.3% and 60%. Despite 11.2% higher solvent yield, butanol yield and butanol ratio were 13% and 12.5% lower compared to lignocellulosic hydrolysate fermentations without extra glucose, which implies that the composition of the sugar mixture has an influence on the product mixture.

For mixed sugar fermentations, the medians of total sugar, glucose, xylose and arabinose utilizations are 89%, 100%, 80.8% and 86%, respectively. Despite the similar initial total substrate concentrations of lignocellulosic hydrolysate with glucose and mixed sugar fermentations, the latter had 20% higher total sugar utilization. This can be due to the difference in concentrations of individual sugars and other medium components. Median values of total ABE solvent yield, butanol yield and butanol ratio were 29.9%, 19.8% and 67%. Both yield values were significantly lower than in lignocellulosic hydrolysate with added glucose fermentations. However, the butanol ratio was 11.7% higher in mixed sugar fermentations.

3.3.4 Correlations between Fermentation Variables

All 22 fermentation variables introduced in the previous section were used. They are initial substrate, glucose, xylose and acetic acid concentrations (S_i , SG_i , SX_i and HAc_i), ratio of glucose and xylose in the initial substrate mixture (SG_{ir} and SX_{ir}), utilized concentrations of total substrate, glucose and xylose (S_u , SG_u and SX_u), percental utilizations of total substrate, glucose and xylose (S_{ur} , SG_{ur} and SX_{ur}), concentrations of acetone, butanol, ethanol, ABE solvents, butyric acid, acetic acid and total acids (Ac , $BuOH$, $EtOH$, ABE , HBu , HAc and $Acids$), ABE solvents and butanol yields (ABE_y and $BuOH_y$), and butanol ratio in ABE solvents ($BuOH_r$). Figure 3.5 shows correlations of 22 fermentation variables of 175 fermentations. For a thorough investigation of the correlation coefficients, it is referred to Table A.1 in the Appendix. All the correlation coefficients discussed below have a p value greater than 0.05, showing that the correlation is statistically significant.

All utilized sugar concentrations (S_u , SG_u , SX_u) increase as their initial concentrations (S_i , SG_i , SX_i) increase, which reflects into positive and

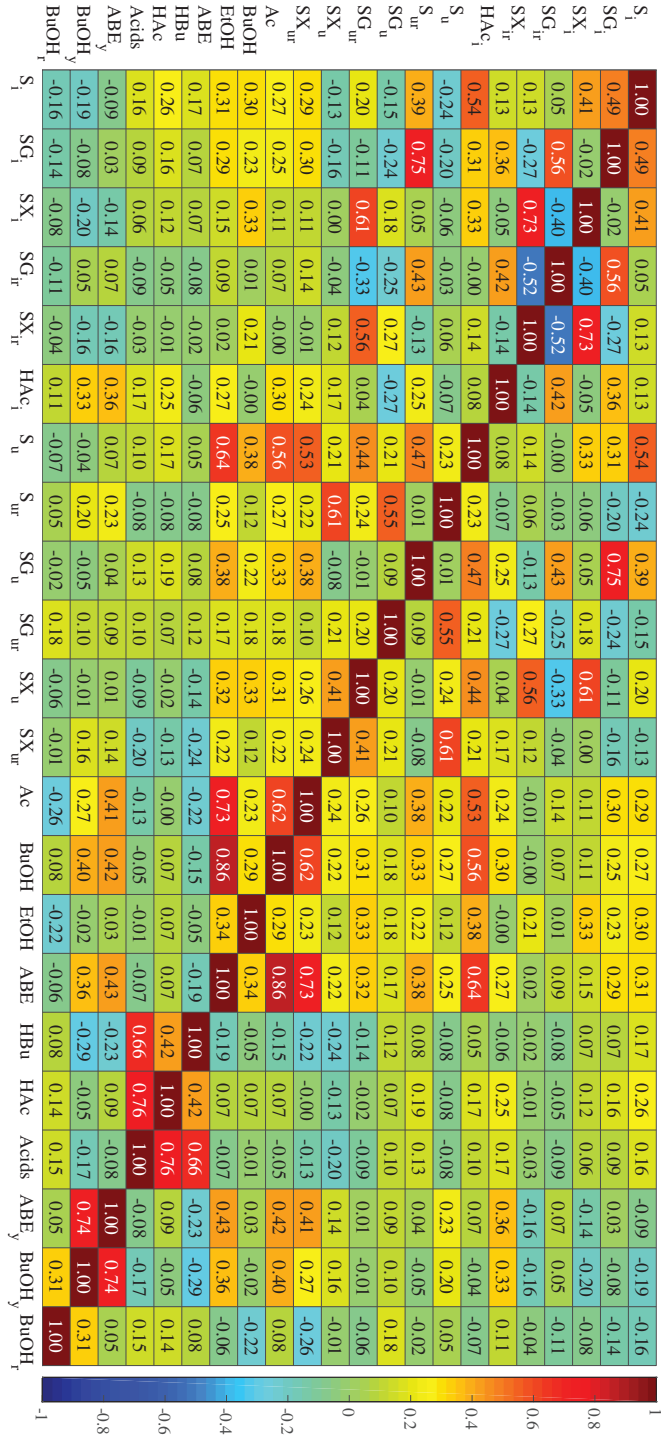


Figure 3.5: Correlations of all fermentation variables

statistically significant correlation coefficients in Figure 3.5. On the other hand, sugar utilizations (S_{ur} , SG_{ur} , SX_{ur}) (%) decrease with increasing initial total sugar (S_i) and glucose concentrations (SG_i). Even though higher sugar concentration improves fermentation to some extent, beyond some threshold, it starts to become inhibitory and this phenomenon is illustrated with negative correlation coefficients. Furthermore, correlation coefficients show that SG_{ur} decreases with increasing initial glucose ratio (SG_{ir}) with correlation coefficient value of -0.25 and increases with increasing initial xylose ratio (SX_{ir}) in the substrate with correlation coefficient value of 0.27. This seems controversial at first sight. However, high SG_{ir} is a result of high SG_i , which leads to lower glucose utilization as explained above.

CCR information is another important feature extracted from the correlations. A higher initial glucose ratio (SG_{ir}) and a lower initial xylose ratio (SX_{ir}) leads to an increasing utilized glucose concentration (SG_u) with a correlation coefficient of -0.13 for the latter. Similarly, the utilized xylose concentration (SX_u) increases with an increasing initial xylose ratio (SX_{ir}), while it decreases as the initial glucose ratio (SG_{ir}) increases with a correlation coefficient of -0.33. Therefore, both sugars repress each other's utilization due to CCR. However, the repression effect is greater from glucose to xylose ($|-0.33| > |-0.13|$) as suggested in our previous work [198].

As the correlation coefficients in Figure 3.5 indicate, all product concentrations increase with increasing initial concentrations of all sugars; acetone (Ac) and butanol ($BuOH$) concentrations are more influenced by initial glucose (SG_i) than xylose (SX_i), and SG_i has a greater influence on Ac (0.30) than on $BuOH$ (0.25). This is in line with previous work where no acetone accumulation was found during fermentation of xylose by *C. acetobutylicum* [112]. Both solvent yield (ABE_y) and butanol yield ($BuOH_y$) decrease with increasing initial xylose concentration (SX_i) and ratio (SX_{ir}), while they increase with elevated initial acetic acid concentration (HAc_i) that is often generated during pretreatment of lignocellulosic biomass. Negative correlation coefficient between xylose and yields could be because the carbon content of one xylose molecule is less than that of glucose, thus one xylose molecule has less capacity to yield products. Positive correlation between ABE_y and $BuOH_y$, and HAc_i can be due to presence of acetic acid in the beginning of fermentation facilitating solvent formation, following metabolic pathway of fermentation [15]. Another crucial performance indicator, the butanol ratio ($BuOH_r$), becomes greater as S_i , SG_i , and SG_{ir} decrease. Furthermore, all product concentrations except HBu and $EtOH$ increase with increasing HAc_i . Some researchers stated that high initial

acetic acid concentrations could facilitate acetone formation, consequently increase the acetone to butanol ratio [106]. However, the correlation coefficient between HAc_i and $BuOH$ is greater than that of HAc_i and Ac , i.e. 0.30 and 0.24, respectively. Therefore, a potential effect of initial acetic acid concentrations in the fermentation medium on product formation needs to be studied in more detail.

Correlation coefficients between utilized sugar concentrations (S_u , SX_u) and sugar utilizations (S_{ur} , SX_{ur}) are positive, indicating the more the utilized sugar concentration, the higher the utilization (%) with respect to its initial concentration. In addition, all solvent concentrations (ABE , Ac , $BuOH$, $EtOH$) increase with increasing S_u , SG_u , SX_u , S_{ur} , SG_{ur} and SX_{ur} . One exception to this trend is that there is no significant correlation between SG_{ur} and Ac . HAc is in positive correlation with and S_u and SG_u , while HBu is in negative correlation with and SX_u and SX_{ur} . Even though both acids are produced as the cells metabolize glucose and xylose, the difference in the effects of specific sugars in the metabolic pathway is apparent.

Ac and $BuOH$ concentrations decrease with increasing HBu concentration, while there is no correlation with HAc . Therefore, HBu concentration alone can be considered as a measure of fermentation completion. $EtOH$ is not correlated with any of the acids, which is in good agreement with the metabolic model developed by Shinto et al., 2008 [145].

3.4 Conclusions

This chapter presented operating conditions in terms of substrate properties together with performance indicators and product mixture properties by developing an extensive data set including information of 175 fermentations, which to the author's knowledge, is the largest collection assembled so far. The main contributions of this chapter can be stated as below:

- This is the first attempt to identify and define performance indicators for the ABE fermentation process.
- Presented substrate and product mixture properties provide a basis for fermentation process design.
- Interconnectedness between the fermentation variables was investigated for the first time by employing exploratory data analysis.

-
- Results of the exploratory data analysis were linked to individual observations presented in the research articles to provide a holistic view and a platform for discussing the usefulness of the measures applied to improve fermentation performance.
 - Exploratory data analysis revealed the effect of substrate composition and concentration on the fermentation for the first time, which was supported by other research results in the field.
 - The relationships between performance indicators provided by the data analysis can be utilized to predict fermentation performance without having to determine every variable.

By using the results and observation from this chapter, the study in the next Chapter 4 was designed. In addition, experimental conditions such as the representative sugars, their compositions and concentrations were decided accordingly.

Chapter 4

Butanol Production from Lignocellulosic Sugars in Microbioreactors

Contents of this chapter were covered in Paper VI.

4.1 Introduction

Systematic bioprocess development involving strain and cultivation optimization and testing is often needed to increase yield and productivity. These efforts require screening of strains, medium compositions, and operating conditions, which are traditionally carried out in shake flasks or microtiter plates. However, these methods have some downsides, such as the lack of online data monitoring and control [199]. Microbioreactor technology can eliminate some of these drawbacks by offering easy handling, online monitoring of key parameters and control capability, in addition to the possibility to run multiple cultures in parallel. Disposable and miniaturized versions of bench-scale bioreactors are today available for performing fermentation experiments. Moreover, such technology has the advantage of low power consumption, less space requirements, small quantities of reagents and cells per batch as well as flexibility and portability due their small size [200]. To exploit these advantages for studying fermentative butanol production, mixed sugar fermentation experiments were performed in microbioreactors. A BioLector[®] (m2p-labs GmbH, Baesweiler, Germany) instrument was used as the microbioreactor unit. The BioLector[®] is a powerful tool with proven capabilities of high-throughput fermentation with simul-

taneous online monitoring of cell mass growth (by light scattering), fluorescence, pH and dissolved oxygen (DO) [201]. To date, the BioLector[®] has not been used for the purpose of studying fermentative butanol production before. The objectives of the present chapter were therefore i) to demonstrate the possibility to use BioLector[®] for butanol production under anaerobic conditions, ii) to investigate the effect of scale and experimental setup by parallel use of BioLector[®] and serum flasks, and iii) to show the effect of different sugar mixtures on fermentation.

4.2 Materials and Methods

4.2.1 Microorganism and Medium

Clostridium beijerinckii NCIMB 8052 was used, since it is known to utilize different lignocellulosic sugars for growth and butanol production [202]. The culture was pre-grown in medium described in Section B.2.1 and under the conditions explained in Section B.4.1 in the Appendix. The fermentation medium contained 5 and 10 g/l sugar, and rest of the medium components are given in Table B.2.

In total 12 different sugar compositions at 2 different total sugar concentrations and 6 different glucose to xylose ratios were used and studied in parallel. The cultures containing 5 g/l total sugar, and glucose (G) to xylose (X) ratios of 100:0, 80:20, 60:40, 40:60, 20:80 and 0:100 are referred to as 5-G100:X0, 5-G80:X20, 5-G60:X40, 5-G40:X60, 5-G20:X80 and 5-G0:X100, respectively throughout the study. Similarly, the cultures containing 10 g/l total sugar, and glucose to xylose ratios of 100:0, 80:20, 60:40, 40:60, 20:80 and 0:100 are referred to as 10-G100:X0, 10-G80:X20, 10-G60:X40, 10-G40:X60, 10-G20:X80 and 10-G0:X100, respectively. Analysis of variance (ANOVA) was applied to test significance of the effect of sugar concentration and glucose to xylose ratio, the details are in Section B.6 in the Appendix.

4.2.2 Fermentations

Fermentations performed in microbioreactors are explained in Section B.4.3 together with the details of the online monitoring and the BioLector[®] setup was shown in Figure B.1. To benchmark the microbioreactor fermentations, fermentations were also done in serum flasks as explained in Section B.4.2. Both microbioreactor and serum flask experiments had the same mixture of medium and inoculum to prevent the errors due to medium preparation and inoculation. Experiments were terminated after 79 hours.

Samples were taken at the start and the end of the fermentations, which were analyzed by using high-performance liquid chromatography (HPLC) for quantification of sugars and butanol as described in Section B.3. Data shown represent the mean values from experiments performed in quadruples. Error bars show the standard deviation. A representation of experimental design of fermentations performed both in microbioreactors and serum flasks is shown in Figure 4.1.

4.3 Results and Discussion

4.3.1 Evaluation of Growth in BioLector[®] Microbioreactor Fermentations

All glucose contained in fermentation medium was utilized entirely in all 12 conditions. On the other hand, cultures 10-G80:X20, 10-G40:X60, 10-G20:X80, 10-G0:X100 and 5-G0:X100 had 0.040, 0.037, 0.060, 0.086 and 0.014 g/l residual xylose, respectively. Average xylose utilizations were 99.8 and 98.9% for cultures with 5 and 10 g/l total sugar.

Figure 4.2 and Figure 4.3 show online logged data of fermentations done in BioLector[®] in terms of cell mass (scattered light) and pH allowing the continuous monitoring of the growth during the course of the fermentation (79 hours). Right after the start, there occurred lag phases of approximately 1.5 hours and 1 hour for cultures containing 5 and 10 g/l total sugar, respectively, likely due to the adaptation of the cells to their new environment [166].

After the lag phase, exponential growth was observed, during which *C. beijerinckii* is known to produce acids and pH in the fermentation broth decreases as a result. At the same time, cell mass increases exponentially. Exponential growth phase was followed by a stationary growth phase during which cell mass increased at a slower rate in all cultures. Moreover, pH increased due to re-assimilation of acids to solvents. Standard deviations were considerably smaller during the exponential growth phase compared to the rest of the fermentation for both cell mass and pH values.

For the best understanding of carbon turnover and product formation, fermentation progress in standard bioreactors is followed continuously by online measurements of pH, DO, and off-gas CO₂, while cell mass, sugar and product concentrations are usually determined intermittently by offline spectrophotometry and HPLC, respectively. Such experiments are, however, laborious and costly, and the first phase of process optimization, involving

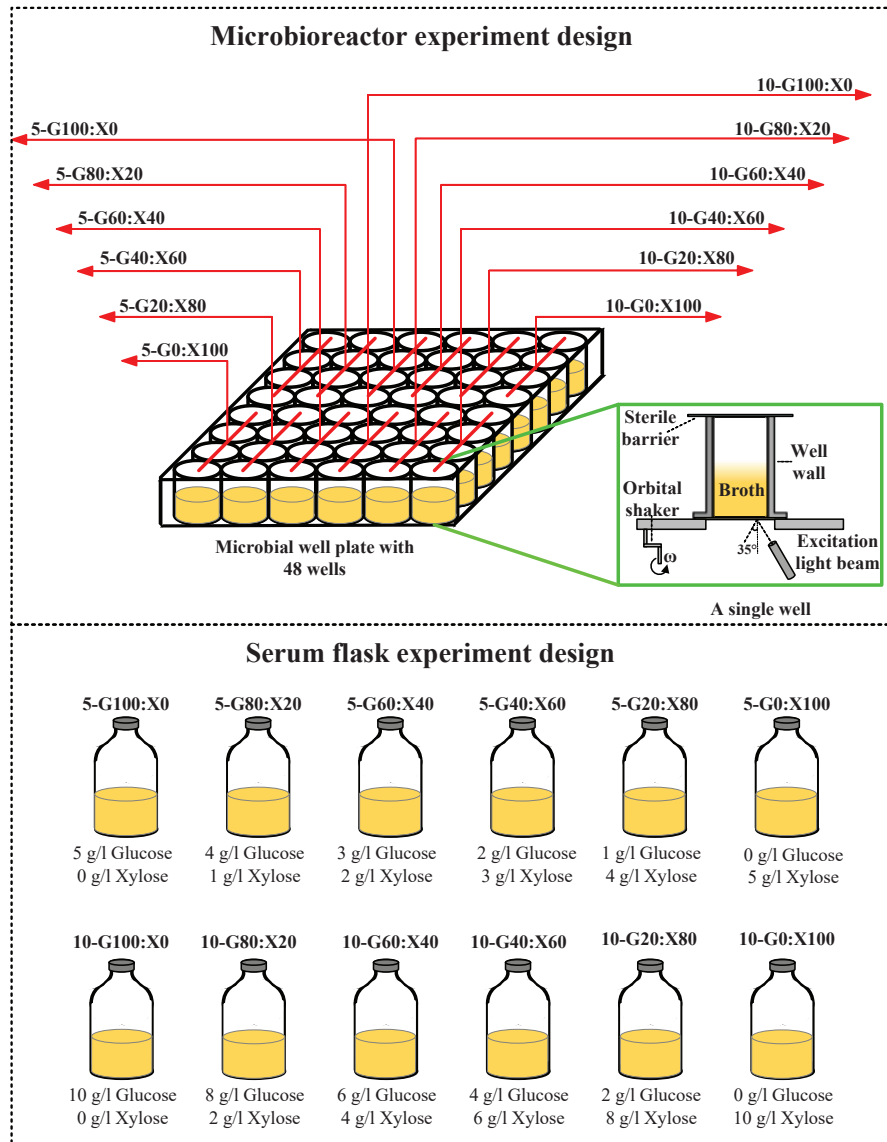


Figure 4.1: Experiment design of fermentations performed in serum flasks (top) and microbioreactors with a schematic representation of a single well (bottom).

e.g. different parameters and strains, is therefore often performed in serum flasks. The cell mass monitoring allowed the direct calculation of growth rates during cultivations, whereas the pH measurements provided online information about sugar consumption and switching of *clostridial* metabol-

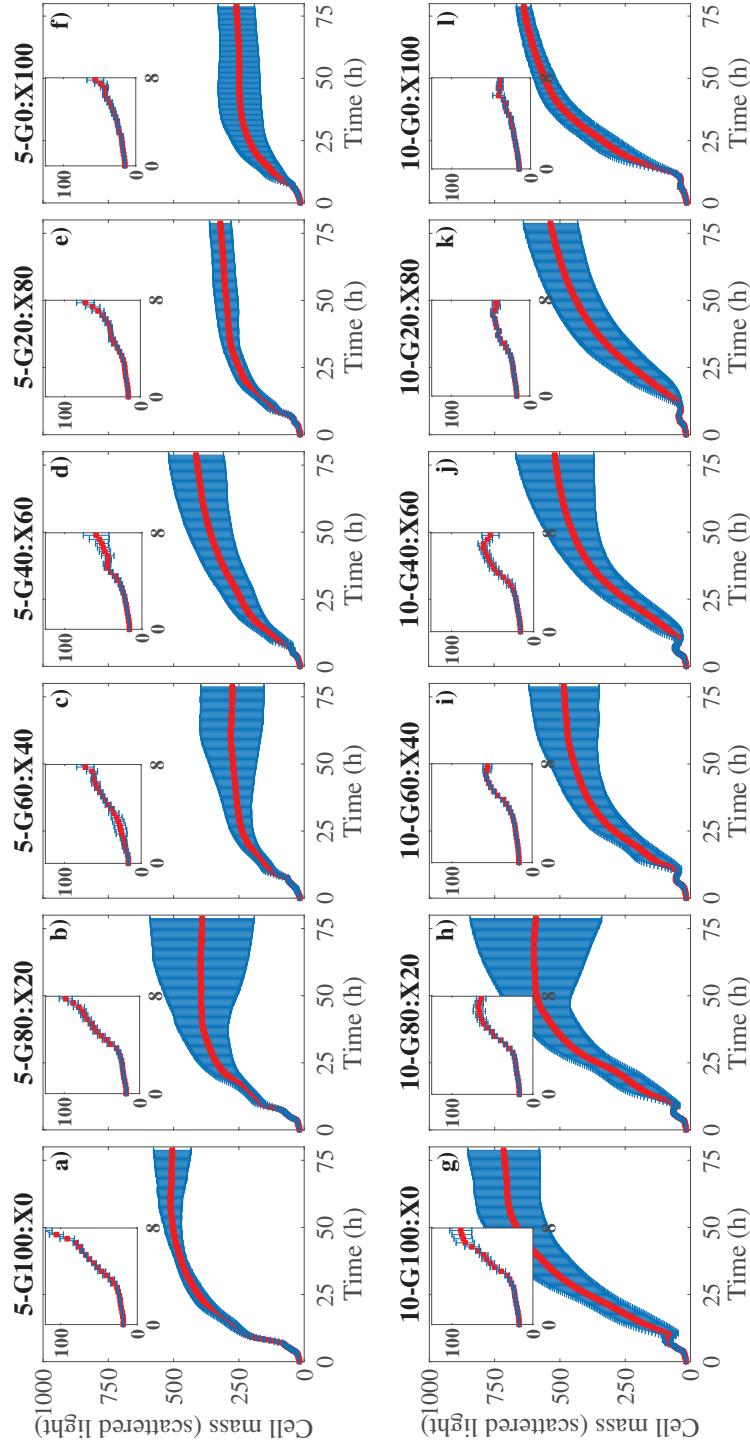


Figure 4.2: Cell mass versus time plots of fermentations done in BioLector[®] using 5 and 10 g/l total sugar and varied glucose (G) to xylose (X) ratios, a) 5-G100:X0, b) 5-G80:X20, c) 5-G60:X40, d) 5-G40:X60, e) 5-G20:X80, f) 5-G0:X100, g) 10-G100:X0, h) 10-G80:X20, i) 10-G60:X40, j) 10-G40:X60, k) 10-G20:X80, and l) 10-G0:X100. Mean values of the 4 replicates are shown together with error bars representing standard deviation, and the magnified parts of each subplot placed on top left corner.

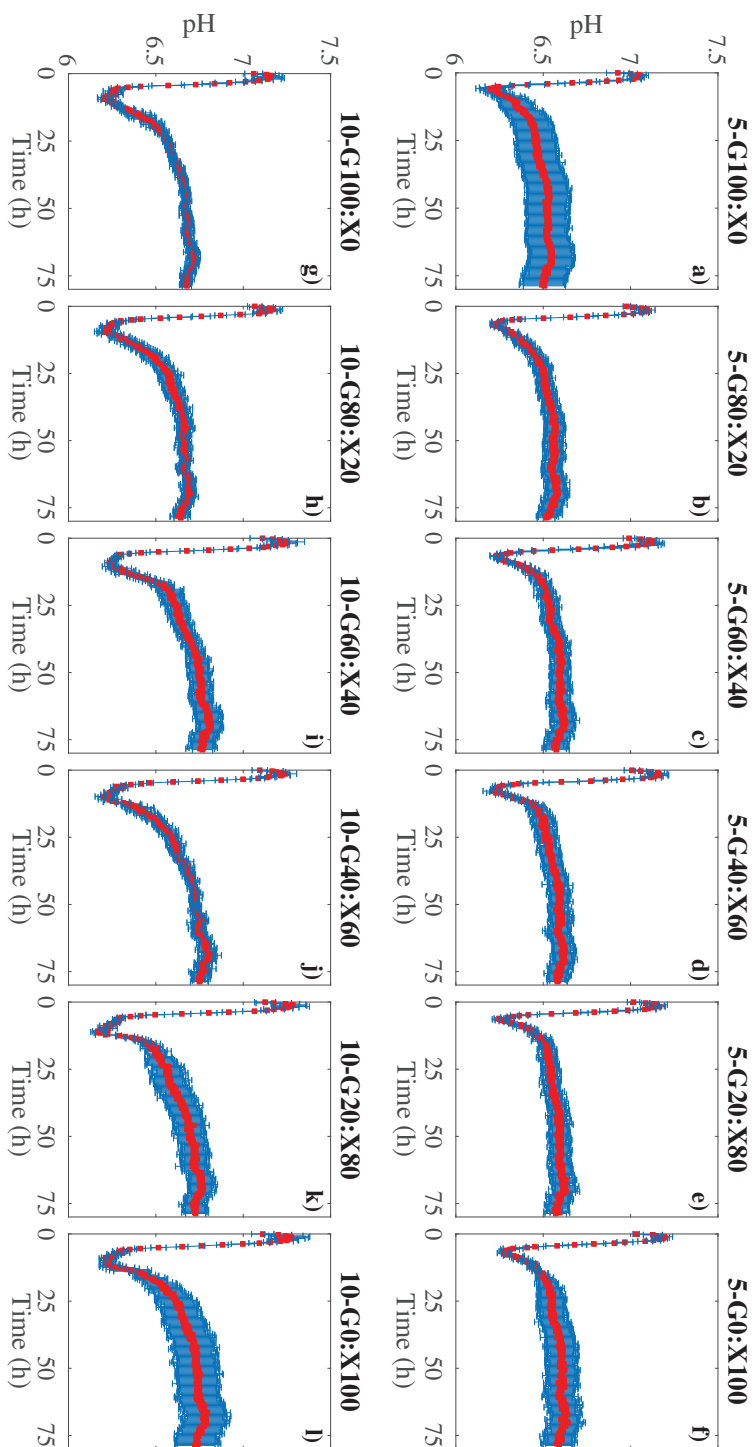


Figure 4.3: pH plots of fermentations done in BioLector[®] using 5 and 10 g/l total sugar and varied glucose (G) to xylose (X) ratios, a) 5-G100:X0, b) 5-G80:X20, c) 5-G60:X40, d) 5-G40:X60, e) 5-G20:X80, f) 5-G0:X100, g) 10-G100:X0, h) 10-G80:X20, i) 10-G60:X40, j) 10-G40:X60, k) 10-G20:X80, and l) 10-G0:X100. Mean values of the 4 replicas are shown together with error bars representing standard deviation.

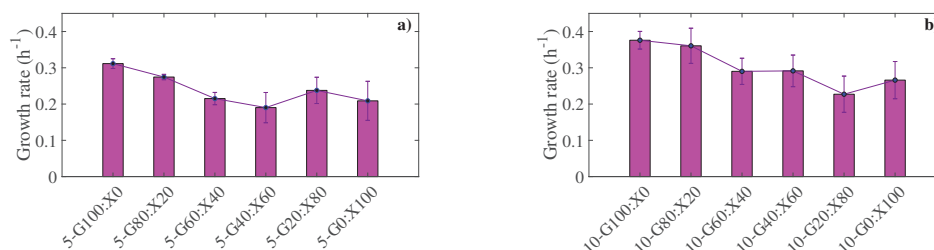


Figure 4.4: Growth rate (h⁻¹) values during exponential growth for all 12 experiments done in the BioLector[®] setup were determined from the BioLector[®] online data.

ism from acetogenic to solventogenic phase. This represents an improvement over standard offline measurement methods in the evaluation of *clostridial* fermentations, even though off-gas CO₂, sugars and product concentrations are still not measured online.

Figure 4.4 shows that growth rate (h⁻¹) values were greater for cultures with 10 g/l total sugar. Average growth rate values for cultures containing 5 and 10 g/l were 0.240 and 0.302 h⁻¹. However, the change in growth rate with respect to glucose to xylose ratio exhibited the opposite trend for ratios of G100:X0, G80:X20 and G60:X40. Highest and lowest growth rates were 0.376 and 0.190 h⁻¹ observed for 10-G100:X0 and 5-G40:X60 cultures.

For experiments done in BioLector[®], all cultures containing xylose had a slower growth rate than the cultures with glucose as the sole sugar, essentially due to glucose being the preferred carbon source over xylose and the effect of CCR [97]. Therefore, the results in this section confirm that cell mass growth was affected by CCR during the fermentation by *C. beijerinckii* NCIMB 8052. The growth rate decreased with decreasing glucose ratio in the medium and increased while xylose was the sole sugar (G0:X100) compared to G20:X80 cultures. This trend can be assigned to interaction between sugars which is discussed in detail in the following sections in this thesis. The standard deviation values of cell mass data increased significantly in stationary phase compared to exponential growth phase as shown in Figure 4.4. Different glucose to xylose ratios resulted in different standard deviations as well. The reason can be the changes in the morphology of cells affecting the online cell mass monitoring in the BioLector[®] unit [203, 204], since *Clostridia* are known to go through morphological changes during fermentation [205], and variation of standard deviation might indicate that the sugar composition affects the morphology of the cells. The same trend was observed for online logged pH data; standard deviations were greater when the cultures reached the stationary phase. A side study was done to

investigate if any particular replicas deviated from the mean value due to its location on the well plate; however, no obvious correlation was obtained, and further systematic examination is required to rule out potential position effects. The sugar ratio also had impact on butanol concentration and yield, which were inversely proportional with the growth rate. These results are in accordance with a previous study, which showed that a higher growth rate results in a lower butanol concentration, since sugars were used for cell mass growth and not for butanol production [206].

4.3.2 Comparison of Fermentations Performed in Microbioreactors and Serum Flasks

A comparative overview of the results for serum flask and microbioreactor setups are provided in this section. In serum flasks experiments, both glucose and xylose contained in fermentation medium was utilized entirely in all 12 conditions, while there was residual xylose in microbioreactor experiments as given in the results above. Butanol concentration (g/l) and butanol yield (g butanol/g sugar) values of all were shown in Figure 4.5.

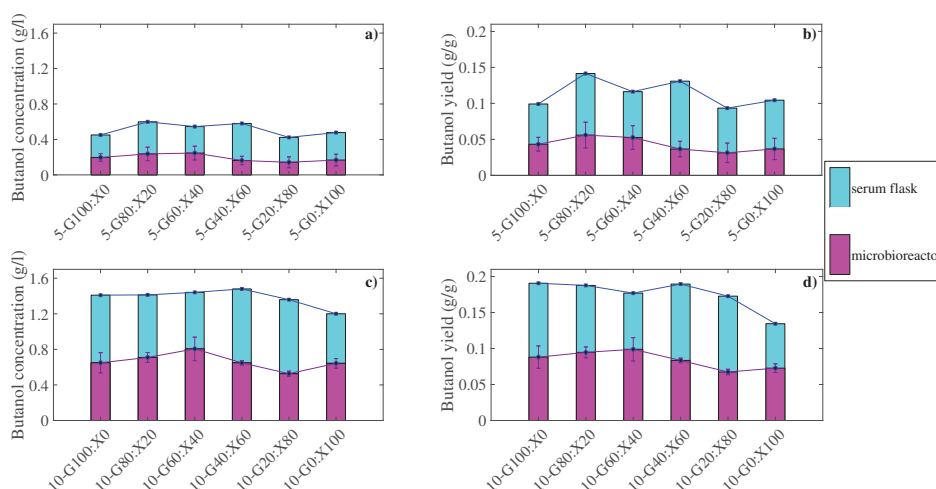


Figure 4.5: Butanol concentration a) and c), and butanol yield b) and d) values of fermentations done in BioLector[®] and serum flasks with 5 and 10 g/l total sugar, respectively. Mean values of the 4 replicas are shown together with error bars representing standard deviation for BioLector[®] results.

Figure 4.5 shows that butanol concentrations and yields were greater for cultures containing 10 g/l total sugar for all 6 different glucose to xylose ratios in both setups. For BioLector[®], average butanol concentration and

butanol yield values of 6 experiments with 5 and 10 g/l were 0.192 and 0.664 g/l, 0.043 and 0.084 g/g, respectively. Both butanol concentrations and yields increased with increasing xylose ratios from 0 to 40, decreased when xylose ratio increased from 40 to 80, and increased again when the ratio was G0:100X for cultures with 5 and 10 g/l total sugar. Highest butanol concentration and butanol yield were 0.806 g/l and 0.099 g/g achieved in the 10-G60:X40 culture, while lowest values 0.142 g/l and 0.031 g/g were observed in 5-G20:X80.

For serum flask setup, average butanol concentration and butanol yield values of 6 experiments with 5 and 10 g/l were 0.513 and 1.384 g/l, 0.114 and 0.176 g/g, respectively. Therefore, higher total sugar resulted in a higher butanol production and yields, which agrees with the results obtained in BioLector[®] fermentations. Highest butanol concentration and butanol yield were 1.480 g/l and 0.190 g/g, achieved in the 10-G40:X60 culture, while lowest values were 0.422 g/l and 0.093 g/g observed in 5-G20:X80, which coincide with results of BioLector[®] as well.

Comparison of fermentations performed in microbioreactors and serum flasks can provide important insight for scale up studies. Growth rates estimated using online logged cell mass data of BioLector[®] were in the range of 0.190-0.312 h⁻¹ for the cultures with 5 g/l total sugar, which is lower than the range of 0.681-1.076 h⁻¹ obtained in Chapter 6 for experiments done in serum flasks using the same sugar concentration and strain. Similarly, the average growth rate of 0.240 h⁻¹ in microbioreactors was 70% lower than the value of 0.819 h⁻¹ acquired in serum flasks. Different growth rate values obtained in microbioreactors and serum flasks can be explained by the difference in cell mass measurement methods. A study comparing shake flasks and BioLector[®] microbioreactors showed that cell mass measurements in BioLector[®] (scattered light intensity) and measurements with photometer (optical density) were in good agreement for the growths of *E. coli* and *K. lactic*. Contrarily, cell mass values for growth of *G. oxydans* differed greatly, which was explained by the morphological changes [204]. Therefore, it is important to have good knowledge about the physiology of the strain used when comparing different experimental setups with different monitoring units.

The effect of sugar ratio on butanol concentration and yield were not as distinguishable for fermentations done in serum flasks as for the microbioreactor fermentations. However, highest butanol productions and yields were observed in 10-G60:X40 and 10-G40:X60 cultures, while lowest values observed in 5-G20:X80 cultures in both experimental setups. Average

butanol concentration and butanol yield values of 0.428 g/l and 0.063 g/g were 54.9% and 56.5% lower in microbioreactors than in serum flask fermentations with average values of 0.948 g/l and 0.145 g/g. Even though butanol concentrations were low due to low sugar concentrations used in the fermentations of this chapter, average butanol yield value obtained in serum flasks is comparable with the butanol yield found as 0.198 g/g in the exploratory data analysis performed by using data of 79 fermentations with lignocellulosic sugars as discussed in Chapter 3. The agreement in butanol yield values is noteworthy, since it is a measure of cells' efficiency to convert substrate to desired product. Even though same inoculated media were used in microbioreactors and serum flasks to have identical starting conditions, there were significant deviations in butanol concentration and butanol yield values, which can be related to the differences in experimental setups. Microbial well plates in microbioreactor setup was continuously shaken and flushed with nitrogen to ensure and anaerobic conditions. This might have caused stripping effect for the volatile components present in fermentation broth, since gas stripping is a commonly applied method for butanol removal [35]. Although an evaporation-limiting layer was used, it might still be permeable to butanol fume. On the other hand, serum flask fermentations were performed under static conditions without any gas flow through the flasks. Moreover, flasks were sealed with rubber stoppers to sustain anaerobic conditions and the stoppers were taken off when the experiments were terminated. Therefore, gas stripping effect was not prevailing as in microbioreactors, which resulted in a greater average butanol concentration, thus average butanol yield.

A two-way ANOVA was used to assess if the effect of changing total sugar concentrations and glucose to xylose ratios on fermentation were significant. Two tests were performed for fermentations done in BioLector[®] and in serum flasks, p values are given in Table 4.1 and Table 4.2, respectively.

Table 4.1: p values obtained from ANOVA for fermentations done in BioLector[®].

	Butanol concentration (g/l)	Butanol yield (g/g)	Specific growth rate (h⁻¹)
Total sugar concentration (g/l)	1.54E-08	1.54E-08	3.71E-05
Sugar ratio (g/g)	0.00063	0.00025	2.88E-05

Table 4.1 shows that both total sugar concentration (g/l) and glucose to xylose sugar ratio have significant effect on butanol concentration (g/l), butanol yield (g butanol/g sugar) and growth rate (h^{-1}), since all the p values are smaller than the set limit of 0.05. It is important to note that the effect of total sugar concentration on butanol concentration (g/l) and butanol yield (g butanol/g sugar) were greater than that of sugar ratio with p values of 1.54E-08 and 1.54E-08, and 0.00063 and 0.00025, respectively. On the other hand, significance of effects for total sugar concentration and sugar ratio were very similar for specific growth rate with p values of 3.71E-05 and 2.88E-05, respectively. Therefore, specific growth rate was equally sensitive to both factors.

Table 4.2: p values obtained from ANOVA for fermentations done in serum flasks.

	Butanol concentration (g/l)	Butanol yield (g/g)
Total sugar concentration (g/l)	1.54E-08	1.54E-08
Sugar ratio (g/g)	0.00063	0.00025

Table 4.2 shows that the effects of total sugar concentration on butanol concentration and butanol yield were significant with p values smaller than 0.05. Nevertheless, sugar ratio did not have a significant effect. An in-depth metabolic study would be useful to investigate the effects of carbon sources on *C. beijerinckii* NCIMB 8052.

4.4 Conclusions

Fermentations of glucose and xylose at 6 different ratios and 2 different total sugar concentrations were done by *C. beijerinckii* NCIMB 8052 in microbioreactors and serum flasks to demonstrate the possibility to use BioLector[®], to investigate the effect of scale and experimental setup, and to show the effect of different sugar mixtures on fermentation. The main contributions of this chapter are summarized below:

- All cultures could be successfully grown in the BioLector[®] system under anaerobic conditions, metabolized both glucose and xylose, and produced butanol.

- The online monitoring of cell mass and pH in the BioLector[®] enabled following the progress of the fermentations at unprecedented time-resolution.
- Growth rate, butanol production and butanol yield values were 70.7, 54.9 and 56.6% lower, respectively in microbioreactors compared to serum flasks experiments.
- Glucose to xylose ratio affects both growth and production.

In conclusion, the information obtained in this chapter will support further research in bioreactor and bioprocess design and scale-up, which are very important aspects of industrial fermentations of lignocellulosic biomass.

Chapter 5

Effect of Pre-growth Conditions on Fermentation

Contents of this chapter were covered in Paper II.

5.1 Introduction

Fermentative butanol production faces feedstock availability and low yield problems, and lignocellulosic biomass is a favorable feedstock, which can help to tackle those problems as discussed in Chapter 2. Even though lignocellulosic sugars is a mixture of pentose and hexose sugars, current methodologies still mainly focus on the fermentation of hexose sugars, mainly glucose, while discarding the rest of the feedstock or using it as a source for process energy. Therefore, full exploitation of all the sugars bound in lignocellulosic biomass can contribute to solving the low yield problem. However, the cells' efficiency at utilizing different sugars in mixed form tends to decrease due to Carbon Catabolite Repression as thoroughly explained in Section 2.3.

Developing strains capable of co-utilizing hexose and pentose for butanol production by metabolic engineering is an active research topic [75, 97, 98, 118, 119]. Even though Lee et al. (2016) [2] stated metabolic engineering is required for simultaneous utilization of sugars, researchers have developed pre-growth strategies achieving co-utilization without any strain manipulation [60, 120–125]. The suggested pre-growth methods comprised of subjecting a culture to a less favorable carbon source, mostly sole xylose for early activation of its utilization pathway. When a mixture of a sugars, usually

glucose and xylose, was then added to the fermentation medium, the culture pre-grown on xylose could simultaneously utilize them. In the light of these findings, the objective was defined as: i) understanding the effect of the feeding strategy on fermentation of glucose and xylose mixtures, and ii) developing a feeding strategy to tackle CCR and sequential utilization problems without having to manipulate the strain.

5.2 Materials and Methods

5.2.1 Microorganism and Medium

Clostridium beijerinckii NCIMB 8052 was used. The culture was pre-grown in medium described in Section B.2.1 and under the conditions explained in Section B.4.1. The fermentation medium contained 5 g/l sugar, and rest of the medium components are given in Table B.2.

5.2.2 Fermentations

Fermentations were performed under the conditions as explained in Section B.4.4. There were two fermenters: one had only xylose (G0:X100) as the initial sugar (fermenter 1) and the other one had only glucose (G100:X0) (fermenter 2). Mixtures of glucose and xylose were fed to fermenter 1 by gradually increasing the glucose (G) to xylose (X) ratio in the feed G20:X80, G40:X60, G60:X40, G80:X20 and G100:X0. Similarly, mixtures were fed to fermenter 2 by gradually decreasing the glucose (G) to xylose (X) ratio in the feed G80:X20, G60:X40, G40:X60 and G20:X80. Total sugar concentration in the fermenters were kept at 5 g/l so that the sugar utilization patterns could be clearly observed. Liquid level in the fermenters were kept constant by using concentrated sugar solutions and removing equal amounts as feed during sampling to reduce dilution effects. Samples were taken to follow the progress of the fermentations, which were analyzed by using high-performance liquid chromatography (HPLC) for quantification of sugars and butanol as described in Section B.3.

5.3 Results and Discussion

5.3.1 Progress of Fermentations

Progress of fermentation started with xylose as the initial sugar is shown in Figure 5.1 in terms of the amounts of the sugars fed and consumed, and productions of cell mass and butanol. The first feed containing xylose

(G0:X100) as the sole sugar was consumed within 6 hours with rate of 0.67 g/l.h^{-1} , and cell mass concentration increased exponentially in the first feed interval (0-6 hours).

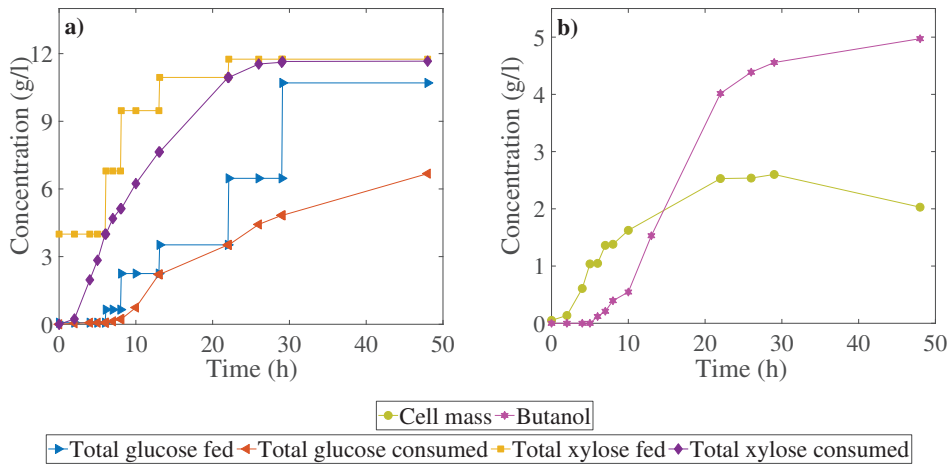


Figure 5.1: Glucose and xylose a), and butanol and cell mass b) profiles for fermenter 1 with xylose as the initial sugar.

The second feed to fermenter 1 was a mixture of 20% glucose and 80% xylose, G20:X80. In the second feed interval (6-8 hours), glucose and xylose were co-utilized at rates of 0.12 and 0.63 g/l.h^{-1} , respectively. Cell mass concentration increased steadily, and butanol was detected first after 7 hours. The third feed contained 40% glucose and 60% xylose, G40:X60, which were co-utilized at 0.40 and 0.50 h^{-1} . Cell mass growth rate decreased, while butanol production rate reached 0.33 g/l.h^{-1} . At 13 hours, the fourth feed with 60% glucose and 40% xylose, G60:X40 was fed to fermenter 1, and sugars were simultaneously utilized as well at rates of 0.64 and 0.37 g/l.h^{-1} . Butanol production rate was the same as in the third feed interval and its concentration became 3.98 g/l , and cell mass continued to increase steadily. The fifth feed consisting of 80% glucose and 20% xylose, G80:X20 was fed at hour 22. Even though co-utilization was observed again, glucose and xylose consumption rates decreased to 0.19 and 0.10 g/l.h^{-1} , respectively. There was no apparent change in cell mass concentration, while butanol production rate decreased to 0.08 g/l.h^{-1} . In the sixth feed interval, feed contained only glucose (G100:X0), with the slowest utilization rate of 0.097 g/l.h^{-1} observed in fermenter 1. Cell mass concentration decreased due to decay phase, and butanol concentration increased to 4.98 g/l . 11.7 g/l xylose was fed in total and all of it was consumed, while 10.7 g/l glucose was

fed and 4 g/l remained in fermenter 1. Fermenter 1 terminated after 48 hours with respect to start of the fermentation determined by off-gas CO₂ monitoring.

Progress of fermentation 2, with glucose as the initial sugar is shown in Figure 5.2 in terms of the amounts of the sugars fed and consumed, and productions of cell mass and butanol. The first feed containing glucose (G100:X0) as the sole sugar was consumed within 5 hours with respect to the start of the fermentation. In the first feed interval, glucose utilization rate was 0.75 g/l.h⁻¹, and cell mass growth was exponential.

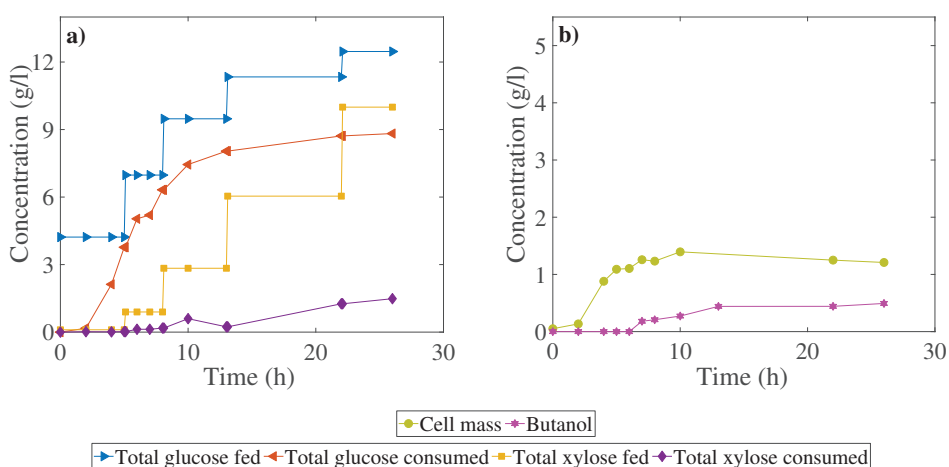


Figure 5.2: Glucose and xylose a), and butanol and cell mass b) profiles for fermenter 2 with glucose as the initial sugar.

The second feed with 80% glucose and 20% xylose, G80:X20 was fed to fermenter 2 at time 5 hours. Steady growth was observed for cell mass, and glucose and xylose utilization rates were 0.85 and 0.05 g/l.h⁻¹ in the second feed interval. Butanol was detected for the first time at 7 hours. 60% glucose and 40% xylose, G60:X40 was the third feed to fermenter 2. There was an apparent co-utilization of sugars, steady growth of cell mass and butanol production in the third feed interval. The fourth feed contained 40% glucose and 60% xylose, G40:X60, which were co-utilized at 0.075 and 0.114 g/l.h⁻¹. Cell mass concentration decreased and butanol production became very low. In the fifth feed interval of fermenter 2, sugar utilization rates decreased drastically, cell mass decay continued and a small butanol production was observed. In total, 12.47 g/l glucose was fed to fermenter 2 of which 8.822 g/l was consumed. 9.996 g/l xylose was fed of which 1.485 g/l was consumed. Final butanol concentration was 0.5 g/l in fermenter 2.

Fermenter 2 terminated after 26 hours with respect to start of the fermentation.

5.3.2 Kinetic Coefficients

Maximum specific growth rate, μ_{max} , cell mass yield on sugar, $Y_{X/S}$, butanol yield on sugar, $Y_{B/S}$, butanol yield on cell mass, $Y_{B/X}$, glucose utilization, SG_{ur} , xylose utilization, SX_{ur} and total sugar utilization, S_{ur} were the kinetic coefficients used to compare the two fermentations. The coefficients, determined as described in Section B.7 for fermenter 1 and fermenter 2, are shown in Table 5.1.

Table 5.1: Kinetic coefficients for fermenter 1 and fermenter 2.

Kinetic coefficient	Fermenter 1	Fermenter 2
μ_{max} (h^{-1})	0.68	0.94
$Y_{X/S}$ (g/g)	0.1	0.12
$Y_{B/S}$ (g/g)	0.28	0.05
$Y_{B/X}$ (g/g)	2.8	0.42
SG_{ur} (%)	62	71
SX_{ur} (%)	100	1
S_{ur} (%)	81	46

Maximum specific growth rate, μ_{max} , 0.94 h^{-1} and cell mass yield on sugar, $Y_{X/S}$, $0.12 \text{ g butanol/g sugar}$ were higher in fermenter 2 than in fermenter 1 with μ_{max} value of 0.68 h^{-1} and $Y_{X/S}$ value of $0.1 \text{ g cell mass/g sugar}$. In fermenter 1, butanol yield on sugar, $Y_{B/S}$ and butanol yield on cell mass, $Y_{B/X}$ were $0.28 \text{ g butanol/g sugar}$ and $2.8 \text{ g butanol/g cell mass}$, respectively, while they were 0.05 g/g and 0.42 g/g in fermenter 2. All xylose fed to fermenter 1 was utilized while only a small amount of the total fed xylose was utilized in fermenter 2; therefore, total xylose utilization, SX_{ur} was 100% in fermenter 1, and 1% in fermenter 2. On the contrary, total glucose utilization, SG_{ur} was higher in fermenter 2 with a value of 71% than 62% obtained in fermenter 1. Total sugar utilization was greater in fermenter 2, 81%, than in fermenter 1, 46%.

As Table 5.1 shows, fermenter 1 was superior to fermenter 2 by means of total sugar and xylose utilizations, butanol concentration and butanol yield. Even though glucose is the preferred carbon source for *Clostridia*, having only xylose in fermenter 1 as the initial sugar obviously activated the xylose metabolism. Therefore, mixtures of glucose and xylose were fed, sugars were co-utilized. Results of fermenter 2 confirm this observation, since it had glucose as the initial sugar, and glucose utilization was prominent when sugar mixtures were fed. Faster growth of cell mass in fermenter 2 was due to rapid glucose consumption, which resulted in a greater cell mass concentration, thus higher cell mass yield, $Y_{X/S}$ compared to fermenter 1. Even though high cell mass density is desirable to achieve high butanol productivity, an earlier study showed that higher growth rate results in a lower butanol concentration, since more sugar was used for cell mass growth and not for butanol production [206].

There has been different approaches to improve utilization of sugars in mixed form by tackling Carbon Catabolite Repression. Metabolic engineering targeted disrupting the genes responsible for CCR and overexpression of genes responsible for xylose transport and catalytic enzymes [75,77,118,119] which resulted in better utilization of xylose and higher butanol production. Even though engineered strains have shown improved performance compared to their wild type strains, researchers have developed pre-growth strategies achieving co-utilization without any manipulation [60,104,120–124]. To compare these two approaches, utilized glucose, xylose and arabinose concentrations (g/l), SG_u , SX_u and SA_u , butanol yield on sugar (g/g), $Y_{B/S}$ and butanol concentration (g/l), $BuOH$ values are summarized in Table 5.2.

Butanol yield (0.28 g/g) was the highest in fermenter 1 compared to all other mixed sugar fermentations. Reported values in Table 5.2 show the results of batch fermentations, while fermenter 1 and fermenter 2 were operated in fed-batch mode by keeping the total sugar concentration in the broth (10 g/l) relatively low compared to common practice (60 g/l). Combined effects of the operating mode and limited sugar concentration might have also promoted better sugar utilization and higher butanol production.

In addition to the effect of initial sugar fed to the fermenter or present in the pre-growth medium, glucose to xylose ratio has an influence on fermentation kinetics. Both in fermenter 1 and fermenter 2, glucose utilization increased with increasing glucose ratio in the feed and vice versa for xylose.

Table 5.2: Comparison of results with previous studies.

Strain	SG_u (g/l)	SX_u (g/l)	SA_u (g/l)	$Y_{B/S}$ (g/g)	$BuOH$ (g/l)	Ref.
<i>C. beijerinckii</i> NCIMB 8052	6.70	17.70	-	0.28	4.98	Ferm.1
<i>C. beijerinckii</i> NCIMB 8052	8.80	1.50	-	0.05	0.50	Ferm.2
<i>C. beijerinckii</i> NCIMB 8052	7.18	20.30	3.50	0.22	6.80	[119]
<i>C. beijerinckii</i> NCIMB 8052xylR	7.18	29.30	7.40	0.25	10.82	[119]
<i>C. beijerinckii</i> NCIMB 8052xylR-xylT _{ptb}	7.18	33.60	8.70	0.23	11.27	[119]
<i>C. beijerinckii</i> SE-2	20.20	19.80	-	0.18	7.30	[126]
<i>C. beijerinckii</i> SE-2	21.10	20.60	-	0.17	7	[126]
<i>C. beijerinckii</i> SE-2	20	18.50	-	0.21	8	[126]
<i>C. acetobutylicum</i> ATCC 824	19	2.60	-	0.12	2.50	[118]
<i>C. acetobutylicum</i> ATCC 824	28	6.40	-	0.19	6.40	[118]
<i>C. acetobutylicum</i> ATCC 824	41	7.30	-	0.18	8.80	[118]
<i>C. acetobutylicum</i> ATCC 824-tal	19	13	-	0.18	5.80	[118]
<i>C. acetobutylicum</i> ATCC 824-tal	28	11	-	0.19	7.50	[118]
<i>C. acetobutylicum</i> ATCC 824-tal	41	9	-	0.18	8.80	[118]
<i>C. acetobutylicum</i> ATCC 824	33	30	-	0.19	12.05	[97]
<i>C. acetobutylicum</i> ATCC 824 (glucose pre-grown)	35	4	-	0.13	5	[121]
<i>C. acetobutylicum</i> ATCC 824 (xylose pre-grown)	34	15	-	0.17	8.50	[121]
<i>C. acetobutylicum</i> ATCC 824 (glucose & xylose pre-grown)	36	35	-	0.23	16.60	[104]
<i>C. acetobutylicum</i> ATCC 824 (glucose pre-grown)	52	10	-	0.23	14.30	[104]
<i>C. acetobutylicum</i> ATCC 824 (xylose pre-grown)	25	43	-	0.22	14.60	[104]

Both metabolic engineering and pre-growth strategies provide improvement in terms of co-utilization of sugars in mixed form. However, simultaneous utilization alone does not guarantee that CCR was tackled. A recent transcriptional study showed that during fermentation of glucose and xylose to produce butanol by *C. beijerinckii* SE-2, glucose inhibition on xylose metabolism-related genes were still present even though the sugars were co-utilized [126].

5.4 Conclusions

Effects of different feeding strategies on fermentation were studied to cope with CCR and sequential utilization problems. Main findings of this chapter are summarized below:

- Fermenter 1 with only xylose as the initial carbon source could co-utilize sugars for all mixed sugar feeds, while fermenter 2 with only glucose as the initial sugar suffered from sequential utilization.
- Xylose in fermenter 2 accumulated while glucose was present; its utilization became apparent only after the glucose was completely exhausted.
- Total sugar utilization, butanol concentration and butanol yield on sugar were greater for fermenter 1, while specific growth rate of cell mass and cell mass yield on sugar were higher for fermenter 2.

The effect of the sugar type in the initial growth medium on fermentation was prevailing. Transcriptional studies need to be performed to understand in depth if CCR is active or not, as well as to understand the co-utilization mechanism for improvement of the proposed feeding approach. Observations and findings of this chapter created a motive for further investigation of mixed sugar utilization and were employed for development of a two-stage pre-growth strategy in Chapter 6.

Chapter 6

Modelling The Binary Substrate Growth

Contents of this chapter were covered in Paper I and Paper III.

6.1 Introduction

In the previous chapter, it was shown that the exposure of active cells to xylose as the sole carbon source enhanced utilization of sugars in mixed form and avoided the sequential utilization problem. However, co-utilization alone does not guarantee that CCR was inactive [126]. Therefore, the limited quantitative knowledge about the effect and extend of CCR on mixed sugar utilization remains as a bottleneck, and indicates the importance of studying the growth on mixed sugars to elucidate the synergic effects stressed by earlier studies [207]. This bottleneck is targeted in this chapter by using *Response Surface Methodology* (RSM). RSM is a statistical tool, which includes an experimental design with a minimum number of experiments and builds a model that can predict the interaction and correlation between a set of independent variables and responses [208].

Even if it is apparent that there is interaction between the sugar utilization paths, the type of interaction would remain unknown, and successful design of lignocellulosic fermentation processes requires the kinetic model for accurately predicting the cell mass growth. Therefore, objectives of this chapter are i) to apply RSM to understand the utilization of xylose and glucose as representative lignocellulosic sugars, and ii) to develop a model describing the cell mass growth as well as the interaction between the sugars.

6.2 Materials and Methods

6.2.1 Microorganism and Medium

Clostridium beijerinckii NCIMB 8052 was used. A two-stage pre-growth strategy was applied based on Chapter 5. First, the culture was pre-grown in medium described in Section B.2.1 and under the conditions explained in Section B.4.1. Then, the culture was pre-grown on a medium containing 5 g/l xylose and components given in Table B.2. After the second pre-growth in the xylose containing medium, experiments started in fermentation media containing different amounts of glucose and xylose according to Table 6.1. The rest of the medium components are listed in Table B.2.

6.2.2 Fermentations

Fermentations were performed in serum flasks as explained in Section B.4.2. 2 ml samples were taken every 2 hours from the start of the experiments until the end of the exponential growth phase. Optical density (OD) was used as a measure for cell mass concentration, explained in Section B.3.

6.2.3 Design of Experiments

A circumscribed central composite (CCC) design for 2 factors, glucose and xylose concentrations was used for designing the experiment. CCC design resulted in 16 experimental runs with 8 of them in the centre point to reduce the effects of correlations between the factors. Further explanation about CCC design can be found in Section B.8. Minimum and maximum values of factors were chosen as 1 g/l and 4 g/l, then real values for each experiment were obtained according to the coded levels of the respective CCC design, which are shown together in Table 6.1.

Table 6.1: Real and coded values of circumscribed central composite design for 2 factors.

Factor	Symbol	Coded				
		-1.4142	-1	0	1	1.4142
Glucose (g/l)	X_1	1	1.4393	2.5000	3.5606	4
Xylose (g/l)	X_2	1	1.4393	2.5000	3.5606	4

6.2.4 Model Fitting

A quadratic linear model was fitted with the experimental data obtained. R-squared value was used to assess the quality of the fit. p value for F-statistic and p value for t-statistic were used to assess significance of linear regression model and model coefficients, respectively. Details can be seen in Section B.9.1 in the Appendix.

Binary substrate growth models were fitted with the experimental growth data by using Levenberg-Marquardt nonlinear least squares algorithm. Sum of squared error (SSE) was used to assess the quality of the fit. 95% confidence intervals for the model parameters were obtained by using the covariance matrix, which is then converted to correlation matrix. Raw residuals were used to visualize the difference between the simulated and observed values of the growth rate. Details can be seen in Section B.9.2 in the Appendix.

6.3 Results and Discussion

6.3.1 Characterization of the Growth on Mixtures of Glucose and Xylose

Table 6.2 shows resulting response values (specific growth rates) estimated as shown in Section B.7 for each experiment together with the factor levels (sugar concentrations) defined by CCC design.

The experimental data given in Table 6.2 were fitted to the model, Equation B.19 presented in the Appendix by linear regression given in Section B.9.1. Model fitting resulted in Equation 6.1 with the actual variables (glucose and xylose concentrations) and the predicted response (growth rate).

$$\begin{aligned} \text{Growth rate} = & 0.0178 + 0.6073 \times \text{Glucose} + 0.0486 \times \text{Xylose} \\ & - 0.0585 \times \text{Glucose}^2 + 0.0498 \times \text{Xylose}^2 \\ & - 0.1266 \times \text{Glucose} \times \text{Xylose} \end{aligned} \quad (6.1)$$

Fit results provided insight into the quality of the fit. The R-squared value was 0.939, which means that the model can explain 93.9% of the variability in the response variable, growth rate, while 6.1% of the variability cannot be represented by this model. The p value for F-statistic for the model was 8.83e-06 indicating that the model was significant.

Table 6.2: Experimental values of circumscribed central composite design and responses.

Experiment No.	Glucose (g/l)	Xylose (g/l)	Growth rate (h ⁻¹)
1	1.4393	1.4393	0.7095
2	1.4393	3.5606	1.0760
3	3.5606	1.4393	0.8514
4	3.5606	3.5606	0.6811
5	1	2.5000	0.6153
6	4	2.5000	0.7045
7	2.5000	1	0.9313
8	2.5000	4	0.8396
9	2.5000	2.5000	0.8877
10	2.5000	2.5000	0.7343
11	2.5000	2.5000	1.0580
12	2.5000	2.5000	0.8380
13	2.5000	2.5000	0.8426
14	2.5000	2.5000	0.7039
15	2.5000	2.5000	0.7544
16	2.5000	2.5000	0.8755

Residuals from the least squares are important for assessing the accuracy of the model. Therefore, normal probability distribution of residuals is shown in Figure 6.1, which confirmed that the normality assumption was satisfied since the probability of the residuals fell on a straight line.

After the quality of the fit was found satisfactory, response surface was plotted by using the model in Equation 6.1, the resulting response surface and its contour plot are presented in Figures 6.2 and 6.3, respectively.

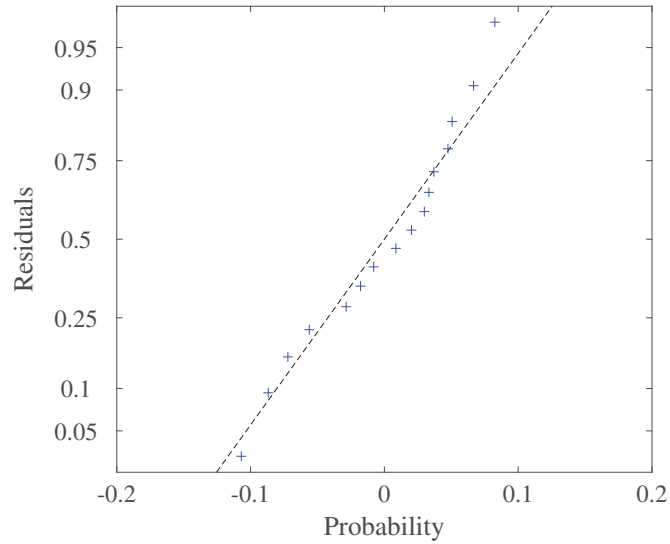


Figure 6.1: Normal probability distribution of residuals.

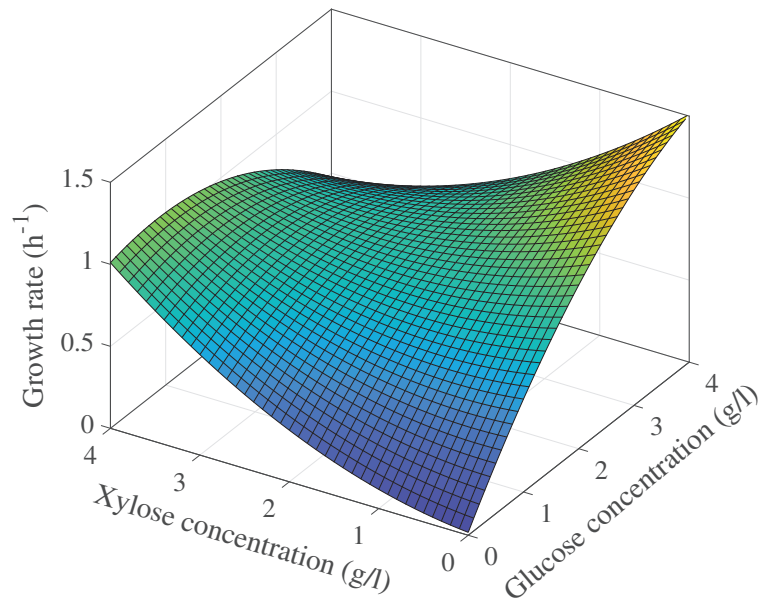


Figure 6.2: Response surface of glucose and xylose concentrations versus growth rates.

Figure 6.2 shows that a minimum appeared when both variables are zero, since cells cannot grow without any carbon source. When glucose was the only sugar present, growth rate increased as its concentration increased,

and a maximum growth rate value was obtained at the highest glucose concentration. Therefore, the effect of glucose concentration on the growth rate is greater than xylose as it is the preferred carbon source. Even though the growth rate was lower for only xylose containing experiments than for only glucose containing ones, the growth rate was still proportional with the xylose concentration.

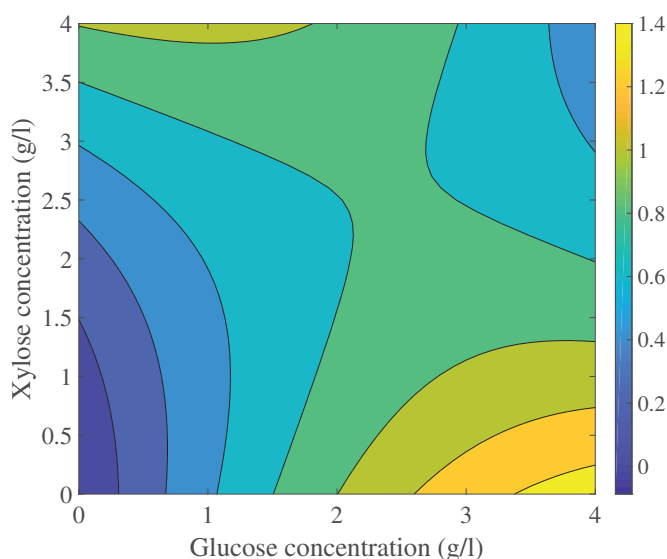


Figure 6.3: Contour plot of glucose and xylose concentrations versus growth rates.

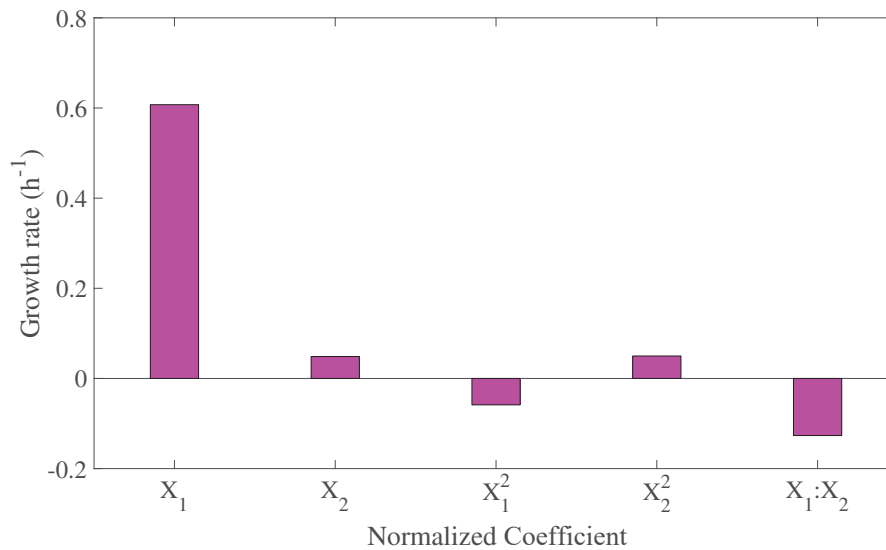
Figure 6.3 shows that the stationary point is a saddle point. From this point near the centre of the experimental design, increasing or decreasing both factors at the same time results in a decreasing response. However, from the stationary point, increasing either factor when decreasing the other one results in an increasing response. This trend demonstrates the importance of interaction between the sugars. Therefore, CCR is still active and both sugars are most likely to be repressing utilization of each other, thus decreasing the growth rate. This is an interesting finding as glucose was found to repress the growth of xylose in earlier studies [97]; while the findings suggest that, the repression effect can apply to both sugars. This might also be due to the developed two-stage pre-growth strategy, where the culture was grown on a medium containing only xylose as the sugar to activate the xylose pathway and achieve co-utilization of sugars.

Table 6.3 shows fit results with the model coefficient estimates, their p values for the t -statistic, and the corresponding statistical significances.

Table 6.3: Model coefficients and corresponding statistical values.

Source	p value	Significance
Intercept	0.7963	-
X_1	9.44e-05	** ($p < 0.01$)
X_2	0.6030	-
X_1^2	0.0259	* ($p < 0.05$)
X_2^2	0.0273	* ($p < 0.05$)
X_1X_2	0.0002	** ($p < 0.01$)

Glucose (X_1) was the most significant variable among all and the only highly significant linear variable affecting the growth rate. Second highly significant variable was the interaction between the variables (X_1X_2). Both quadratic variables (X_1^2 and X_2^2) were significant, while the linear variable of xylose (X_2) was not significant. Figure 6.4 illustrates the effect of each model coefficient on the response.

**Figure 6.4:** Normalized values of model coefficients versus growth rate.

The effects of the model coefficients were examined using Figure 6.4. Linear variable of glucose (X_1) was the most significant variable with the greatest impact on the response. The growth rate increased as glucose concentration increased. The second most significant variable was the interaction between the variables. The interaction term had a negative impact on the growth rate. The quadratic variable of glucose (X_1X_2) had a negative effect on the response, while quadratic variable of xylose (X_2X_2) was increasing the growth rate. Information about the significance of the model coefficients by using p value was confirmed by the plot showing the effect of the coefficients on the response, growth rate.

6.3.2 Modelling the Growth on Mixtures of Glucose and Xylose

Growth data obtained in previous section as a result of the design of experiment was used for model fitting. Glucose and xylose concentrations, SG and SX are predictor variables and the growth rate, μ is the response variable. The coefficients shown in this section are empirical, and due to their dependency on the species, substrate and environmental conditions, they are called parameters. Table 6.4 shows fit results in terms of SSE for the chosen binary substrate growth models.

Table 6.4: Fit results for binary substrate growth models.

Model	Model type	SSE
$\mu = \frac{\mu_{maxG} \cdot SG}{(K_{sG} + SG) \cdot \left(1 + \frac{SX}{K_{sX}}\right)} + \frac{\mu_{maxX} \cdot SX}{(K_{sX} + SX) \cdot \left(1 + \frac{SG}{K_{sG}}\right)}$	Noncompetitive [189]	0.0778
$\mu = \frac{\mu_{maxG} \cdot SG}{K_{sG} + SG \cdot \left(1 + \frac{SX}{K_{sX}}\right)} + \frac{\mu_{maxX} \cdot SX}{K_{sX} + SX \cdot \left(1 + \frac{SG}{K_{sG}}\right)}$	Uncompetitive [189]	0.1516
$\mu = \frac{\mu_{maxG} \cdot SG \cdot SX}{(K_{sG} + SG) \cdot (K_{sX} + SX)}$	Interactive [188]	0.1867
$\mu = \frac{\mu_{maxG} \cdot SG}{K_{sG} + SG} + \frac{\mu_{maxX} \cdot SX}{K_{sX} + SX}$	Noninteractive [190]	0.1847
$\mu = \frac{\mu_{maxG} \cdot SG}{K_{sG} + SG + SX \cdot \left(\frac{K_{sG}}{K_{sX}}\right)} + \frac{\mu_{maxX} \cdot SX}{K_{sX} + SX + SG \cdot \left(\frac{K_{sX}}{K_{sG}}\right)}$	Competitive [191]	0.1928

Fit results showed that the noncompetitive binary substrate growth model delivered the smallest SSE value of 0.0778. Equation 6.2 shows the resulting model with the estimated parameters. The quality of the fit was satisfactory.

$$\mu = \frac{1.435 \cdot SG}{(1.236 + SG) \cdot \left(1 + \frac{SX}{4.601}\right)} + \frac{1.508 \cdot SX}{(4.601 + SX) \cdot \left(1 + \frac{SG}{1.236}\right)} \quad (6.2)$$

Figure 6.5 shows the growth rate (h^{-1}) predictions of noncompetitive binary substrate growth model with respect to glucose and xylose concentrations (g/l).

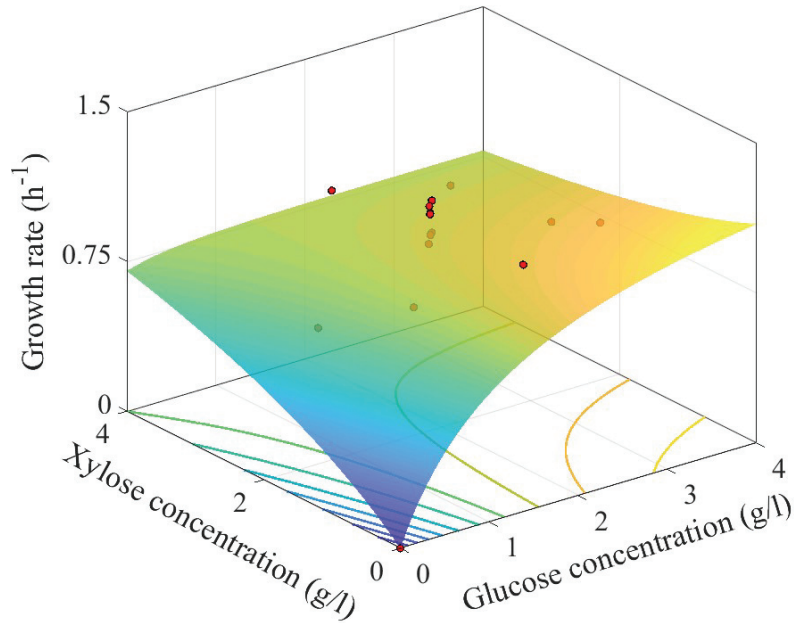


Figure 6.5: Noncompetitive binary substrate growth model predictions and experimental observations.

Figure 6.5 shows that a minimum response, the growth rate, appeared when both glucose and xylose concentrations were zero, since cells cannot grow without any carbon source. When glucose was the sole sugar, the growth rate increased as its concentration increased, and a maximum growth rate value was obtained at its highest concentration. Even though

the growth rate was lower for xylose than for glucose, the growth rate was still proportional with the xylose concentration. Moreover, the projection of the model prediction surface plot illustrates that increasing or decreasing both sugar concentrations at the same time results in a decreasing growth rate. However, increasing either of the sugars when decreasing the other one results in an increasing growth rate.

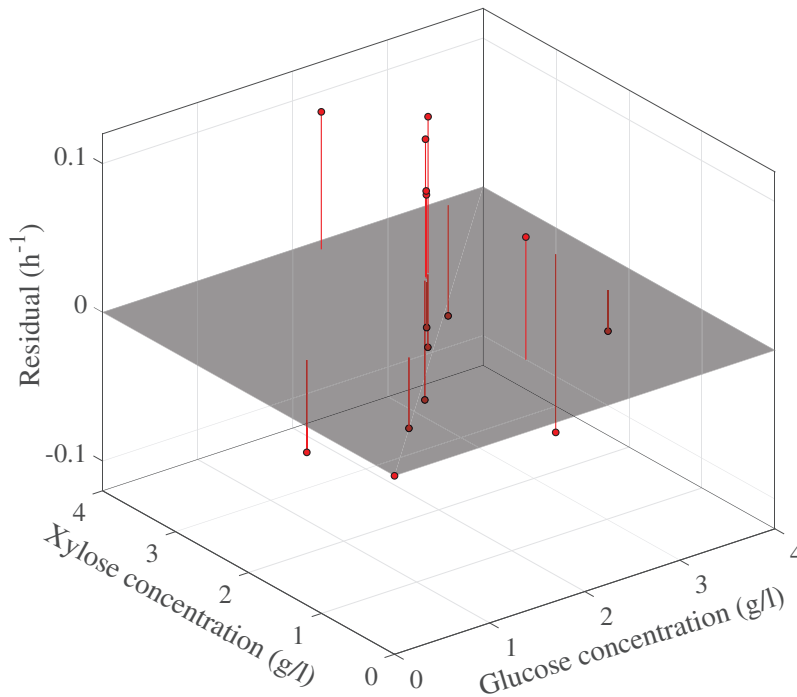


Figure 6.6: Residuals of noncompetitive binary substrate growth model predictions and experimental observations.

Figure 6.6 shows raw residuals, which are the difference between the predicted and observed values of the growth rate. The greatest raw residual value was 0.12 h^{-1} for model prediction of 0.705 h^{-1} , while 0 was the lowest observed when both sugar concentrations were 0.

Table 6.5 shows the parameter estimates and their 95% confidence intervals for the noncompetitive binary substrate growth model. The maximum specific growth rate on glucose, μ_{maxG} was greater than the maximum specific growth rate on xylose, μ_{maxX} . On the other hand, the substrate affinity constant for xylose, K_{sX} was larger than the substrate affinity constant for glucose, K_{sG} .

Table 6.5: Parameters of the noncompetitive binary substrate growth model.

Parameter	Estimate	95% Confidence interval
μ_{maxG}	1.4354	(-2.2643) – 5.1351
K_{sG}	1.2360	(-7.1363) – 9.6082
K_{sX}	4.5996	(-23.9499) – 33.1491
μ_{maxX}	1.5078	(-1.8106) – 4.8262

μ_{maxX} had the smallest confidence interval, thus the uncertainty associated with this parameter was the smallest among others, while K_{sX} had the largest confidence interval. 95% confidence intervals of the parameters in ascending order were μ_{maxX} , μ_{maxG} , K_{sG} and K_{sG} . Correlation matrix for the noncompetitive binary substrate growth model is given in Table 6.6.

Table 6.6: Correlation matrix of noncompetitive binary substrate growth model.

	μ_{maxG}	K_{sG}	K_{sX}	μ_{maxX}
μ_{maxG}	1	0.9918	-0.9945	-0.9728
K_{sG}	0.9918	1	-0.9860	-0.9455
K_{sX}	-0.9945	-0.9860	1	0.9542
μ_{maxX}	-0.9728	-0.9455	0.9542	1

The correlation coefficient ranges from -1 to +1. The greater the absolute value of the correlation coefficient, the stronger the relationship between those parameters. Furthermore, the sign of the correlation coefficient indicates the direction of the relationship. If both parameters tend to increase or decrease simultaneously, the correlation coefficient is positive. Therefore, the greatest correlation of -0.9954 was found between μ_{maxG} and K_{sX} , thus as one parameter decreases as the other one increases. The weakest correlation value was -0.9455 between μ_{maxX} and K_{sG} . The relationships between μ_{maxG} and μ_{maxX} , and K_{sG} and K_{sX} were negative. On the other hand, the relationship between model parameters for individual sugars, μ_{maxG} and

K_{sG} , and μ_{maxX} and K_{sX} were positive.

Effects of the model parameters on the growth rate were illustrated in Figure 6.7 by varying the parameters over their respective confidence intervals and plotting them against the resulting growth rate values. Sugar concentrations (SG and SX) were kept constant at their centre value of 2.5 g/l over the experimental concentration space.

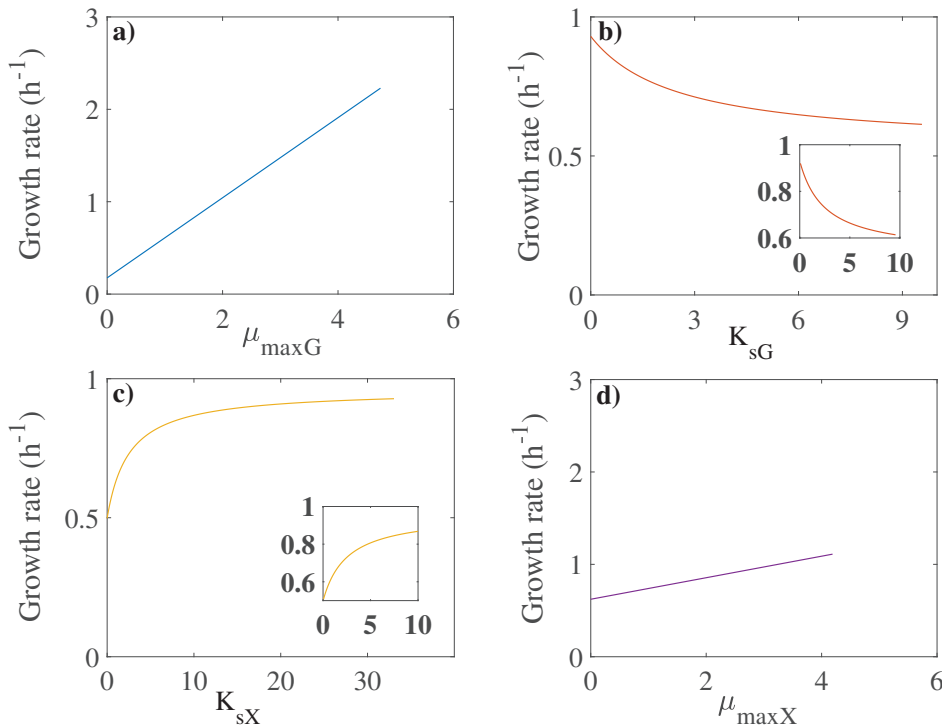


Figure 6.7: Effects of parameters of the noncompetitive binary substrate growth model on the growth rate (h⁻¹).

Increase in both μ_{maxG} and μ_{maxX} resulted in an increased growth rate, μ . However, the effect of μ_{maxG} was greater, since the slope of μ_{maxG} versus μ plot was 0.41, while the slope of μ_{maxX} versus μ was 0.23. The shape of K_{sG} versus μ plot was in the shape of an exponential decay curve, therefore μ increased exponentially with decreasing K_{sG} . On the other hand, K_{sX} versus μ plot was in the shape of an exponential growth curve, thus μ increased exponentially, while K_{sX} was increasing. Furthermore, there is a relation between the sugar concentration and the substrate affinity constant [166]. When $SX < K_{sX}$, the term for repression effect of xylose

on glucose utilization $(1 + SX/KsX)$ decreases with increasing K_{sX} , and vice versa. Therefore, a change in K_{sG} and K_{sX} resulted in different effects on the growth rate, since $SG=2.5$ g/l $>$ $K_{sG}=1.2360$ g/l, and $SX=2.5$ g/l $<$ $K_{sX}=4.5996$ g/l as shown in Figure 6.7.

6.4 Conclusions

A binary substrate growth model was suggested, which describes the cell mass growth on mixtures of glucose and xylose and the interaction between them. Main conclusions of this chapter are given below:

- RSM showed that the interaction between the sugars had a significant influence on the cell mass growth.
- CCR mechanism can be active not only from glucose on xylose utilization, but also vice versa, from xylose on glucose utilization.
- Among the interactive binary substrate models, the model with non-competitive inhibition gave the best fit.

Validation with other sugar concentration values will be necessary to evaluate the prediction capability of the proposed growth model. In the following chapter, the growth model obtained in this chapter was used.

Chapter 7

Modelling Fermentative Butanol Production from Glucose and Xylose

Contents of this chapter were covered in Paper IV.

7.1 Introduction

Fermentative butanol production from mixtures of pentose and hexose suffers from Carbon Catabolite Repression as thoroughly explained in Section 2.3 together with a review of different approaches to tackle this problem. In Chapter 5, a pre-growth strategy was developed, showing that a culture subjected to xylose as the sole sugar could efficiently co-utilize glucose and xylose, and produce butanol. In this chapter, the improvement in mixed sugars fermentations were investigated with respect to the suggested pre-growth strategies.

There are different models describing fermentative butanol production, which serves different purposes and utilizes different types of information as reviewed in Section 2.4. Despite the wide variety of the proposed models [13,127], there is still not a consensus about the most appropriate model to use for process design, control and optimization. Moreover, the majority of models is only valid under certain process conditions and regimes [209]. Dynamic models developed by Shinto et al. (2007, 2008) have been central to the recent modeling attempts [144,145]. Raganati et al. (2015) applied their models for a wider range of pentose and hexose sugars [147]. Diaz

and Willis (2018) extended the model to include CCR for fermentation of glucose and xylose [210] and it was developed simultaneously with the initial model proposed as part of this PhD project [211]. These two are currently the only mixed sugar fermentation models developed for butanol production. Despite their rich information content, the complexity level of Shinto et al.'s (2007, 2008) models is high and they require larger experimental datasets for estimation of larger number of parameters necessary to construct the models. On the contrary, traditional unstructured models are simpler and easier to interpret, thus they are still actively being used for describing butanol production by fermentation [212].

The main objective of this chapter is therefore twofold: i) to establish a dynamic model for fermentative butanol production from mixtures of glucose and xylose, and ii) to investigate the effects of pre-growth strategies on the fermentation kinetics.

7.2 Materials and Methods

7.2.1 Microorganism and Medium

Clostridium beijerinckii NCIMB 8052 was used. The culture was pre-grown in medium described in Section B.2.1 and under the conditions explained in Section B.4.1. The fermentation medium contained different amounts of glucose and xylose as explained in the section below, and rest of the medium components are given in Table B.2.

7.2.2 Fermentations

Fed-batch fermentations were performed in serum flasks as explained in Section B.4.2. 2 ml samples were taken every 2 hours from the start of the experiments until the end of the exponential growth phase. Optical density (OD) was used as a measure for cell mass concentration, explained in Section B.3. 1 ml samples were taken at sampling times of 0, 4, 8, 12, 16, 24, 26, 28, 30, 32, 36, 40 and 48 hours with respect to the start of the experiment. Sugar feeding was done with a concentrated, 232.5 g/l sugar solution containing equal amounts of glucose and xylose. The feeding was done such that the volumes removed during sampling and the volumes added during feeding were equal and the same for all the experiments to reduce dilution effects. The cultures with 15 g/l total sugars (X15 and GX15, validation datasets) were fed with the sugar solution every 8 hours, the ones with 30 g/l (X30 and GX30, parameter estimation datasets) were fed every 16 hours, and the

ones with 45 g/l (X45 and GX45, validation datasets) were fed every 24 hours. Experiments terminated after 48 hours.

Samples were analyzed by using high-performance liquid chromatography (HPLC) for quantification of sugars and butanol, and cell mass concentration was estimated by measuring optical density (OD) as described in Section B.3.

7.3 Model Development

A dynamic model describing cell mass (X) growth, uptake of glucose (SG) and xylose (SX), and butanol (B) production was developed. The model was based on unstructured mathematical models that have typically been used to estimate the state of fermentative butanol production [142]. Kinetic equations were chosen such that they can describe the key characteristics of the process while avoiding the overparameterization of the model. Following assumptions were made by employing the fermentation biochemistry knowledge to establish the proposed model:

- Glucose and xylose are the only limiting substrates.
- There is no nitrogen limitation.
- Growth inhibition sources are
 1. high substrate concentration
 2. butanol accumulation
 3. interaction between sugars
- High substrate inhibition effects are combined for glucose and xylose, and it is in noncompetitive form [166].
- Butanol inhibition is noncompetitive described by parabolic function [143, 166].
- Inhibition effects of substrates on each other is significant and non-competitive [213].
- Substrate assimilation is only for butanol and cell mass production.
- Substrate consumption for maintenance is negligible.
- Luedeking-Piret model with a growth-associated part describes the butanol production.

The model was developed with the light of the assumptions above using the data of Fond et al. (1986) [104], and the experimental data produced during this PhD project separately for cultures pre-grown on xylose, and pre-grown on xylose and glucose. The validity and accuracy were checked using two more datasets for each model. Then, the critical parameters were identified by sensitivity analysis.

In section 6.3.2, the Monod equation was modified to describe the growth on mixtures of glucose and xylose together with noncompetitive inhibition between them. Cell mass growth on glucose, μ_{SG} , and xylose, μ_{SX} , are shown in Equation 7.1 and Equation 7.2, respectively.

$$\mu_{SG} = \frac{\mu_{maxG} \cdot SG}{(K_{sG} + SG) \cdot \left(1 + \frac{SX}{K_{sX}}\right)} \quad (7.1)$$

$$\mu_{SX} = \frac{\mu_{maxX} \cdot SX}{(K_{sX} + SX) \cdot \left(1 + \frac{SG}{K_{sG}}\right)} \quad (7.2)$$

where μ_{maxG} and μ_{maxX} are maximum specific growth rates on glucose and xylose, and K_{sG} and K_{sX} are substrate affinity constants for glucose and xylose, respectively. The growth model was extended with substrate and butanol inhibition terms in this section as shown in Equation 7.3.

$$\mu_g = (\mu_{SG} + \mu_{SX}) \cdot \left(\frac{K_I}{K_I + SG + SX}\right) \cdot \left(1 - \frac{B}{B_{max}}\right)^{i_B} \quad (7.3)$$

where μ_g is the specific growth rate of cell mass, K_I is the substrate inhibition constant, B_{max} is the concentration of butanol at which cell mass growth stops, and i_B is the butanol inhibition constant to cell mass growth. Net growth rate of cell mass, μ_{net} , given in Equation 7.4 is the difference between the specific growth rate and specific death rate, k_d , therefore, the cell mass change over time shown in Equation 7.5.

$$\mu_{net} = \mu_g - k_d \quad (7.4)$$

$$\frac{dX}{dt} = \mu_{net} \cdot X \quad (7.5)$$

Glucose and xylose uptakes are given in terms of the amounts utilized for cell mass growth and butanol formation, which can be seen in Equation 7.6 and Equation 7.7, respectively.

$$\frac{dSG}{dt} = -\mu_{SG} \cdot X \cdot \left(\frac{1}{Y_{X/SG}} + \frac{1}{Y_{B/SG}}\right) \quad (7.6)$$

$$\frac{dSX}{dt} = -\mu_{SX} \cdot X \cdot \left(\frac{1}{Y_{X/SX}} + \frac{1}{Y_{B/SX}} \right) \quad (7.7)$$

where $Y_{X/SG}$ and $Y_{X/SX}$ are cell yields on glucose and xylose, and $Y_{B/SG}$ and $Y_{B/SX}$ are butanol yields on glucose and xylose, respectively. Equation 7.8 shows butanol formation.

$$\frac{dB}{dt} = \mu_{SG} \cdot X \cdot Y_{B/XG} + \mu_{SX} \cdot X \cdot Y_{B/XX} \quad (7.8)$$

where $Y_{B/XG}$ and $Y_{B/XX}$ are butanol yields on cell mass utilizing glucose and xylose. The relationships between cell mass yields, butanol yields on substrates and on cell mass are shown in Equation 7.9 and Equation 7.10.

$$Y_{B/XG} = \frac{Y_{B/SG}}{Y_{X/SG}} \quad (7.9)$$

$$Y_{B/XX} = \frac{Y_{B/SX}}{Y_{X/SX}} \quad (7.10)$$

The empirical coefficients shown in Equations 7.1 - 7.10 are called parameters in the thesis due to their dependency on the species, substrate and environmental conditions.

7.3.1 Parameter Estimation

The proposed model includes 12 parameters listed in the section above that are unknown a priori; therefore, they are estimated using the experimental data of cell mass, glucose, xylose, and butanol concentrations. The parameter estimation poses a constrained nonlinear least-squares optimization problem, which was solved as described in Section B.10. Parameter bounds were the constraints as shown in Table B.3.

After obtaining the parameter estimates, model simulations were done to check the model accuracy, and the average squared correlation coefficients (r^2) were calculated using the model predictions and experimental observations as explained in Section B.11. Sensitivity analysis was done by 10% perturbations in each of 12 parameters as given in Section B.12.

7.4 Results and Discussion

7.4.1 Parameter Estimates

The model parameters were estimated for 4 datasets:

1. Glucose and xylose fermentations by xylose pre-grown culture, X30.
2. Fond et al.'s data of glucose and xylose fermentations by xylose pre-grown culture, FondX [104]
3. Glucose and xylose fermentations by glucose and xylose pre-grown culture, GX30.
4. Fond et al.'s data of glucose and xylose fermentations by glucose and xylose pre-grown culture, FondGX [104].

Parameter estimates for all 4 datasets given in Table 7.1 were interpreted to illustrate the effects of different pre-growth strategies on the fermentation kinetics.

Table 7.1: Parameter estimation results.

Parameter	X30	FondX [104]	GX30	FondGX [104]
$Y_{X/SG}$	0.199	0.097	0.523	0.157
$Y_{X/SX}$	0.292	0.260	0.058	0.223
$Y_{B/SG}$	0.265	0.250	0.196	0.319
$Y_{B/SX}$	0.057	0.389	0.232	0.399
k_d	0.055	0.033	0.076	0.026
B_{max}	15.632	15.796	15.658	17.243
i_B	1.125	2.138	0.616	1.695
K_I	143.629	186.199	171.492	187.667
μ_{maxG}	0.982	1.444	0.730	1.204
K_{sG}	1.842	5.634	1.293	4.637
K_{sX}	2.066	6.974	4.469	5.884
μ_{maxX}	0.487	1.292	0.615	1.025

Cell mass yield on glucose, $Y_{X/SG}$ values were 0.199 and 0.523 g/g, and cell mass yield on xylose, $Y_{X/SX}$ values were 0.292 and 0.058 g/g for xylose

pre-grown culture, X30 and glucose and xylose pre-grown culture, GX30, respectively. Therefore, higher amount of glucose ended up in cell mass in GX30 than in X30, and vice versa for xylose. The reason can be the higher expression levels of glucose utilization enzymes in the glucose and xylose pre-grown culture since it is the preferred carbon source [97]. On the other hand, for the culture pre-grown in only xylose containing medium, xylose assimilation enzymes were readily available when the glucose and xylose mixture was added and could utilize xylose at a higher efficiency for cell mass production. Furthermore, FondGX had higher $Y_{X/SG}$ and lower $Y_{X/SX}$ than FondX showing the same trend. Maximum specific growth rate of cell mass on glucose, μ_{maxG} and substrate affinity constant for glucose, K_{sG} was lower for FondGX and GX30 indicating that the cells pre-grown on glucose and xylose grew slower on glucose and were more attracted to glucose. However, changes in μ_{maxX} and K_{sX} exhibited opposite trends for X30 and GX30 cultures, and FondX and FondGX. This difference in the parameters of xylose growth model can be the result of *C. beijerinckii* (used in experiments of the thesis) having more sets of xylose metabolic pathway genes than *C. acetobutylicum* (used in Fond et al.'s study (1986)) [106]. Thus, different sugar utilization mechanisms may have caused variance in the xylose growth parameters.

Both butanol yield on glucose, $Y_{B/SG}$ and butanol yield on xylose, $Y_{B/SX}$ were greater for glucose and xylose pre-grown culture, FondGX than xylose pre-grown culture, FondX. The same increase was observed for $Y_{B/SX}$ in GX30 compared to X30. Therefore, glucose and xylose pre-grown cultures produced more butanol. The highest $Y_{B/SG}$ was 0.319 g/g and the highest $Y_{B/SX}$ was 0.399 g/g representing the 77.4% of the maximum theoretical butanol yield on glucose, 0.412 g/g, and 80.7% of the maximum theoretical butanol yield on xylose, 0.494 g/g, respectively. The concentrations of butanol at which cell mass growth stops, B_{max} were 15.632, 15.658, 15.796 and 17.243 g/l for X30, GX30, FondX and FondGX, respectively. Therefore, glucose and xylose pre-grown cultures were more tolerant to butanol toxicity. Similarly, butanol inhibition constants to cell mass growth, i_B were 1.125, 0.616, 2.138, 1.695 for X30, GX30, FondX and FondGX, respectively indicating the extent of butanol inhibition is greater for xylose pre-grown cultures. The toxic butanol concentration values and butanol inhibition constants are in good agreement with both previously reported experimental observations [143] and estimations in modeling studies [212]. Further experimental evidence confirms that the inhibitory effects of butanol on *C. acetobutylicum* were more pronounced in xylose-grown cells than in glucose-grown cells, and glucose and xylose permease were inhibited when

butanol concentration reached 12 and 8 g/l, respectively [124].

Substrate inhibition constant, K_I values were 143.629, 171.492, 186.199, and 187.667 g/l for X30, GX30, FondX and FondGX, respectively. Thus, the substrate inhibition on the growth was greater for the xylose pre-grown cultures. K_I estimates coincide with the literature information where it was stated that the cell growth was inhibited strongly when the total substrate concentration was 200 g/l and stopped entirely when it was 250 g/l for a mixture of sugars containing mostly glucose [51]. These results principally agree with the results of Raganati et al. (2015), in which they found that the cultures fed with glucose possessed the highest metabolic activity and lowest tendency to sporulate compared to the cultures with pentose sugars [147]. Even though this might be an indication of a shorter lifespan for xylose pre-grown cells, further investigation is necessary.

7.4.2 Comparison of Model Predictions and Experimental Observations

Simulations were performed by employing the model with the parameter estimates given in Table 7.1. The model predictions and the observed values for the FondX and FondGX datasets are shown in Figure 7.1.

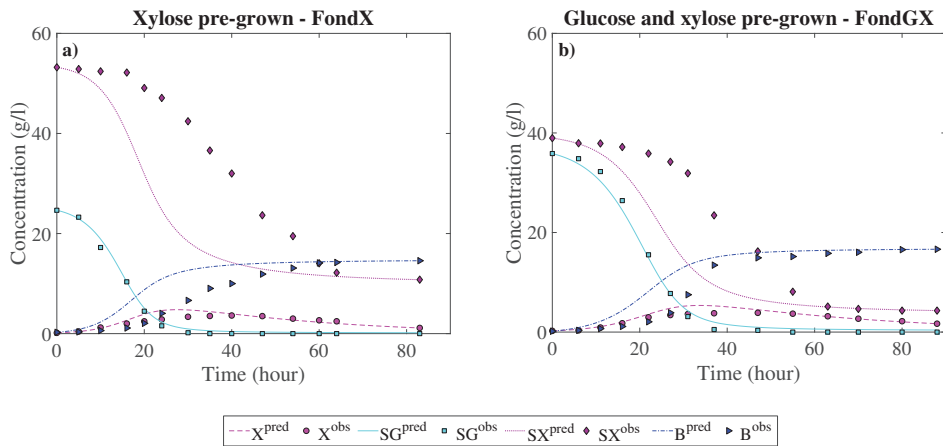


Figure 7.1: Comparison of model predictions and experimental observations with the data from Fond et al. (1986) for a) xylose pre-grown culture, FondX, and b) glucose and xylose pre-grown culture, FondGX [104].

Figure 7.1 (left) shows the predicted and observed values of cell mass, glucose, xylose and butanol concentrations for fermentation of a sugar mixture of 53 g/l xylose and 25 g/l glucose by xylose pre-grown culture, FondX.

Exponential growth phase during which the cell mass increased rapidly was observed until 10 hours with respect to the start of the experiment, and followed by a steady cell mass growth until 40 hours. Glucose utilization started immediately and lasted for 25 hours. Only after complete depletion of glucose, xylose utilization became apparent and lasted until the end of the fermentation with a decreased rate from 64 hours when butanol concentration reached 14 g/l. Butanol production was slow initially, became faster between 16 and 54 hours, and almost stopped around 64 hours. The residual xylose concentration was 11 g/l, and butanol was 14.5 g/l at the end of the fermentation. Figure 7.1 (right) shows the predicted and observed values for fermentation of a sugar mixture of 36 g/l xylose and 39 g/l glucose by glucose and xylose pre-grown culture, FondGX. Exponential growth lasted longer in this fermentation, continued for 22 hours, and then steady growth occurred until 47 hours and cell mass concentration decreased until the end of the experiment. Initially, glucose was consumed rapidly and xylose utilization was very slow. After 22 hours, both sugars were co-utilized almost at the same rate. Glucose was completely depleted at 47 hours, while xylose consumption continued. Xylose consumption rate decreased when butanol concentration was 16 g/l. The residual xylose and butanol concentrations were 4.3 and 16.6 g/l, respectively. Higher butanol concentration and lower residual xylose in FondGX than in FondX are line with the estimated parameters as well as the butanol concentrations when the sugar utilization rates dropped. Therefore, the model can describe the fermentation kinetics for both pre-growth strategies. A more detailed overview of the model accuracy in terms of average squared correlation coefficients (r^2) between the predicted and observed values is given in Table 7.2.

The model predictions and experimental observations done in the thesis for X30 and GX30, parameter estimation experiments, and X15, GX15, X45, and GX45, validation experiments are shown in Figure 7.2.

Figures 7.2 a-c show the predicted and observed values of cell mass (volume corrected), accumulated consumption of glucose, xylose and accumulated butanol concentrations for fed-batch fermentations by xylose pre-grown cultures, X15, X30 and X45. All the cultures showed the same growth pattern; cell mass concentrations increased exponentially as soon as the experiments started followed by a steady growth phase, followed by a decay phase during which the apparent cell mass concentration decreased [166]. In all the experiments, xylose consumption rates were slightly higher and utilizations were simultaneous with glucose. Consumption rates of both glucose and xylose decreased as the fermentations proceeded. Butanol con-

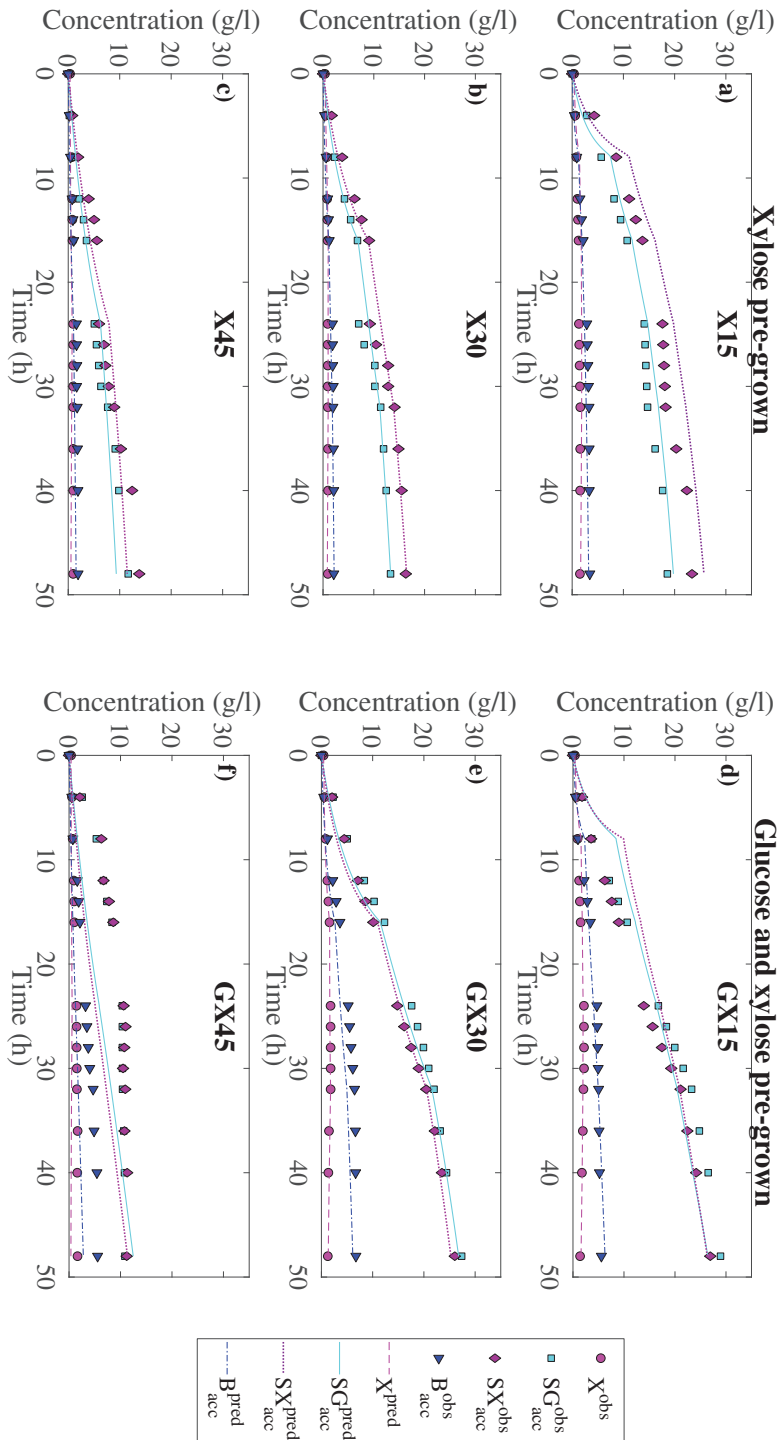


Figure 7.2: Comparison of model predictions and our experimental observations for xylose pre-grown cultures a) X15, b) X30, c) X45, and glucose and xylose pre-grown cultures d) GX15, e) GX30, f) GX45.

centrations showed the same trend as the cell mass confirming the growth-associated production as shown in Equation 7.8.

Figures 7.2 d-f show the model predictions and experimental observations of cell mass (volume corrected), accumulated consumption of glucose, xylose and accumulated butanol concentrations for fed-batch fermentations by glucose and xylose pre-grown cultures, GX15, GX30 and GX45. Cell mass concentrations showed the same growth pattern as in the fermentations with xylose pre-grown cultures explained above. In all experiments, sugar utilizations were simultaneous and almost at the same rate unlike the xylose pre-grown culture experiments in which the xylose consumption rates were higher than those for glucose. Sugar consumption rates became slower as the fermentations continued. Similarly, butanol and cell mass productions were closely linked.

Table 7.2: Average squared correlation coefficients (r^2) between predicted and observed values.

Dataset	Cell mass	Glucose	Xylose	Butanol	Average
X15	0.122	0.944	0.851	0.903	0.705
X30	0.842	0.975	0.973	0.914	0.926
X45	0.552	0.921	0.894	0.524	0.723
GX15	0.754	0.935	0.873	0.925	0.872
GX30	0.934	0.982	0.991	0.778	0.917
GX45	0.752	0.094	0.248	0.221	0.329
FondX	0.595	0.998	0.350	0.591	0.633
FondGX	0.657	0.997	0.623	0.826	0.776
Average	0.651	0.856	0.725	0.710	0.735

In accordance with Fond et al.'s (1986) work, glucose and xylose pre-grown cultures in our experiments showed better tolerance to inhibitions as well as 2-fold increase in butanol production and 1.5-fold increase in sugar utilizations. For all our experiments, cell mass growth rate, total amounts

of sugar utilizations and butanol production increased with decreasing total sugar concentration. The reason is the inhibition due to high substrate concentration and noncompetitive inhibition between sugars. Model predictions and observations were in good agreement as derivable from the r^2 values shown in Table 7.2.

Average squared correlation coefficients (r^2) for the parameter estimation datasets were 0.926, 0.917, 0.633, and 0.776 for X30, GX30, FondX and FondGX, respectively. The results are in the range of r^2 values calculated in similar studies. The r^2 values of Shinto et al.'s findings for the parameter estimation datasets were 0.909 and 0.970; Raganati et al.'s results were 0.894 and 0.890 for fermentations of 65.7 mM (10 g/l) xylose and 70.6 mM (12.7 g/l) glucose, and 60 g/l glucose and 60 g/l xylose, respectively [144,145,147]. It is important to note that the fermentations in these studies were single sugar fermentations. The model proposed for mixed sugar fermentation was by Diaz and Willis (2018), and r^2 was 0.955 for fermentation of 32 g/l xylose and 31 g/l glucose [210]. The higher average squared correlation coefficients can be due to use of a more detailed model considering more metabolites and a variety of different datasets used in parameter estimation.

7.4.3 Sensitivity Analysis on Model Parameters

The critical parameters were identified by performing a sensitivity analysis. The reference trajectory was the concentration profiles from model simulations under the given initial concentrations and model parameters estimated for X30 and GX30. Figure 7.3 shows the sensitivity analysis for the cell mass, glucose, xylose and butanol in terms of end point deviations (%) in concentrations with 10% perturbations in the parameters.

End point deviations (%) were significantly larger in cell mass, glucose and xylose concentrations for GX30 than X30, while in the same range for butanol. Figures 7.3 a and e show that +10% variations of all growth parameters resulted in a greater end point cell mass concentration due to increased net growth rate. While positive influence of μ_{maxG} and μ_{maxX} on growth is apparent, the same impact of K_{sG} and K_{sX} can be explained by decreased competitive inhibition between the sugars when $SG > K_{sG}$ and $SX > K_{sX}$ as shown in Equations 7.1 and 7.2. The greatest end point deviation in cell mass was 49.68% in GX30 with respect to a +10% increase in μ_{maxG} . Another critical parameter was specific death rate of cell mass, k_d and its -10% perturbation caused 11.28 and 18.48% end point deviations in cell mass concentrations in X30 and G30, respectively as a result of increased net growth rate, μ_{net} .

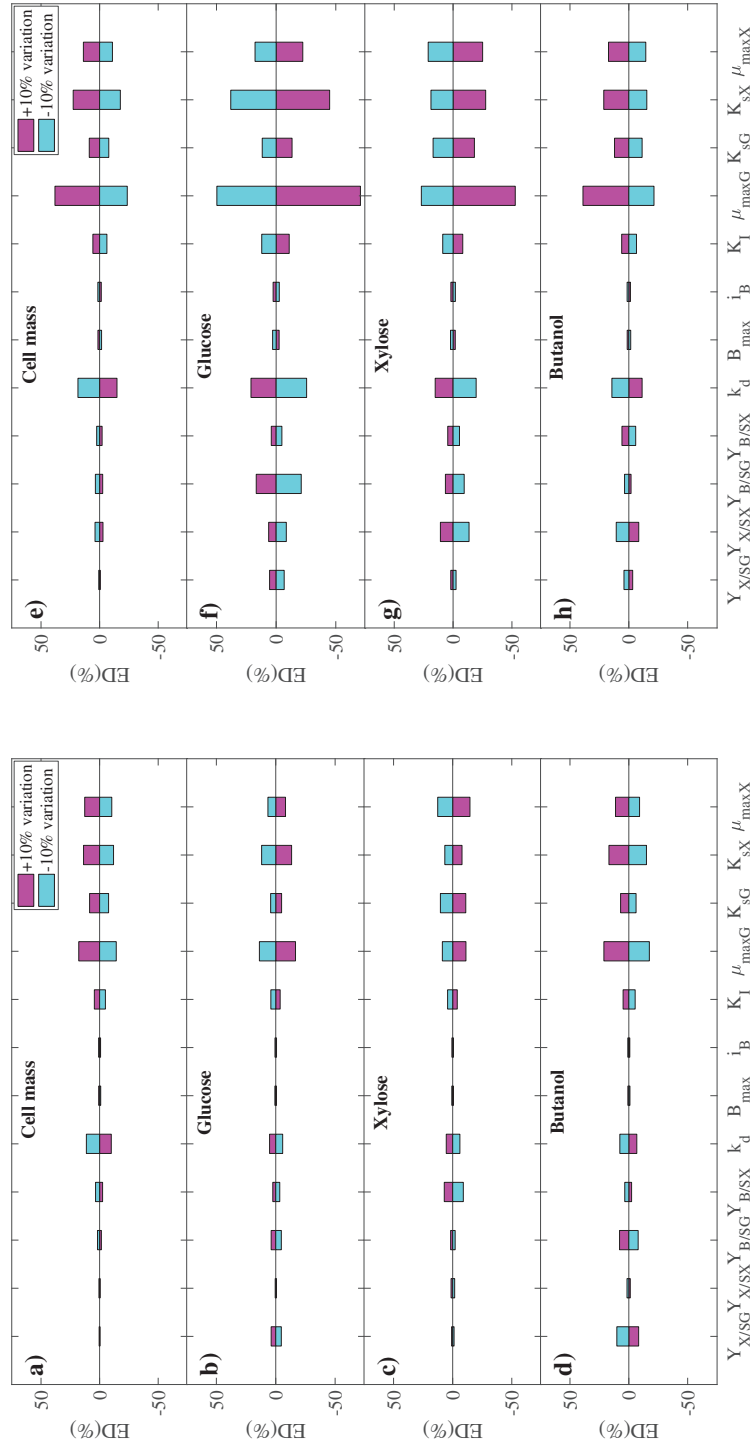


Figure 7.3: Sensitivity analysis on model parameters for a) and e) cell mass, b) and f) glucose, c) and g) xylose, and d) and h) butanol concentrations.

Figures 7.3 b and f illustrate that glucose concentrations were most sensitive to the perturbations in growth parameters due to its correlation with cell mass concentration as given in Equation 7.6. Therefore, any perturbation of any parameter causing an increase in cell mass concentration results in a decrease in glucose concentration. Moreover, +10% variation in $Y_{B/SG}$ yielded 3.84 and 16.68% end point deviations for X30 and GX30, respectively, as a result of greater growth inhibition due to increased butanol level. Figures 7.3 c and g show that the critical parameters were the same for xylose as for glucose. The greatest end point deviations in xylose concentrations were 12.66% for X30 and 52.8% for G30 resulting from -10% variations in μ_{maxX} and μ_{maxG} , respectively.

Growth parameters were the most critical for butanol since its production is dependent on growth and cell mass concentrations as given in Equation 7.8. Figures 7.3 d and h show that +10% variation in the most critical parameter, μ_{maxG} resulted in 21.17 and 38.95% end point deviations, while +10% variation of the second most important parameter, K_{sX} caused 16.88 and 21.27% end point deviations for X30 and GX30, respectively. Sensitivity analysis identified critical parameters, which can be re-estimated with more experimental data to improve the model accuracy.

7.5 Conclusions

A dynamic model structure describing key characteristics of fermentative butanol production from glucose and xylose mixtures was proposed. Parameter estimates revealed that pre-growth has a profound impact on the kinetics, and parameter values coincide with observations done in similar studies. Sugar utilization and butanol production were higher in fermentations by cultures pre-grown on glucose and xylose. Sugar utilization and butanol production decreased with increasing initial sugar concentrations, which is consistent with the results of exploratory data analysis performed by using data of 175 fermentations with lignocellulosic hydrolysates and mixed sugars shown in Chapter 3. Two models developed for both pre-growth strategies were validated with two more experimental datasets, and average squared correlation coefficients between predicted and observed values were satisfactory. Growth parameters were critical for all components as identified by sensitivity analysis. The main contributions of this study can be stated as below:

- This is the first study, which investigates the effect of different pre-growth strategies on kinetics of mixed sugar fermentations.

-
- The proposed model is the first attempt to incorporate the noncompetitive inhibition between sugars together with high substrate and butanol inhibitions.
 - This chapter provides insight into contributions of each sugar to cell mass growth and butanol formation in terms of yield parameters.

The suggested model can serve as a basis for industrial fermentations of lignocellulosic biomass, and its extension with effects of common inhibitors found in the hydrolysates can improve its applicability.

Chapter 8

Concluding Remarks and Future Work

8.1 Concluding Remarks

This thesis dealt with different aspects of fermentative butanol production from lignocellulosic biomass. The research has been motivated by the increasing need to design efficient processes for production of biofuels and green chemicals with improved conversion of feedstock to useful products. However, complexity of fermentation is not well understood, and systematic approach is lacking to tackle low product yield and selectivity, scalability and poor mixed sugar utilization problems, and unavailability of simple models to describe mixed sugar fermentations. Therefore, the aim of this thesis was to obtain a holistic overview of all fermentation variables, gain insight into scalability issues, develop feeding strategies to achieve co-utilization of sugars, and to establish a simple model which can describe fermentative butanol production from lignocellulosic sugars. Experimental studies in different fermentation setups in different scales were done together with modeling and simulations to serve the aim of the thesis. The main contributions of this thesis are summarized below for each chapter.

Chapter 3 presented variables and performance indicators of fermentative butanol production from lignocellulosic biomass and sugars by developing an extensive dataset covering 175 fermentations, which is the largest collection to author's knowledge. Presented substrate and product mixture properties provided as a basis for fermentation process design. This was the first attempt to identify and define performance indicators, and to study

interconnectedness between them and fermentation variables by exploratory data analysis. EDA results were linked to individual observations from research articles to provide a holistic overview and a platform for discussing the usefulness of the measures applied to improve fermentation performance. Exploratory data analysis revealed the effect of substrate mixture properties on the fermentation for the first time, supported by research results in the field. The interconnectedness between the fermentation variables suggested that data analysis can be utilized to predict fermentation performance without having to measure/determine every variable.

By using the findings from this chapter, design of experiments in the following chapters were done, in addition, operating conditions such as representative lignocellulosic sugars, their compositions and concentrations were decided accordingly.

Chapter 4 showed results of glucose and xylose fermentations as representative lignocellulosic sugars at 6 different ratios and 2 different total sugar concentrations by *C. beijerinckii* NCIMB 8052 in microbioreactors and serum flasks. Glucose to xylose ratio affected both cell mass growth and butanol production. All cultures could be successfully grown in the BioLector[®] system under anaerobic conditions, metabolized both glucose and xylose, and produced butanol. The online monitoring of cell mass and pH in the BioLector[®] enabled following the progress of the fermentations at unprecedented time-resolution. Even though applicability of BioLector[®] was successfully demonstrated for the first time, growth rate, butanol production and butanol yield values were lower compared to fermentations done in serum flasks. Therefore, serum flask was chosen in addition to bench-scale fermenters for the experiments presented in the following chapters.

Chapter 5 demonstrated the effect of different feeding strategies, which were designed to cope with Carbon Catabolite Repression and sequential utilization problems on fermentation kinetics. The fermenter with only xylose as the initial carbon source could co-utilize sugars for all mixed sugar feeds, while the fermenter with only glucose as the initial sugar suffered from sequential utilization, thus xylose utilization became apparent only after complete exhaustion of glucose. Therefore, effect of sugar in the initial growth medium on fermentation was prevailing, and this was the first study to investigate the effect in a systematic manner. Observations and findings of this chapter created a motive for further investigation of mixed sugar utilization and were employed for development of a two-stage pre-growth strategy in Chapter 6.

Chapter 6 suggested a binary substrate growth model, which described

the cell mass growth on mixtures of glucose and xylose and the interaction between them. First, results of Response Surface Methodology showed that the interaction between the sugars had a significant influence on the cell mass growth, illustrated that Carbon Catabolite Repression mechanism could be active not only from glucose on xylose utilization, but also vice versa, from xylose on glucose utilization. Then the model fitting for different interactive binary substrate models was done, and the model with noncompetitive inhibition gave the best fit. This was the first model to describe growth of *C. beijerinckii* NCIMB 8052 on mixtures of glucose and xylose.

Chapter 7 proposed a dynamic model describing key characteristics of fermentative butanol production from glucose and xylose mixtures. Estimates of model parameters revealed that the initial sugar in the pre-growth medium had a profound impact on the kinetics, and parameter values coincided with observations done in similar studies. Sugar utilization and butanol production were higher in fermentations by cultures pre-grown on glucose and xylose compared to the ones pre-grown only on xylose. Sugar utilizations and butanol productions decreased with increasing initial sugar concentrations, which was consistent with the results of exploratory data analysis performed by using data of 175 fermentations with lignocellulosic hydrolysates and mixed sugars shown in Chapter 3. Two models developed for both pre-growth strategies were validated with two additional experimental datasets, and average squared correlation coefficients between predicted and observed values were satisfactory. Growth parameters were critical for all components as identified by sensitivity analysis. This was the first study that investigated the effect of different pre-growth strategies on kinetics of mixed sugar fermentations. The proposed model was the first attempt to incorporate the noncompetitive inhibition between sugars together with high substrate and butanol inhibitions, and provided insight into contributions of each sugar to cell mass growth and butanol formation in terms of yield parameters.

The knowledge and experience obtained throughout the thesis work were utilized to provide some directions and suggestions for future work in Section 8.2.

8.2 Recommendations for Future Work

In this thesis, a considerable emphasis has been placed on the batch and fed-batch fermenters due to their prevalence in industry traditionally. However, continuous fermentation is gaining importance as they provide

better utilization of equipment, prolonged operation time and improved productivity. Therefore, there is a significant scope for future development of operating strategies and models for continuous fermenters. Furthermore, industrial fermentation processes utilize biomass, properties of which depend greatly on the type of the biomass and the environmental conditions instead of pure sugars and defined medium used in this thesis. Thus, it is of great importance to test feeding and pre-growth strategies suggested in this thesis for industrial scale fermentations of biomass. In addition, proposed models need to be applied for prediction of those processes, which were not considered in this thesis. Particularly, the following topics should be investigated further.

8.2.1 Experimental Work

Experimental studies of fermentation have several limitations. Prior knowledge about the fermentation process should be sufficient to make a good design of the experiment with regards to the purpose. Low data density of fermentative butanol production from lignocellulosic biomass is a common problem as well. In addition, lack of or insufficient data filtration hinders following the progress of fermentation, and creates uncertainty in models developed with these data. Thus, high performance data acquisition is important to obtain a complete understanding of complex substrate utilization and product formation kinetics. Complete understanding of the effect of different operating conditions on fermentation is lacking and transcriptome analysis can provide complimentary information on metabolic regulation. The suggestions for future work regarding these aspects are discussed more in detail in the sections below.

Experimental setups

During bioprocess development, initial screening of different strains and substrates or medium components are done in microtiter plates. After pre-selection of the tested conditions, experiments are done in a larger scale, typically in shake or serum flasks. Similarly, some of those conditions are selected and tested in bench-scale fermenters. This process stretches to pilot scale and industrial scale bioreactors. Therefore, different scales of fermentation are typically done in different types of bioreactors/setups, and each of them has drawbacks and benefits regarding the monitoring, sampling, operating and control options and capabilities. Hence, it is important to make a considerate selection of the experimental setup depending on the purpose of the experiment. For example, the microbioreactor unit used in

this thesis is advantageous if the objective is to scan as many parameters as possible in one run. On the other hand, taking and analyzing samples for quantification of sugars or other products during the fermentation are not possible in microbioreactors. Consequently, an attentive evaluation of experimental setups is necessary for scale up studies as well as for producing data specific to the purpose of the experiment.

Running replicates of experiments in parallel can help to demonstrate the reproducibility and to provide information about the inherent variability of the process. Therefore, it is beneficial to design the experiments and arrange the setups, which enable parallel runs of replicates. Then the results of replicates can be used to calculate standard deviations for each data point of each sugar and product providing a measure of uncertainty. Moreover, having replicates for every different operating condition can help to illustrate their effects on fermentation more clearly. Even though the operation of several bioreactors in parallel can be laborious, the improvement in results makes it worthwhile.

Measurement methods

Low data density of fermentative butanol production from lignocellulosic biomass is limiting the modeling and optimization of the process. Off-gas (CO_2), temperature and pH can be measured on-line with a relatively high frequency during the course of fermentation. On the other hand, quantification of sugars and metabolites (alcohols, acids) are done off-line by using chromatographic methods, which are time consuming and erroneous, and results in insufficient data. Therefore, it is significant to develop and employ on-line measurement methods that can provide reliable and adequate data points. Bench-top Raman analyzers with integrated auto-samplers are compact and easy-to-use units with shown possibility to use in fermentation applications. Use of Raman analyzers coupled with real time data analysis has the potential to overcome low data density problem of fermentation. Increased volume of real-time data can help to quantify and filter measurement errors as well, since it becomes tedious to distinguish error when data density is low.

Measurement of cell mass concentration has similar issues. Even though there is a number of methods available for its quantification, they only provide an approximation of the actual amount of active cells. Moreover, it is known that a fermentation culture consists of cells at different physiological states, which are associated with different metabolisms. Therefore, it is important to track the change in physiological states of the cells and

their distribution among the population to gain better understanding of the fermentation. Raman microscopes have been used for this purpose recently. However, analysis and filtering of the microscopic data would be required. All in all, there is a great number of measurement methods, which can be exploited with better utilization of on-line data analysis and filtering tools.

Transcriptome analysis

Transcriptome analysis reveals information about expression levels of genes encoding enzymes and gives a detailed view on gene regulation at genome scale. Expressions of the different genes encoding the enzymes as catalysts of different reactions in the metabolic pathway can be identified by transcriptome analysis. As mentioned throughout the thesis, cells go through different phases and physiological states, which are important for understanding fermentation. These changes in the cells and their metabolism can be detected and monitored by transcriptome analysis. Effects of sugar composition and concentration on fermentation are studied thoroughly with illustrated improvement in sugar utilization by the suggested pre-growth strategies. Transcriptome analysis can be used to support the usefulness of these strategies as well by determining the expression levels of enzymes responsible from using different sugars. To sum up, information about the changes in the transcriptome during changing operating conditions can support the findings of this thesis, and can be utilized further in Systems Biology level model development.

8.2.2 Modeling Work

Fermentation models are often criticized for having poor accuracy and predictability within a limited operating space. These issues are linked to insufficient, unfiltered or poor quality experimental data. Lack of models for describing fermentative butanol production from lignocellulosic hydrolysates needs to be addressed as well. The recommendations regarding these are discussed in the sections below.

Model fine-tuning

Improving quality of the experimental data can in return improve the quality of the model developed using them. As discussed in Section 8.2.1, increasing the number of data points (sampling frequency) will increase the degrees of freedom when estimating the model parameters, and then the confidence intervals will get smaller, thus the uncertainty associated

with the parameters will be lower. Similarly, filtering measurement errors improves the quality of data.

Averages of the data from replicated experiments and the standard deviations as weights can be used in weighted regression for parameter estimation. This extra information input to the modeling can increase the reliability.

Modeling fermentative butanol production from lignocellulosic hydrolysates

The models suggested in this thesis are describing the fermentation of pure sugars; glucose and xylose. However, there are typically more sugars present in the lignocellulosic biomass hydrolysates as presented in Figure 3.1. Therefore, extension of the proposed model with more sugars can be beneficial in terms of more realistic description of the process. To approach the real application even closer, a model for lignocellulosic biomass hydrolysate fermentation is necessary. Comparison of the models developed by using all the sugars present in the hydrolysate and the actual hydrolysate will reveal very important information about the effect of inhibitors present in the hydrolysate as discussed in Section 2.2.3, and will help to quantify those effects. For development of these models, the methodology of this thesis can be followed. First, the characterization and modeling of the cell mass growth on those particular sugar mixtures/hydrolysates, and then the development of the model describing the substrate utilizations as well as the butanol production, in addition to the cell mass growth. Validation of these models is required to demonstrate the application range of the model.

APPENDICES
A-B

Appendix A

Correlations

Correlations between fermentation variables are shown in Table A.1.

Table A.1: Kendall's correlation coefficients for correlations between 22 fermentation variables.

S_i	SG_i	SX_i	$SG_{i,r}$	$SX_{i,r}$	HAc_i	S_u	S_{ur}	SG_u	SG_{ur}	SX_u	SX_{ur}	Ac	$BuOH$	$EtOH$	ABE	HBu	HAc	$Acids$	ABE_y	$BuOH_y$	$BuOH_r$	
S_i	1.00	0.49	0.41	0.05	0.13	0.13	-0.24	0.39	-0.15	0.20	-0.13	0.29	0.27	0.30	0.31	0.17	0.26	0.16	-0.09	-0.19	-0.16	
SG_i	0.49	1.00	-0.02	0.56	-0.27	0.36	-0.20	0.75	-0.24	-0.11	-0.16	0.30	0.25	0.23	0.29	0.07	0.16	0.09	0.03	-0.08	-0.14	
SX_i	0.41	-0.02	1.00	-0.40	0.73	-0.05	0.33	-0.06	0.18	0.61	0.00	0.11	0.11	0.33	0.15	0.07	0.12	0.06	-0.14	-0.20	-0.08	
$SG_{i,r}$	0.05	0.56	-0.40	1.00	-0.52	0.42	0.00	-0.03	0.43	-0.25	-0.33	0.14	0.07	0.01	0.09	-0.08	-0.05	-0.09	0.07	0.05	-0.11	
$SX_{i,r}$	0.13	-0.27	0.73	-0.52	1.00	-0.14	0.14	0.06	-0.13	0.27	0.56	-0.01	0.00	0.21	0.02	-0.02	-0.01	-0.03	-0.16	-0.16	-0.04	
HAc_i	0.13	0.36	-0.05	0.42	-0.14	1.00	0.08	-0.07	0.25	-0.27	0.04	0.17	0.24	0.30	0.27	-0.06	0.25	0.17	0.36	0.33	0.11	
S_u	0.54	0.31	0.33	0.00	0.14	0.08	1.00	0.23	0.47	0.21	0.44	0.21	0.53	0.56	0.64	0.05	0.17	0.10	0.07	-0.04	-0.07	
S_{ur}	-0.24	-0.20	-0.06	-0.03	0.06	-0.07	0.23	1.00	0.01	0.55	0.24	0.61	0.22	0.27	0.12	0.25	-0.08	-0.08	0.23	0.20	0.05	
SG_u	0.39	0.75	0.05	0.43	-0.13	0.25	0.47	1.00	0.09	-0.01	-0.08	0.38	0.33	0.22	0.38	0.08	0.19	0.13	0.04	-0.05	-0.02	
SG_{ur}	-0.15	-0.24	0.18	-0.25	0.27	-0.27	0.21	0.55	0.09	1.00	0.20	0.21	0.18	0.18	0.17	0.12	0.07	0.10	0.09	0.10	0.18	
SX_u	0.20	-0.11	0.61	-0.33	0.56	0.04	0.44	0.24	-0.01	0.20	1.00	0.41	0.26	0.31	0.32	-0.14	-0.02	-0.09	0.01	-0.01	-0.06	
SX_{ur}	-0.13	-0.16	0.00	-0.04	0.12	0.17	0.21	0.61	-0.08	0.21	0.41	1.00	0.24	0.22	0.22	-0.24	-0.13	-0.20	0.14	0.16	-0.01	
Ac	0.29	0.30	0.11	0.14	-0.01	0.24	0.53	0.22	0.38	0.10	0.26	0.24	1.00	0.62	0.73	-0.22	0.00	-0.13	0.41	0.27	-0.26	
$BuOH$	0.27	0.25	0.11	0.07	0.00	0.30	0.56	0.27	0.33	0.18	0.31	0.22	0.62	1.00	0.86	-0.15	0.07	-0.05	0.42	0.40	0.08	
$EtOH$	0.30	0.23	0.33	0.01	0.21	0.00	0.38	0.12	0.22	0.18	0.33	0.12	0.23	0.29	1.00	0.34	-0.05	0.07	-0.01	0.03	-0.22	
ABE	0.31	0.29	0.15	0.09	0.02	0.27	0.64	0.25	0.38	0.17	0.32	0.22	0.73	0.86	1.00	-0.19	0.07	-0.07	0.43	0.36	-0.06	
HBu	0.17	0.07	0.07	-0.08	-0.02	-0.06	0.05	-0.08	0.08	0.12	-0.14	-0.24	-0.22	-0.15	-0.05	1.00	0.42	0.66	-0.23	-0.29	0.08	
HAc	0.26	0.16	0.12	-0.05	-0.01	0.25	0.17	-0.08	0.19	0.07	-0.02	-0.13	0.00	0.07	0.07	0.42	1.00	0.76	0.09	-0.05	0.14	
$Acids$	0.16	0.09	0.06	-0.09	-0.03	0.17	0.10	-0.08	0.13	0.10	-0.09	-0.20	-0.13	-0.05	-0.01	0.66	0.76	1.00	-0.08	-0.17	0.15	
ABE_y	-0.09	0.03	-0.14	0.07	-0.16	0.36	0.07	0.23	0.04	0.09	0.01	0.14	0.41	0.42	0.03	0.43	-0.23	0.09	1.00	0.74	0.05	
$BuOH_y$	-0.19	-0.08	-0.20	0.05	-0.16	0.33	-0.04	0.20	-0.05	0.10	-0.01	0.16	0.27	0.40	-0.02	0.36	-0.29	-0.05	-0.17	1.00	0.31	
$BuOH_r$	-0.16	-0.14	-0.08	-0.11	-0.04	0.11	-0.07	0.05	-0.02	0.18	-0.06	-0.01	-0.26	0.08	-0.22	-0.06	0.08	0.14	0.15	0.05	0.31	1.00

Appendix B

Materials and Methods

B.1 Bacterial Strain

An industrial, wild type *Clostridium beijerinckii* NCIMB 8052 strain, provided by the Biotechnology and Nanomedicine group in SINTEF Industry was used. Work ampoules (1 ml) were prepared by pre-growing the strain provided in frozen form in Reinforced *Clostridial* Medium (CM0149), and then mixing them with 20% glycerol solution to prevent damage due to freezing. All the work ampoules were stored at the deep freezer at -80°C . The work ampoules prepared in the same batch were used in the experiments.

B.2 Media

Two different types of media were used in the experiments presented in this thesis. They are presented in detail below.

B.2.1 Pre-growth Media

The revival of frozen work ampoules were done by a 14 hour pre-growth in the Reinforced *Clostridial* Medium (RCM)(CM0149) by Oxoid, Thermo Scientific designed by Hirsch and Grinstead¹ for the cultivation and enumeration of *Clostridia* [214]. The RCM medium was in powder form, and 38 g of it was suspended in 1 litre of distilled water. Then, it was brought to the boil to dissolve completely followed by sterilization with autoclave at 121°C for 15 minutes. The autoclaved media were flushed with biological grade nitrogen gas upon cooling to have anaerobic conditions. Final pH of

the medium was 6.8 ± 0.2 . Typical composition of the Reinforced *Clostridial* Medium (RCM) is shown in Table B.1.

Table B.1: Typical composition of Reinforced *Clostridial* Medium, CM0149.

Component	Molecular formula	Concentration (g/l)
Yeast extract	-	13
Peptone	-	10
Glucose	$C_6H_{12}O_6$	5
Soluble starch	$(C_6H_{12}O_6)_n \cdot H_2O$	5
Sodium chloride	NaCl	5
Sodium acetate	$C_2H_3NaO_2$	3
Cysteine hydrochloride	$HSCH_2CH(NH_2)COOH \cdot HCl$	0.5
Agar	-	0.5

B.2.2 Fermentation Media

The cultures pre-grown on the RCM medium presented above were used as the inocula for fermentation experiments performed both in serum flasks and fermenters. Except the sugar(s), composition of the fermentation media were the same in all experiments. Components of the fermentation medium are shown in Table B.2 together with their concentrations (g/l) for 1 l medium. Separate stock solutions were prepared for every component as shown in Table B.2. In serum flask experiments, 232.5 g/l sugar solutions containing equal amounts of glucose and xylose and in the fermentation experiments, separate glucose and xylose solutions with 232.5 g/l concentrations were used. Vitamins were filter sterilized and stored in the freezer at $-20^\circ C$ and the rest were stored in the fridge at $4^\circ C$.

For the medium preparation, respective amounts (volume in ml) of the components were mixed with the sterile and anaerobic distilled water to have the designated the liquid volume of the particular experiment. Sodium acetate, yeast extract, ammonium sulfate, sodium chloride, magnesium sulfate heptahydrate and manganese sulfate monohydrate comprise the base medium and were autoclaved together. Potassium salts, KH_2PO_4

and K_2HPO_4 , and sugar solutions were autoclaved separately. Iron solution was filter sterilized as well as the vitamins. All the components were mixed and stirred thoroughly in a magnetic stirrer while flushed with biological grade nitrogen gas.

Table B.2: Medium components used in fermentation and flask test experiments.

Component	Molecular formula	Concentration (g/l)	Stock solution used
Sodium acetate	$C_2H_3NaO_2$	2.5	250 g/l
Yeast extract	-	5	200 g/l
Ammonium sulfate	$(NH_4)_2SO_4$	2	400 g/l
Sodium chloride	NaCl	0.01	0.01 g/ml
Magnesium sulfate heptahydrate	$MgSO_4 \cdot 7H_2O$	0.2	40 g/l
Manganese(II) sulfate monohydrate	$MnSO_4 \cdot H_2O$	0.01	0.079 g/ml
Monopotassium phosphate	KH_2PO_4	0.75	15 g/100 ml
Dipotassium phosphate	K_2HPO_4	1.50	30 g/100 ml
Iron(II) sulfate heptahydrate	$FeSO_4 \cdot 7H_2O$	0.01	100 mg/ml
p-aminobenzoic acid		0.01	50 mg/ml
Biotin		0.01	50 mg/ml
Thiamine		0.01	50 mg/ml

B.3 Analytical Methods

B.3.1 Optical Density Measurement

Optical density (OD) was used as a measure for cell mass concentration, measured at 660 nm with a UV-vis spectrophotometer UV-1700 (Shimadzu)

with water as the reference. Samples exceeding 0.4 OD were diluted with water so that the Beer-Lambert Law is applied. The OD readings were converted to cell mass concentrations as explained below.

B.3.2 Dry Cell Weight Estimation

The dry cell mass samples were centrifuged (10000 rpm) at 5 °C for 5 minutes and pelleted cell mass washed with deionized water for three times. The cells were then dried at 120 °C until constant weight was obtained.

B.3.3 High Performance Liquid Chromatography

The samples for determining concentrations of glucose, xylose and butanol were filtrated (Millipore filter, 0.2 micrometre) before analysis by using a HPLC system (Shimadzu Model 9) equipped with UV (210 nm) and RI detector and an Aminex HPX-87H column (Biorad). Samples were eluted with 5 mM H₂SO₄ buffer, flow rate 0.6 ml/min at 45 °C. Quantification was performed using standards for each component.

B.4 Growth Conditions

There were two types of fermentations, done in the serum flasks and in the fermenters. Both were started upon inoculation with active cultures, pre-grown on the RCM media. Details of the growth conditions are given the chapters below.

B.4.1 Pre-growth Conditions

The RCM media were anaerobically prepared with 50 ml volume in 120 ml serum bottles sealed with rubber stoppers. The fresh media were inoculated with 1 ml of frozen work ampoules (2% v/v). The inoculated media were then incubated at 37 °C under static conditions for 14 hours, which was found as the optimal for *C. beijerinckii* [215].

B.4.2 Serum Flask Experiments

Serum flask experiments were done in 120 ml serum bottles with 50 ml working volume, inoculum size of 4% v/v, at 37 °C static and anaerobic conditions.

B.4.3 Microbioreactor Experiments

Fermentations were performed in round-well plates with 48x 3 ml microbioreactor wells with 1.5 ml working volume. Anaerobic conditions were sustained by flushing with biological grade nitrogen gas at 37 °C and shaking at 400 rpm in a BioLector[®] instrument (m2p-labs; Baesweiler, Germany). Cultures in the wells were started with inoculum size of 4% v/v. The BioLector[®] measures cell mass density by scattered light, which was measured every 20 minutes in the present study. A gain of 20 (EX: 620 nm, EM:620 nm) was used for the experiments to avoid saturation at high optical densities. pH was measured every 20 minutes with a gain of 19 (EX: 470 nm, EM: 525 nm). Photo of the BioLector[®], microbioreactor setup is shown in Figure B.1 together with a microbial well plate and a single well.

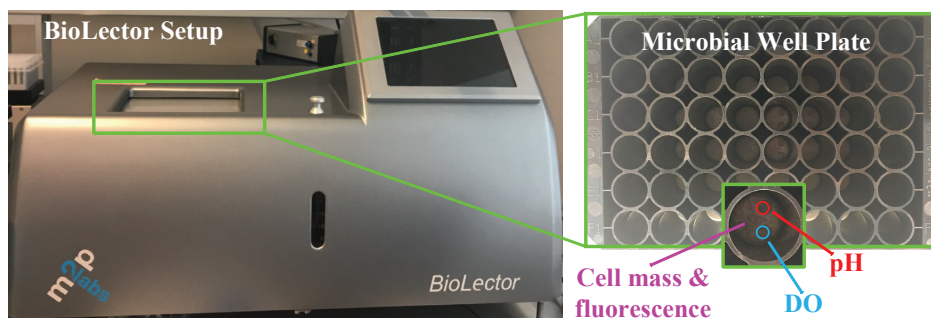


Figure B.1: BioLector[®] setup, round-well plate, and a single well showing the sensors for dissolved oxygen (DO), pH, cell mass and fluorescence.

B.4.4 Fermentation Experiments

Fermentation experiments were done in 2 l Applikon fermenters with 1 l working volume, inoculum size of 4% v/v, at 37 °C stirred at 150 rpm and flushed with biological grade nitrogen gas (0.5 l/min) to sustain anaerobic conditions. There was no pH control applied.

B.5 Exploratory Data Analysis

Exploratory data analysis was performed to statistically visualize the fermentation variables and the correlations between them by means of box-plots and correlation plots, respectively. Further explanations can be found in the chapters below.

B.5.1 Boxplot

Boxplots are typically used for visualization of statistics and shown as rectangles. Matlab function, `boxplot` is used. On each rectangle, the central mark indicates 50th percentile that is the median, and the left and right edges of the box indicate the 25th and 75th percentiles, respectively, for a boxplot stretching along the x-axis. A percentile is a measure indicating the value below which a given percentage of data in a data set fall.

Whisker are the dashed lines extending from the boxes. Their default value is approximately $\pm 2.7\sigma$ and 99.3 percent coverage if the data are normally distributed. The plotted whisker extends to the adjacent value, which is the most extreme data value that is not an outlier. Outliers are plotted individually using the '+' symbol, if they are greater than $q3 + w \times (q3 - q1)$ or less than $q1 - w \times (q3 - q1)$, where w is the maximum whisker length, and $q1$ and $q3$ are the 25th and 75th percentiles of the data set, respectively.

B.5.2 Correlations

Kendall's correlation coefficient shows the correlations among pairs of variables in a data set. Matlab function, `corr` is used for this purpose with pairwise option so that correlation coefficient is computed only for the rows with no missing values in columns i or j . Kendall's τ is based on counting the number of (i,j) pairs, for $i < j$, that are concordant. That is for which $X_{a,i} - X_{a,j}$ and $Y_{b,i} - Y_{b,j}$ have the same sign. The equation for Kendall's tau includes an adjustment for ties in the normalizing constant. For column X_a in matrix X and column Y_b in matrix Y , Kendall's τ coefficient is given in Equation B.1.

$$\tau = \frac{2K}{n(n-1)} \quad (\text{B.1})$$

where $K = \sum_{i=1}^{n-1} \sum_{j=i+1}^n \xi^*(X_{a,i}, X_{a,j}, Y_{b,i}, Y_{b,j})$ and

$$\xi^*(X_{a,i}, X_{a,j}, Y_{b,i}, Y_{b,j}) = \begin{cases} 1 & \text{if } (X_{a,i} - X_{a,j})(Y_{b,i} - Y_{b,j}) > 0 \\ 0 & \text{if } (X_{a,i} - X_{a,j})(Y_{b,i} - Y_{b,j}) = 0 \\ -1 & \text{if } (X_{a,i} - X_{a,j})(Y_{b,i} - Y_{b,j}) < 0 \end{cases}$$

The coefficient has a value between -1 and +1 where +1 is total positive correlation, 0 is no correlation, -1 and is total negative correlation. When the p value is less than the significance level of 0.05, it indicates rejection of the hypothesis that no correlation exists between the two columns.

B.6 Analysis of Variance

Analysis of variance (ANOVA) is a procedure to assign sample variance to different sources and to decide whether the variation arises within or among different population groups. A two-way, nonparametric ANOVA method, Friedman's test is used in this thesis. Friedman's test assumes that all data come from populations having the same continuous distribution, apart from possibly different locations due to column and row effect, and all observations are mutually independent [216]. It does not test for row effects or interaction effects. Friedman's test is appropriate when columns represent treatments that are under study, and rows represent nuisance effects (blocks) that need to be taken into account but are not of any interest.

The different columns of X represent changes in a factor A. The different rows represent changes in a blocking factor B. If there is more than one observation for each combination of factors, input reps indicates the number of replicates and it must be constant. The matrix below illustrates the format for a set-up where column factor A has three levels, row factor B has two levels, and there are two replicates (reps=2). The subscripts indicate row, column, and replicate, respectively.

$$X = \begin{bmatrix} x_{111} & x_{121} & x_{131} \\ x_{112} & x_{122} & x_{132} \\ x_{211} & x_{221} & x_{231} \\ x_{212} & x_{222} & x_{232} \end{bmatrix}$$

Friedman's test assumes a model of the form shown in Equation B.2.

$$x_{ijk} = \mu + \alpha_i + \beta_j + \varepsilon_{ijk} \quad (\text{B.2})$$

where μ is an overall location parameter, α_i and β_j represent the column and row effects, respectively, and ε_{ijk} represents the error. This test ranks the data within each level of B, and tests for a difference across levels of A.

Friedman's test makes the following assumptions about the data in X :

- Data does not need to come from a normal distribution.
- All data come from populations having the same continuous distribution, apart from possibly different locations due to column and row effects.
- All observations are mutually independent.

The p value that friedman returns is the probability that a chi-square statistic with a specific degrees of freedom, df is more extreme than calculated value of chi-square. If the p value is near zero, this casts doubt on the null hypothesis. A sufficiently small p value suggests that at least one column-sample median is significantly different than the others; i.e., there is a main effect due to factor A. It is common to declare a result significant if the p value is less than 0.05 or 0.01. The chi-square test statistic is shown in Equation B.3.

$$T = (n - 1) \left(\frac{s}{\sigma_0} \right)^2 \quad (\text{B.3})$$

where n is the sample size, s is the sample standard deviation, and σ is the hypothesized standard deviation. The denominator is the ratio of the sample standard deviation to the hypothesized standard deviation. The further this ratio deviates from 1, the more likely you are to reject the null hypothesis. The test statistic, T has a chi-square distribution with $(n - 1)$ degrees of freedom under the null hypothesis.

B.7 Determination of Kinetic Coefficients and Fermentation Variables

The kinetic coefficients can be used to characterize a fermentation process and asses its performance. The coefficients used in this thesis are shown below.

The maximum specific growth rate, μ_{max} (h^{-1}) is equal to specific growth rate, μ (h^{-1}) during exponential growth phase as shown in Equation B.4, since the nutrient concentration is high enough so that the growth rate is independent of nutrient concentration.

$$\frac{dX}{dt} = \mu \cdot X \quad (\text{B.4})$$

The specific growth rate is determined during the exponential growth phase by integration of Equation B.4, which yields Equation B.5.

$$\ln \left(\frac{X}{X_0} \right) = \mu \cdot t \quad (\text{B.5})$$

where t is time (h), and X and X_0 are the cell mass concentrations (g/l) at time t and $t = 0$, respectively.

Cell mass yield, $Y_{X/S}$ (g cell/g sugar), butanol yield, $Y_{B/S}$ ($BuOH_y$) (g butanol/g sugar), butanol yield on cell mass, $Y_{B/X}$ (g butanol/g cell),

solvent yield, ABE_y (g solvent/g sugar) are shown in Equations B.6, B.7, B.8, and B.9, respectively. Butanol ratio in solvent mixture, $BuOH_r$ (g butanol/g ABE solvents) is given in Equation B.10.

$$Y_{X/S} = \frac{X_f - X_i}{S_i - S_f} \quad (\text{B.6})$$

$$Y_{B/S} = \frac{BuOH}{S_i - S_f} \quad (\text{B.7})$$

$$Y_{B/X} = \frac{BuOH}{X_f - X_i} \quad (\text{B.8})$$

$$ABE_y = \frac{ABE}{S_i - S_f} \quad (\text{B.9})$$

$$BuOH_r = \frac{BuOH}{ABE} \quad (\text{B.10})$$

where X_i and X_f are initial and final cell mass concentrations (g/l), S_i and S_f are initial and final total sugar concentrations (g/l), $BuOH$ is total butanol production (g/l), ABE is total solvent production (g/l).

Glucose and xylose ratios in the sugar mixture (%), SG_{ir} and SX_{ir} are shown in Equation B.11 and Equation B.12.

$$SG_{ir} = \frac{SG_i}{S_i} \times 100\% \quad (\text{B.11})$$

$$SX_{ir} = \frac{SX_i}{S_i} \times 100\% \quad (\text{B.12})$$

where SX_i and S_i are initial glucose and xylose concentrations (g/l).

Utilized amounts of total sugar, glucose and xylose, S_u , SG_u and SX_u (g/l), and their percental utilizations S_{ur} , SG_{ur} and SX_{ur} (%) are shown in Equations B.13, B.14, B.15, B.16, B.17 and B.18.

$$S_u = (S_i - S_f) \quad (\text{B.13})$$

$$SG_u = (SG_i - SG_f) \quad (\text{B.14})$$

$$SX_u = (SX_i - SX_f) \quad (\text{B.15})$$

$$S_{ur} = \left(\frac{S_i - S_f}{S_i} \right) \times 100\% \quad (\text{B.16})$$

$$SG_{ur} = \left(\frac{SG_i - SG_f}{SG_i} \right) \times 100\% \quad (\text{B.17})$$

$$SX_{ur} = \left(\frac{SX_i - SX_f}{SX_i} \right) \times 100\% \quad (\text{B.18})$$

B.8 Design of Experiments

Design of experiments enables planning experiments with systematic data collection. *Central Composite Design* (CCD), also referred as Box-Wilson Design, is a five-level fractional factorial design of experiments. Circumscribed, inscribed, and face-centered are the three types of CCDs. Circumscribed central composite (CCC) design was used in this thesis due to its ability to provide good accuracy of estimation over the entire design space using built-in Matlab function `ccdesign`. Figure B.2 shows a geometrical representation of the CCC design.

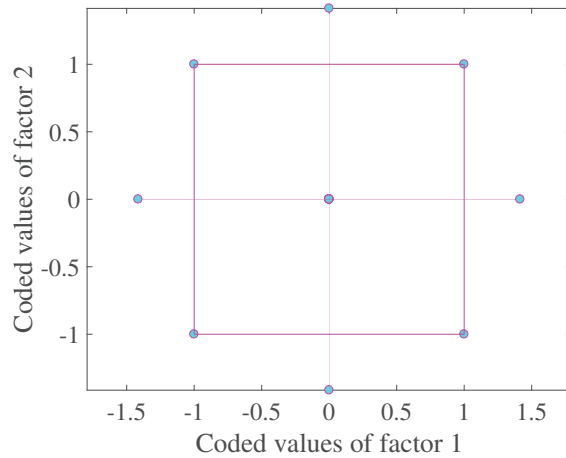


Figure B.2: A geometrical representation of the CCC design with two factors.

The five-level coded values of each factor are represented by $[-\alpha, -1, 0, 1, +\alpha]$. For a two factor CCC design, α is equal to 1.4142, and the design consists of 16 experimental runs with 8 of them in the centre point to reduce the effects of correlations between the factors. The minimum and maximum values for the factors were determined first, then the real values for each experiment were obtained according to the coded values.

B.9 Regression

B.9.1 Linear Regression

A quadratic linear model given in Equation B.19 is fitted with experimental data obtained from CCC design of experiments by using Matlab

function fitlm for linear regression analysis applying least squares method.

$$Y = A_0 + \sum A_i X_i + \sum A_{ii} X_i^2 + \sum A_{ij} X_i X_j \quad (\text{B.19})$$

where Y is the response, A_0 is the constant coefficient, A_i is the linear coefficient, A_{ii} is the quadratic coefficient and A_{ij} is the interaction coefficient. X_i and X_j are factor level values determined by CCC design.

p value for F-statistic

In linear regression, the F-statistic is the test statistic, which tests whether the model fits significantly better than a degenerate model consisting of only a constant term. When the null hypothesis is true, the F-statistic follows the F-distribution. p value for the F-statistic is used to determine the significance.

p value for t-statistic

In linear regression, the t-statistic is used to make inferences about the regression coefficients. t-statistic for each coefficient to test the null hypothesis that the corresponding coefficient is zero, which means that the corresponding term is not significant versus the alternate hypothesis that the coefficient is different from zero.

$$tStat = \frac{A_i}{SE_i} \quad (\text{B.20})$$

where A_i is the coefficient estimate and SE_i is the standard error of the estimated coefficient, A_i .

p value for the t-statistic of the hypothesis test that the corresponding coefficient is equal to zero or not.

B.9.2 Nonlinear Regression

The binary substrate growth models given in the chapter were fitted by using the Matlab function nlinfit for nonlinear regression, which uses the Levenberg-Marquardt nonlinear least squares algorithm. The parameter estimates minimize the least squares equation, Equation B.21.

$$\sum_{i=1}^N (Y_i - f(X_i, b))^2 \quad (\text{B.21})$$

where $f(X_i, b)$ is the nonlinear function, X_i are the predictors for i^{th} observation, $i = 1, \dots, N$, and b are the parameters.

95% confidence intervals for the model parameters were obtained by using `nlparci`, and `CovB` output argument of `nlinfit` gives covariance matrix, which was then converted to a correlation matrix by using `corrcoef` function. `R` argument of the `nlinfit` function was used to get raw residuals data to visualize the difference between the simulated and observed values of the growth rate.

B.10 Parameter Estimation

The model parameters were unknown a priori; therefore, they were estimated from experimental data. Observed concentrations of cell mass, glucose, xylose, and butanol are used:

$$y = [[X] [SG] [SX] [B]]^T$$

for estimation of parameters

$$\Theta = [Y_{X/SG} Y_{X/SX} Y_{B/SG} Y_{B/SX} k_d B_{max} i_B K_I \mu_{maxG} K_{sG} K_{sX} \mu_{maxX}]^T$$

The parameter estimation poses a nonlinear least-squares optimization problem

$$\hat{\Theta} = \underset{\Theta}{\operatorname{argmin}} \sum_{i=1}^{N_m} \sum_{j=1}^{N_v} (y_{ij}^{obs} - y_{ij}^{pred})^2 \quad (\text{B.22})$$

where $\hat{\Theta}$ denotes the estimated values of the parameters Θ ; and y^{obs} and y^{pred} denote the observed and predicted concentrations of the components. Number of components, N_m , is 4. Number of observations, N_v , is 14. The subscript ij denotes the j^{th} value of the i^{th} component.

The objective of the parameter estimation problem in Equation B.22 is to determine the parameters, Θ , by minimizing the squared difference between the observed and predicted concentrations of the components in y . The constrained nonlinear optimization problem is solved using `fmincon` in MATLAB 2017b Optimization Toolbox based on the interior point algorithm together with `ode45` solver.

B.10.1 Determination of Parameter Bounds

The bounds for yield coefficients were determined using stoichiometric relations between the components [127, 166], which are shown below.





Rest of the parameter bounds were taken from literature [212]. The optimization problem was initialized by with the initial points, which were the middle points between the upper and lower bounds of the parameters. The parameter bounds considered in the optimization problem are given in Table B.3 together with the initial points.

Table B.3: Model parameters, their bounds and initial points used for initialization.

Parameter	Unit	Lower bound	Upper bound	Initial point
$Y_{X/SG}$	g/g	0	0.689	0.345
$Y_{X/SX}$	g/g	0	0.689	0.345
$Y_{B/SG}$	g/g	0	0.412	0.206
$Y_{B/SX}$	g/g	0	0.494	0.247
k_d	h^{-1}	0	0.100	0.050
B_{max}	g/l	10	20	15
i_B	-	0	10	5
K_I	g/l	125	250	187
μ_{maxG}	h^{-1}	0	1	0.500
K_{sG}	g/l	0	10	5
K_{sX}	g/l	0	10	5
μ_{maxX}	h^{-1}	0	1	0.500

B.11 Index of Model Accuracy

Average squared correlation coefficient, r^2 was employed as the model accuracy index and it was calculated as shown below. Equation B.27 shows

sum of squared error (SSE) between the observed and predicted values of the components.

$$SSE = \sum_{t=0}^{t_{end}} (y_i^{obs}(t) - y_i^{pred}(t))^2 \quad (\text{B.27})$$

where $y_i^{obs}(t)$ and $y_i^{pred}(t)$ denote the observed and predicted concentrations of the components, $i = X, SG, SX, B$ at time t , and the subscript i denotes value of the i^{th} measured component.

Sum of squared total (SST), which is a quantification of the observations', $y_i^{obs}(t)$ variation around their mean, \bar{y}_i^{obs} was calculated as in Equation B.28.

$$SST = \sum_{t=0}^{t_{end}} (y_i^{obs}(t) - \bar{y}_i^{obs})^2 \quad (\text{B.28})$$

By using SSE and SST values, average squared correlation coefficients for each component was calculated with the formula given in Equation B.29.

$$r^2 = 1 - \frac{SSE}{SST} \quad (\text{B.29})$$

B.12 Sensitivity Analysis

Sensitivity analysis was conducted by 10% perturbations in each of 12 parameters. The sensitivity can be measured by comparing the final concentrations with perturbed and unperturbed parameters. End point deviations (ED) of cell mass, glucose, xylose and butanol as a result of each parameter perturbation are assessed. ED values were calculated as in Equation B.30.

$$ED_i^P(\%) = \frac{y_i(\Theta \pm \Delta\Theta, t_{end}) - y_i^{ref}(\Theta, t_{end})}{y_i^{ref}(\Theta, t_{end})} \quad (\text{B.30})$$

where $y_i(\Theta, t_{end})$ and $y_i(\Theta \pm \Delta\Theta, t_{end})$ represent the predicted concentration of i^{th} component at time t_{end} associated with unperturbed parameter Θ and perturbed parameter $\Theta \pm \Delta\Theta$, respectively. $y_i^{ref}(\Theta, t_{end})$ is the end concentration of the i^{th} component in the reference, where $i = X, SG, SX, B$.

References

- [1] Y. Jiang, J. Liu, W. Jiang, Y. Yang, and S. Yang, "Current status and prospects of industrial bio-production of n-butanol in china," *Biotechnology Advances*, vol. 33, no. 7, pp. 1493–1501, 2015.
- [2] S.-H. Lee, E. J. Yun, J. Kim, S. J. Lee, Y. Um, and K. H. Kim, "Biomass, strain engineering, and fermentation processes for butanol production by solventogenic clostridia," *Applied Microbiology and Biotechnology*, vol. 100, no. 19, pp. 8255–8271, 2016.
- [3] A. Ranjan and V. S. Moholkar, "Biobutanol: science, engineering, and economics," *International Journal of Energy Research*, vol. 36, no. 3, pp. 277–323, 2012.
- [4] T. G. Solomons and C. B. Fryhle, *Organic Chemistry John Wiley and Sons Inc.*, 2000.
- [5] C. Jin, M. Yao, H. Liu, F. L. Chia-fon, and J. Ji, "Progress in the production and application of n-butanol as a biofuel," *Renewable and Sustainable Energy Reviews*, vol. 15, no. 8, pp. 4080–4106, 2011.
- [6] H. Liu, G. Wang, and J. Zhang, *The promising fuel-biobutanol*. InTech, 2013.
- [7] S. B. Bankar, S. A. Survase, H. Ojamo, and T. Granström, "Biobutanol: the outlook of an academic and industrialist," *RSC Advances*, vol. 3, no. 47, pp. 24 734–24 757, 2013.
- [8] L. J. Visioli, H. Enzweiler, R. C. Kuhn, M. Schwaab, and M. A. Mazutti, "Recent advances on biobutanol production," *Sustainable Chemical Processes*, vol. 2, no. 1, p. 15, 2014.
- [9] J. Campos-Fernández, J. M. Arnal, J. Gómez, and M. P. Dorado, "A comparison of performance of higher alcohols/diesel fuel blends in a diesel engine," *Applied Energy*, vol. 95, pp. 267–275, 2012.

- [10] C. A. Heaton, *The chemical industry*. Springer Science and Business Media, 2012.
- [11] S. Nejame, “Butanol as a fuel—view from the field,” *Promotum, presentation to NREL*, 2010.
- [12] E. M. Green, “Fermentative production of butanol—the industrial perspective,” *Current Opinion in Biotechnology*, vol. 22, no. 3, pp. 337–343, 2011.
- [13] T. Millat and K. Winzer, “Mathematical modelling of clostridial acetone-butanol-ethanol fermentation,” *Applied Microbiology and Biotechnology*, vol. 101, no. 6, pp. 2251–2271, 2017.
- [14] L. Pasteur, “Quelques résultats nouveaux relatifs aux fermentations acétique et butyrique,” *Bull Soc Chim Paris*, pp. 52–53, 1862.
- [15] D. T. Jones and D. R. Woods, “Acetone-butanol fermentation revisited,” *Microbiological Reviews*, vol. 50, no. 4, p. 484, 1986.
- [16] H. G. Moon, Y.-S. Jang, C. Cho, J. Lee, R. Binkley, and S. Y. Lee, “One hundred years of clostridial butanol fermentation,” *FEMS Microbiology Letters*, vol. 363, no. 3, 2016.
- [17] S. C. Beesch, “Acetone-butanol fermentation of sugars,” *Industrial and Engineering Chemistry*, vol. 44, no. 7, pp. 1677–1682, 1952.
- [18] A. H. Rose, *Industrial microbiology*. Butterworths, 1961.
- [19] P. Dürre, “New insights and novel developments in clostridial acetone/butanol/isopropanol fermentation,” *Applied Microbiology and Biotechnology*, vol. 49, no. 6, pp. 639–648, 1998.
- [20] P. Rogers, J.-S. Chen, and M. J. Zidwick, *Organic acid and solvent production*. Springer, 2006, pp. 511–755.
- [21] V. Zverlov, O. Berezina, G. Velikodvorskaya, and W. Schwarz, “Bacterial acetone and butanol production by industrial fermentation in the soviet union: use of hydrolyzed agricultural waste for biorefinery,” *Applied Microbiology and Biotechnology*, vol. 71, no. 5, pp. 587–597, 2006.
- [22] B. Bharathiraja, J. Jayamuthunagai, T. Sudharsanaa, A. Bharghavi, R. Praveenkumar, M. Chakravarthy, and D. Yuvaraj, “Biobutanol—an impending biofuel for future: A review on upstream and downstream processing techniques,” *Renewable and Sustainable Energy Reviews*, vol. 68, pp. 788–807, 2017.
- [23] P. Dürre, “Butanol formation from gaseous substrates,” *FEMS Microbiology Letters*, vol. 363, no. 6, 2016.
- [24] L. D. Gottumukkala, K. Haigh, and J. Görgens, “Trends and advances in conversion of lignocellulosic biomass to biobutanol: Microbes, bioprocesses and industrial viability,” *Renewable and Sustainable Energy Reviews*, vol. 76, pp. 963–973, 2017.

- [25] Y. Jang, J. Lee, A. Malaviya, J. H. Cho, and S. Y. Lee, "Butanol production from renewable biomass: rediscovery of metabolic pathways and metabolic engineering," *Biotechnology Journal*, vol. 7, no. 2, pp. 186–198, 2012.
- [26] G. Jurgens, S. Survase, O. Berezina, E. Sklavounos, J. Linnekoski, A. Kurkijärvi, M. Väkevä, A. van Heiningen, and T. Granström, "Butanol production from lignocellulosics," *Biotechnology Letters*, vol. 34, no. 8, pp. 1415–1434, 2012.
- [27] S. Maiti, G. Gallastegui, S. J. Sarma, S. K. Brar, Y. Le Bihan, P. Drogui, G. Buelna, and M. Verma, "A re-look at the biochemical strategies to enhance butanol production," *Biomass and Bioenergy*, vol. 94, pp. 187–200, 2016.
- [28] N. Qureshi and T. C. Ezeji, "Butanol, 'a superior biofuel' production from agricultural residues (renewable biomass): recent progress in technology," *Biofuels, Bioproducts and Biorefining*, vol. 2, no. 4, pp. 319–330, 2008.
- [29] Y. Wang, S.-H. Ho, H.-W. Yen, D. Nagarajan, N.-Q. Ren, S. Li, Z. Hu, D.-J. Lee, A. Kondo, and J.-S. Chang, "Current advances on fermentative biobutanol production using third generation feedstock," *Biotechnology Advances*, 2017.
- [30] C. Xue, J. Zhao, F. Liu, C. Lu, S.-T. Yang, and F.-W. Bai, "Two-stage in situ gas stripping for enhanced butanol fermentation and energy-saving product recovery," *Bioresource Technology*, vol. 135, pp. 396–402, 2013.
- [31] P. Dürre, "Fermentative production of butanol—the academic perspective," *Current Opinion in Biotechnology*, vol. 22, no. 3, pp. 331–336, 2011.
- [32] S. Nanda, D. Golemi-Kotra, J. C. McDermott, A. K. Dalai, I. Gökalp, and J. A. Kozinski, "Fermentative production of butanol: perspectives on synthetic biology," *New Biotechnology*, vol. 37, pp. 210–221, 2017.
- [33] P. Patakova, J. Kolek, K. Sedlar, P. Koscova, B. Branska, K. Kupkova, L. Paulova, and I. Provaznik, "Comparative analysis of high butanol tolerance and production in clostridia," *Biotechnology Advances*, 2017.
- [34] E. P. Knoshaug and M. Zhang, "Butanol tolerance in a selection of microorganisms," *Applied Biochemistry and Biotechnology*, vol. 153, no. 1-3, pp. 13–20, 2009.
- [35] A. Kujawska, J. Kujawski, M. Bryjak, and W. Kujawski, "Abe fermentation products recovery methods—a review," *Renewable and Sustainable Energy Reviews*, vol. 48, pp. 648–661, 2015.
- [36] Y.-S. Jang, A. Malaviya, C. Cho, J. Lee, and S. Y. Lee, "Butanol production from renewable biomass by clostridia," *Bioresource Technology*, vol. 123, pp. 653–663, 2012.
- [37] Y. Gu, Y. Jiang, S. Yang, and W. Jiang, "Utilization of economical substrate-derived carbohydrates by solventogenic clostridia: pathway dissection, regulation and engineering," *Current Opinion in Biotechnology*, vol. 29, pp. 124–131, 2014.

- [38] P. Patakova, M. Linhova, M. Rychtera, L. Paulova, and K. Melzoch, "Novel and neglected issues of acetone–butanol–ethanol (abe) fermentation by clostridia: Clostridium metabolic diversity, tools for process mapping and continuous fermentation systems," *Biotechnology Advances*, vol. 31, no. 1, pp. 58–67, 2013.
- [39] C. Xue, J. Zhao, L. Chen, S.-T. Yang, and F. Bai, "Recent advances and state-of-the-art strategies in strain and process engineering for biobutanol production by clostridium acetobutylicum," *Biotechnology Advances*, vol. 35, no. 2, pp. 310–322, 2017.
- [40] H. Huang, H. Liu, and Y.-R. Gan, "Genetic modification of critical enzymes and involved genes in butanol biosynthesis from biomass," *Biotechnology Advances*, vol. 28, no. 5, pp. 651–657, 2010.
- [41] F. Hillmann, R. Fischer, F. Saint-Prix, L. Girbal, and H. Bahl, "Perr acts as a switch for oxygen tolerance in the strict anaerobe clostridium acetobutylicum," *Molecular Microbiology*, vol. 68, no. 4, pp. 848–860, 2008.
- [42] S. Y. Lee, J. H. Park, S. H. Jang, L. K. Nielsen, J. Kim, and K. S. Jung, "Fermentative butanol production by clostridia," *Biotechnology and Bioengineering*, vol. 101, no. 2, pp. 209–228, 2008.
- [43] J. Zaldivar, J. Nielsen, and L. Olsson, "Fuel ethanol production from lignocellulose: a challenge for metabolic engineering and process integration," *Applied Microbiology and Biotechnology*, vol. 56, no. 1-2, pp. 17–34, 2001.
- [44] F. Carvalheiro, L. C. Duarte, and F. M. Gírio, "Hemicellulose biorefineries: a review on biomass pretreatments," *Journal of Scientific and Industrial Research*, pp. 849–864, 2008.
- [45] K. Kalogiannis, S. Stefanidis, A. Marianou, C. Michailof, A. Kalogianni, and A. Lappas, "Lignocellulosic biomass fractionation as a pretreatment step for production of fuels and green chemicals," *Waste and Biomass Valorization*, vol. 6, no. 5, pp. 781–790, 2015.
- [46] P. Sannigrahi and A. J. Ragauskas, "Fundamentals of biomass pretreatment by fractionation," *Aqueous Pretreatment of Plant Biomass for Biological and Chemical Conversion to Fuels and Chemicals*, pp. 201–222, 2013.
- [47] C. Baldry, C. Bucke, and J. Coombs, "Progressive release of carboxylating enzymes during mechanical grinding of sugar cane leaves," *Planta*, vol. 97, no. 4, pp. 310–319, 1971.
- [48] X. Kong, H. Xu, H. Wu, C. Wang, A. He, J. Ma, X. Ren, H. Jia, C. Wei, and M. Jiang, "Biobutanol production from sugarcane bagasse hydrolysate generated with the assistance of gamma-valerolactone," *Process Biochemistry*, vol. 51, no. 10, pp. 1538–1543, 2016.
- [49] W. Lan, C.-F. Liu, F.-X. Yue, R.-C. Sun, and J. F. Kennedy, "Ultrasound-assisted dissolution of cellulose in ionic liquid," *Carbohydrate Polymers*, vol. 86, no. 2, pp. 672–677, 2011.

- [50] J.-P. Mikkola, A. Kirilin, J.-C. Tuuf, A. Pranovich, B. Holmbom, L. M. Kustov, D. Y. Murzin, and T. Salmi, "Ultrasound enhancement of cellulose processing in ionic liquids: from dissolution towards functionalization," *Green Chemistry*, vol. 9, no. 11, pp. 1229–1237, 2007.
- [51] N. Qureshi, B. C. Saha, and M. A. Cotta, "Butanol production from wheat straw hydrolysate using *clostridium beijerinckii*," *Bioprocess and Biosystems Engineering*, vol. 30, no. 6, pp. 419–427, 2007.
- [52] H. Su, G. Liu, M. He, and F. Tan, "A biorefining process: Sequential, combinational lignocellulose pretreatment procedure for improving biobutanol production from sugarcane bagasse," *Bioresource Technology*, vol. 187, pp. 149–160, 2015.
- [53] Y. Zhang, T. Hou, B. Li, C. Liu, X. Mu, and H. Wang, "Acetone–butanol–ethanol production from corn stover pretreated by alkaline twin-screw extrusion pretreatment," *Bioprocess and Biosystems Engineering*, vol. 37, no. 5, pp. 913–921, 2014.
- [54] C. Bellido, M. L. Pinto, M. Coca, G. González-Benito, and M. T. García-Cubero, "Acetone–butanol–ethanol (abe) production by *clostridium beijerinckii* from wheat straw hydrolysates: Efficient use of penta and hexa carbohydrates," *Bioresource Technology*, vol. 167, pp. 198–205, 2014.
- [55] T. Ezeji and H. P. Blaschek, "Fermentation of dried distillers' grains and solubles (ddgs) hydrolysates to solvents and value-added products by solventogenic clostridia," *Bioresource Technology*, vol. 99, no. 12, pp. 5232–5242, 2008.
- [56] K. Liu, H. K. Atiyeh, O. Pardo-Planas, T. C. Ezeji, V. Ujor, J. C. Overton, K. Berning, M. R. Wilkins, and R. S. Tanner, "Butanol production from hydrothermolysis-pretreated switchgrass: quantification of inhibitors and detoxification of hydrolyzate," *Bioresource Technology*, vol. 189, pp. 292–301, 2015.
- [57] Z. Sun and S. Liu, "Production of n-butanol from concentrated sugar maple hemicellulosic hydrolysate by *clostridia acetobutylicum atcc824*," *Biomass and Bioenergy*, vol. 39, pp. 39–47, 2012.
- [58] L. Wang and H. Chen, "Increased fermentability of enzymatically hydrolyzed steam-exploded corn stover for butanol production by removal of fermentation inhibitors," *Process Biochemistry*, vol. 46, no. 2, pp. 604–607, 2011.
- [59] H. Amiri, K. Karimi, and H. Zilouei, "Organosolv pretreatment of rice straw for efficient acetone, butanol, and ethanol production," *Bioresource Technology*, vol. 152, pp. 450–456, 2014.
- [60] A. Boonsombuti, K. Komolpis, A. Luengnaruemitchai, and S. Wongkasemjit, "Enhancement of abe fermentation through regulation of ammonium acetate and d-xylose uptake from acid-pretreated corncobs," *Annals of Microbiology*, vol. 64, no. 2, pp. 431–439, 2014.

- [61] J.-C. Ding, G.-C. Xu, R.-Z. Han, and Y. Ni, "Biobutanol production from corn stover hydrolysate pretreated with recycled ionic liquid by clostridium saccharobutylicum dsm 13864," *Bioresource Technology*, vol. 199, pp. 228–234, 2016.
- [62] K. Gao, S. Boiano, A. Marzocchella, and L. Rehm, "Cellulosic butanol production from alkali-pretreated switchgrass (*panicum virgatum*) and phragmites (*phragmites australis*)," *Bioresource Technology*, vol. 174, pp. 176–181, 2014.
- [63] L. D. Gottumukkala, B. Parameswaran, S. K. Valappil, K. Mathiyazhakan, A. Pandey, and R. K. Sukumaran, "Biobutanol production from rice straw by a non acetone producing clostridium sporogenes be01," *Bioresource Technology*, vol. 145, pp. 182–187, 2013.
- [64] C. N. Hipolito, E. Crabbe, C. M. Badillo, O. C. Zarrabal, M. A. M. Mora, G. P. Flores, M. d. A. H. Cortazar, and A. Ishizaki, "Bioconversion of industrial wastewater from palm oil processing to butanol by clostridium saccharoperbutylacetonicum n1-4 (atcc 13564)," *Journal of Cleaner Production*, vol. 16, no. 5, pp. 632–638, 2008.
- [65] J.-E. Lee, E.-J. Seo, D.-H. Kweon, K.-M. Park, and Y.-S. Jin, "Fermentation of rice bran and defatted rice bran for butanol production using clostridium beijerinckii ncimb 8052," *Journal of Microbiology and Biotechnology*, vol. 19, no. 5, pp. 482–490, 2009.
- [66] H. Li, L. Xiong, X. Chen, C. Wang, G. Qi, C. Huang, M. Luo, and X. Chen, "Enhanced enzymatic hydrolysis and acetone-butanol-ethanol fermentation of sugarcane bagasse by combined diluted acid with oxidate ammonolysis pretreatment," *Bioresource Technology*, vol. 228, pp. 257–263, 2017.
- [67] Z. Liu, Y. Ying, F. Li, C. Ma, and P. Xu, "Butanol production by clostridium beijerinckii atcc 55025 from wheat bran," *Journal of Industrial Microbiology and Biotechnology*, vol. 37, no. 5, pp. 495–501, 2010.
- [68] C. Lu, J. Zhao, S.-T. Yang, and D. Wei, "Fed-batch fermentation for n-butanol production from cassava bagasse hydrolysate in a fibrous bed bioreactor with continuous gas stripping," *Bioresource Technology*, vol. 104, pp. 380–387, 2012.
- [69] F. Moradi, H. Amiri, S. Soleimani-Zad, M. R. Ehsani, and K. Karimi, "Improvement of acetone, butanol and ethanol production from rice straw by acid and alkaline pretreatments," *Fuel*, vol. 112, pp. 8–13, 2013.
- [70] N. Qureshi, T. C. Ezeji, J. Ebener, B. S. Dien, M. A. Cotta, and H. P. Blaschek, "Butanol production by clostridium beijerinckii. part i: use of acid and enzyme hydrolyzed corn fiber," *Bioresource Technology*, vol. 99, no. 13, pp. 5915–5922, 2008.
- [71] N. Qureshi, B. C. Saha, B. Dien, R. E. Hector, and M. A. Cotta, "Production of butanol (a biofuel) from agricultural residues: Part i—use of barley straw hydrolysate," *Biomass and Bioenergy*, vol. 34, no. 4, pp. 559–565, 2010.

- [72] N. Qureshi, B. C. Saha, R. E. Hector, and M. A. Cotta, "Removal of fermentation inhibitors from alkaline peroxide pretreated and enzymatically hydrolyzed wheat straw: production of butanol from hydrolysate using *clostridium beijerinckii* in batch reactors," *Biomass and Bioenergy*, vol. 32, no. 12, pp. 1353–1358, 2008.
- [73] C. Tang, Y. Chen, J. Liu, T. Shen, Z. Cao, J. Shan, C. Zhu, and H. Ying, "Sustainable biobutanol production using alkali-catalyzed organosolv pretreated cornstalks," *Industrial Crops and Products*, vol. 95, pp. 383–392, 2017.
- [74] Y. Wang and H. P. Blaschek, "Optimization of butanol production from tropical maize stalk juice by fermentation with *clostridium beijerinckii* ncimb 8052," *Bioresource Technology*, vol. 102, no. 21, pp. 9985–9990, 2011.
- [75] F. Xin, Y. Wu, and J. He, "Simultaneous fermentation of glucose and xylose to butanol by *clostridium* species strain boh3," *Applied and Environmental Microbiology*, pp. AEM. 00 337–14, 2014.
- [76] M. Yang, J. Zhang, S. Kuittinen, J. Vepsäläinen, P. Soininen, M. Keinänen, and A. Pappinen, "Enhanced sugar production from pretreated barley straw by additive xylanase and surfactants in enzymatic hydrolysis for acetone–butanol–ethanol fermentation," *Bioresource Technology*, vol. 189, pp. 131–137, 2015.
- [77] L. Yu, M. Xu, I. Tang, and S. Yang, "Metabolic engineering of *clostridium tyrobutyricum* for n-butanol production through co-utilization of glucose and xylose," *Biotechnology and Bioengineering*, vol. 112, no. 10, pp. 2134–2141, 2015.
- [78] H. Jørgensen, J. B. Kristensen, and C. Felby, "Enzymatic conversion of lignocellulose into fermentable sugars: challenges and opportunities," *Biofuels, Bioproducts and Biorefining*, vol. 1, no. 2, pp. 119–134, 2007.
- [79] T. Ezeji, N. Qureshi, and H. P. Blaschek, "Production of acetone–butanol–ethanol (abe) in a continuous flow bioreactor using degermed corn and *clostridium beijerinckii*," *Process Biochemistry*, vol. 42, no. 1, pp. 34–39, 2007.
- [80] P. T. Pienkos and M. Zhang, "Role of pretreatment and conditioning processes on toxicity of lignocellulosic biomass hydrolysates," *Cellulose*, vol. 16, no. 4, pp. 743–762, 2009.
- [81] Y. Sun, Y. Jin, X. Gao, X. Li, Y. Xiao, and Z. Yao, "Effects of byproducts from acid hydrolysis of lignocelluloses on butanol fermentation by *clostridium acetobutylicum* cicc8012," *Chinese Journal of Applied and Environmental Biology*, vol. 16, no. 6, pp. 845–850, 2010.
- [82] S. Wang, Y. Zhang, H. Dong, S. Mao, Y. Zhu, R. Wang, G. Luan, and Y. Li, "Formic acid triggers the "acid crash" of acetone-butanol-ethanol fermentation of *clostridium acetobutylicum*," *Applied and Environmental Microbiology*, 2011.

- [83] I. Maddox, E. Steiner, S. Hirsch, S. Wessner, N. Gutierrez, J. Gapes, and K. Schuster, "The cause of" acid crash" and" acidogenic fermentations" during the batch acetone-butanol-ethanol(abe-) fermentation process," *Journal of Molecular Microbiology and Biotechnology*, vol. 2, no. 1, pp. 95–100, 2000.
- [84] N. Qureshi, B. C. Saha, R. E. Hector, B. Dien, S. Hughes, S. Liu, L. Iten, M. J. Bowman, G. Sarath, and M. A. Cotta, "Production of butanol (a biofuel) from agricultural residues: Part ii–use of corn stover and switchgrass hydrolysates," *Biomass and Bioenergy*, vol. 34, no. 4, pp. 566–571, 2010.
- [85] J. S. Terracciano and E. R. Kashket, "Intracellular conditions required for initiation of solvent production by clostridium acetobutylicum," *Applied and Environmental Microbiology*, vol. 52, no. 1, pp. 86–91, 1986.
- [86] Q. He and H. Chen, "Improved efficiency of butanol production by absorbed lignocellulose fermentation," *Journal of Bioscience and Bioengineering*, vol. 115, no. 3, pp. 298–302, 2013.
- [87] N. Qureshi, B. A. Annous, T. C. Ezeji, P. Karcher, and I. S. Maddox, "Biofilm reactors for industrial bioconversion processes: employing potential of enhanced reaction rates," *Microbial Cell Factories*, vol. 4, no. 1, p. 24, 2005.
- [88] S.-Y. Li, R. Srivastava, S. L. Suib, Y. Li, and R. S. Parnas, "Performance of batch, fed-batch, and continuous a–b–e fermentation with ph-control," *Bioresource Technology*, vol. 102, no. 5, pp. 4241–4250, 2011.
- [89] T. Ezeji, N. Qureshi, and H. Blaschek, "Acetone butanol ethanol (abe) production from concentrated substrate: reduction in substrate inhibition by fed-batch technique and product inhibition by gas stripping," *Applied Microbiology and Biotechnology*, vol. 63, no. 6, pp. 653–658, 2004.
- [90] C. Lu, J. Dong, and S.-T. Yang, "Butanol production from wood pulping hydrolysate in an integrated fermentation–gas stripping process," *Bioresource Technology*, vol. 143, pp. 467–475, 2013.
- [91] Z. Sun, "The design and technology of acetone–butanol continuous fermentation," *Industrial Microbiology*, vol. 11, pp. 31–37, 1981.
- [92] W.-C. Huang, D. E. Ramey, and S.-T. Yang, "Continuous production of butanol by clostridium acetobutylicum immobilized in a fibrous bed bioreactor," in *Proceedings of the Twenty-Fifth Symposium on Biotechnology for Fuels and Chemicals Held May 4–7, 2003, in Breckenridge, CO*. Springer, 2003, Conference Proceedings, pp. 887–898.
- [93] N. Qureshi, L. Lai, and H. Blaschek, "Scale-up of a high productivity continuous biofilm reactor to produce butanol by adsorbed cells of clostridium beijerinckii," *Food and Bioproducts Processing*, vol. 82, no. 2, pp. 164–173, 2004.
- [94] Y. Jang, A. Malaviya, and S. Y. Lee, "Acetone–butanol–ethanol production with high productivity using clostridium acetobutylicum bkm19," *Biotechnology and Bioengineering*, vol. 110, no. 6, pp. 1646–1653, 2013.

- [95] Y. Tashiro, K. Takeda, G. Kobayashi, K. Sonomoto, A. Ishizaki, and S. Yoshino, "High butanol production by clostridium saccharoperbutylacetonicum n1-4 in fed-batch culture with ph-stat continuous butyric acid and glucose feeding method," *Journal of Bioscience and Bioengineering*, vol. 98, no. 4, pp. 263–268, 2004.
- [96] Y. Jiang, C. Xu, F. Dong, Y. Yang, W. Jiang, and S. Yang, "Disruption of the acetoacetate decarboxylase gene in solvent-producing clostridium acetobutylicum increases the butanol ratio," *Metabolic Engineering*, vol. 11, no. 4-5, pp. 284–291, 2009.
- [97] C. Ren, Y. Gu, S. Hu, Y. Wu, P. Wang, Y. Yang, C. Yang, S. Yang, and W. Jiang, "Identification and inactivation of pleiotropic regulator ccpa to eliminate glucose repression of xylose utilization in clostridium acetobutylicum," *Metabolic Engineering*, vol. 12, no. 5, pp. 446–454, 2010.
- [98] H. Xiao, Y. Gu, Y. Ning, Y. Yang, W. J. Mitchell, W. Jiang, and S. Yang, "Confirmation and elimination of xylose metabolism bottlenecks in glucose phosphoenolpyruvate-dependent phosphotransferase system-deficient clostridium acetobutylicum for simultaneous utilization of glucose, xylose, and arabinose," *Applied and Environmental Microbiology*, vol. 77, no. 22, pp. 7886–7895, 2011.
- [99] M.-J. Heo, H.-M. Jung, J. Um, S.-W. Lee, and M.-K. Oh, "Controlling citrate synthase expression by crispr/cas9 genome editing for n-butanol production in escherichia coli," *ACS synthetic biology*, vol. 6, no. 2, pp. 182–189, 2016.
- [100] Y. Wang, Z.-T. Zhang, S.-O. Seo, K. Choi, T. Lu, Y.-S. Jin, and H. P. Blaschek, "Markerless chromosomal gene deletion in clostridium beijerinckii using crispr/cas9 system," *Journal of biotechnology*, vol. 200, pp. 1–5, 2015.
- [101] N. Qureshi, B. C. Saha, R. E. Hector, S. R. Hughes, and M. A. Cotta, "Butanol production from wheat straw by simultaneous saccharification and fermentation using clostridium beijerinckii: Part i—batch fermentation," *Bio-mass and Bioenergy*, vol. 32, no. 2, pp. 168–175, 2008.
- [102] Y. Jiang, D. Guo, J. Lu, P. Dürre, W. Dong, W. Yan, W. Zhang, J. Ma, M. Jiang, and F. Xin, "Consolidated bioprocessing of butanol production from xylan by a thermophilic and butanogenic thermoanaerobacterium sp. m5," *Biotechnology for Biofuels*, vol. 11, no. 1, p. 89, 2018.
- [103] K. Ounine, H. Petitdemange, G. Raval, and R. Gay, "Acetone-butanol production from pentoses by clostridium acetobutylicum," *Biotechnology Letters*, vol. 5, no. 9, pp. 605–610, 1983.
- [104] O. Fond, J. Engasser, G. Matta-El-Amouri, and H. Petitdemange, "The acetone butanol fermentation on glucose and xylose. i. regulation and kinetics in batch cultures," *Biotechnology and Bioengineering*, vol. 28, no. 2, pp. 160–166, 1986.

- [105] Y. Gu, Y. Ding, C. Ren, Z. Sun, D. A. Rodionov, W. Zhang, S. Yang, C. Yang, and W. Jiang, "Reconstruction of xylose utilization pathway and regulons in firmicutes," *BMC Genomics*, vol. 11, no. 1, p. 255, 2010.
- [106] J. Nölling, G. Breton, M. V. Omelchenko, K. S. Makarova, Q. Zeng, R. Gibson, H. M. Lee, J. Dubois, D. Qiu, and J. Hitti, "Genome sequence and comparative analysis of the solvent-producing bacterium *Clostridium acetobutylicum*," *Journal of Bacteriology*, vol. 183, no. 16, pp. 4823–4838, 2001.
- [107] Y. Chen, T. Zhou, D. Liu, A. Li, S. Xu, Q. Liu, B. Li, and H. Ying, "Production of butanol from glucose and xylose with immobilized cells of *Clostridium acetobutylicum*," *Biotechnology and Bioprocess Engineering*, vol. 18, no. 2, pp. 234–241, 2013.
- [108] W. Jiang, Z. Wen, M. Wu, H. Li, J. Yang, J. Lin, Y. Lin, L. Yang, and P. Cen, "The effect of pH control on acetone–butanol–ethanol fermentation by *Clostridium acetobutylicum* ATCC 824 with xylose and D-glucose and D-xylose mixture," *Chinese Journal of Chemical Engineering*, vol. 22, no. 8, pp. 937–942, 2014.
- [109] Y. Wu, C. Xue, L. Chen, W. Yuan, and F. Bai, "Synergistic effect of calcium and zinc on glucose/xylose utilization and butanol tolerance of *Clostridium acetobutylicum*," *FEMS Microbiology Letters*, vol. 363, no. 5, 2016.
- [110] A. Poehlein, J. D. M. Solano, S. K. Flitsch, P. Krabben, K. Winzer, S. J. Reid, D. T. Jones, E. Green, N. P. Minton, and R. Daniel, "Microbial solvent formation revisited by comparative genome analysis," *Biotechnology for Biofuels*, vol. 10, no. 1, p. 58, 2017.
- [111] Y. Shi, Y.-X. Li, and Y.-Y. Li, "Large number of phosphotransferase genes in the *Clostridium beijerinckii* NCIMB 8052 genome and the study on their evolution," *BMC Bioinformatics*, vol. 11, no. 11, p. S9, 2010.
- [112] C. Grimmler, C. Held, W. Liebl, and A. Ehrenreich, "Transcriptional analysis of catabolite repression in *Clostridium acetobutylicum* growing on mixtures of D-glucose and D-xylose," *Journal of Biotechnology*, vol. 150, no. 3, pp. 315–323, 2010.
- [113] L. Liu, L. Zhang, W. Tang, Y. Gu, Q. Hua, S. Yang, W. Jiang, and C. Yang, "Phosphoketolase pathway for xylose catabolism in *Clostridium acetobutylicum* revealed by ¹³C-metabolic flux analysis," *Journal of Bacteriology*, pp. JB. 00 713–12, 2012.
- [114] D. A. Rodionov, A. A. Mironov, and M. S. Gelfand, "Transcriptional regulation of pentose utilisation systems in the *Bacillus/Clostridium* group of bacteria," *FEMS Microbiology Letters*, vol. 205, no. 2, pp. 305–314, 2001.
- [115] M. Servinsky, K. Germane, S. Liu, J. Kiel, A. Clark, J. Shankar, and C. Sund, "Arabinose is metabolized via a phosphoketolase pathway in *Clostridium acetobutylicum* ATCC 824," *Journal of Industrial Microbiology and Biotechnology*, vol. 39, no. 12, pp. 1859–1867, 2012.

- [116] M. D. Servinsky, J. T. Kiel, N. F. Dupuy, and C. J. Sund, "Transcriptional analysis of differential carbohydrate utilization by clostridium acetobutylicum," *Microbiology*, vol. 156, no. 11, pp. 3478–3491, 2010.
- [117] L. Zhang, S. A. Leyn, Y. Gu, W. Jiang, D. A. Rodionov, and C. Yang, "Ribulokinase and transcriptional regulation of arabinose metabolism in clostridium acetobutylicum," *Journal of Bacteriology*, pp. JB. 06241–11, 2011.
- [118] Y. Gu, J. Li, L. Zhang, J. Chen, L. Niu, Y. Yang, S. Yang, and W. Jiang, "Improvement of xylose utilization in clostridium acetobutylicum via expression of the tala gene encoding transaldolase from escherichia coli," *Journal of Biotechnology*, vol. 143, no. 4, pp. 284–287, 2009.
- [119] H. Xiao, Z. Li, Y. Jiang, Y. Yang, W. Jiang, Y. Gu, and S. Yang, "Metabolic engineering of d-xylose pathway in clostridium beijerinckii to optimize solvent production from xylose mother liquid," *Metabolic Engineering*, vol. 14, no. 5, pp. 569–578, 2012.
- [120] C. Birgen, S. Markussen, A. Wentzel, and H. A. Preisig, "The effect of feeding strategy on butanol production by clostridium beijerinckii ncimb 8052 using glucose and xylose," *Chemical Engineering Transactions*, vol. 65, pp. 283–288, 2018.
- [121] A. El Kanouni, I. Zerdani, S. Zaafa, M. Znassni, M. Loutfi, and M. Boudouma, "The improvement of glucose/xylose fermentation by clostridium acetobutylicum using calcium carbonate," *World Journal of Microbiology and Biotechnology*, vol. 14, no. 3, pp. 431–435, 1998.
- [122] B. L. Magalhães, M. C. B. Grassi, G. A. Pereira, and M. Brocchi, "Improved n-butanol production from lignocellulosic hydrolysate by clostridium strain screening and culture-medium optimization," *Biomass and Bioenergy*, vol. 108, pp. 157–166, 2018.
- [123] T. Noguchi, Y. Tashiro, T. Yoshida, J. Zheng, K. Sakai, and K. Sonomoto, "Efficient butanol production without carbon catabolite repression from mixed sugars with clostridium saccharoperbutylacetonicum n1-4," *Journal of Bioscience and Bioengineering*, vol. 116, no. 6, pp. 716–721, 2013.
- [124] K. Ounine, H. Petitdemange, G. Raval, and R. Gay, "Regulation and butanol inhibition of d-xylose and d-glucose uptake in clostridium acetobutylicum," *Applied and Environmental Microbiology*, vol. 49, no. 4, pp. 874–878, 1985.
- [125] M. Wayman and S. Yu, "Acetone-butanol fermentation of xylose and sugar mixtures," *Biotechnology Letters*, vol. 7, no. 4, pp. 255–260, 1985.
- [126] J. Zhang, W. Zhu, H. Xu, Y. Li, D. Hua, F. Jin, M. Gao, and X. Zhang, "Simultaneous glucose and xylose uptake by an acetone/butanol/ethanol producing laboratory clostridium beijerinckii strain se-2," *Biotechnology Letters*, vol. 38, no. 4, pp. 611–617, 2016.

- [127] R. Mayank, A. Ranjan, and V. S. Moholkar, "Mathematical models of abe fermentation: review and analysis," *Critical Reviews in Biotechnology*, vol. 33, no. 4, pp. 419–447, 2013.
- [128] E. T. Papoutsakis, "Equations and calculations for fermentations of butyric acid bacteria," *Biotechnology and Bioengineering*, vol. 67, no. 6, pp. 813–826, 1984.
- [129] R. P. Desai, L. K. Nielsen, and E. T. Papoutsakis, "Stoichiometric modeling of clostridium acetobutylicum fermentations with non-linear constraints," *Journal of Biotechnology*, vol. 71, no. 1-3, pp. 191–205, 1999.
- [130] Y. Wang, X. Li, Y. Mao, and H. P. Blaschek, "Single-nucleotide resolution analysis of the transcriptome structure of clostridium beijerinckii ncimb 8052 using rna-seq," *BMC Genomics*, vol. 12, no. 1, p. 479, 2011.
- [131] R. S. Senger and E. T. Papoutsakis, "Genome-scale model for clostridium acetobutylicum: Part i. metabolic network resolution and analysis," *Biotechnology and Bioengineering*, vol. 101, no. 5, pp. 1036–1052, 2008.
- [132] —, "Genome-scale model for clostridium acetobutylicum: Part ii. development of specific proton flux states and numerically determined sub-systems," *Biotechnology and Bioengineering*, vol. 101, no. 5, pp. 1053–1071, 2008.
- [133] J. Lee, H. Yun, A. M. Feist, B. . Palsson, and S. Y. Lee, "Genome-scale reconstruction and in silico analysis of the clostridium acetobutylicum atcc 824 metabolic network," *Applied Microbiology and Biotechnology*, vol. 80, no. 5, pp. 849–862, 2008.
- [134] M. J. McAnulty, J. Y. Yen, B. G. Freedman, and R. S. Senger, "Genome-scale modeling using flux ratio constraints to enable metabolic engineering of clostridial metabolism in silico," *BMC Systems Biology*, vol. 6, no. 1, p. 42, 2012.
- [135] S. B. Crown, D. C. Indurthi, W. S. Ahn, J. Choi, E. T. Papoutsakis, and M. R. Antoniewicz, "Resolving the tea cycle and pentose-phosphate pathway of clostridium acetobutylicum atcc 824: Isotopomer analysis, in vitro activities and expression analysis," *Biotechnology Journal*, vol. 6, no. 3, pp. 300–305, 2011.
- [136] D. Amador-Noguez, X.-J. Feng, J. Fan, N. Roquet, H. Rabitz, and J. D. Rabinowitz, "Systems-level metabolic flux profiling elucidates a complete, bifurcated tricarboxylic acid cycle in clostridium acetobutylicum," *Journal of Bacteriology*, vol. 192, no. 17, pp. 4452–4461, 2010.
- [137] S. Dash, T. J. Mueller, K. P. Venkataramanan, E. T. Papoutsakis, and C. D. Maranas, "Capturing the response of clostridium acetobutylicum to chemical stressors using a regulated genome-scale metabolic model," *Biotechnology for Biofuels*, vol. 7, no. 1, p. 144, 2014.

- [138] M. Yoo, G. Bestel-Corre, C. Croux, A. Riviere, I. Meynial-Salles, and P. Soucaille, "A quantitative system-scale characterization of the metabolism of clostridium acetobutylicum," *mBio*, vol. 6, no. 6, pp. e01 808–15, 2015.
- [139] C. B. Milne, J. A. Eddy, R. Raju, S. Ardekani, P.-J. Kim, R. S. Senger, Y.-S. Jin, H. P. Blaschek, and N. D. Price, "Metabolic network reconstruction and genome-scale model of butanol-producing strain clostridium beijerinckii nciimb 8052," *BMC Systems Biology*, vol. 5, no. 1, p. 130, 2011.
- [140] J. Votruba, B. Volesky, and L. Yerushalmi, "Mathematical model of a batch acetone–butanol fermentation," *Biotechnology and Bioengineering*, vol. 28, no. 2, pp. 247–255, 1986.
- [141] L. Yerushalmi, B. Volesky, and J. Votruba, "Modelling of culture kinetics and physiology for c. acetobutylicum," *The Canadian Journal of Chemical Engineering*, vol. 64, no. 4, pp. 607–616, 1986.
- [142] A. Srivastava and B. Volesky, "Updated model of the batch acetone-butanol fermentation," *Biotechnology Letters*, vol. 12, no. 9, pp. 693–698, 1990.
- [143] X. Yang and G. T. Tsao, "Mathematical modeling of inhibition kinetics in acetone-butanol fermentation by clostridium acetobutylicum," *Biotechnology Progress*, vol. 10, no. 5, pp. 532–538, 1994.
- [144] H. Shinto, Y. Tashiro, M. Yamashita, G. Kobayashi, T. Sekiguchi, T. Hanai, Y. Kuriya, M. Okamoto, and K. Sonomoto, "Kinetic modeling and sensitivity analysis of acetone–butanol–ethanol production," *Journal of Biotechnology*, vol. 131, no. 1, pp. 45–56, 2007.
- [145] H. Shinto, Y. Tashiro, G. Kobayashi, T. Sekiguchi, T. Hanai, Y. Kuriya, M. Okamoto, and K. Sonomoto, "Kinetic study of substrate dependency for higher butanol production in acetone–butanol–ethanol fermentation," *Process Biochemistry*, vol. 43, no. 12, pp. 1452–1461, 2008.
- [146] R.-D. Li, Y.-Y. Li, L.-Y. Lu, C. Ren, Y.-X. Li, and L. Liu, "An improved kinetic model for the acetone-butanol-ethanol pathway of clostridium acetobutylicum and model-based perturbation analysis," *BMC Systems Biology*, vol. 5, no. 1, p. S12, 2011.
- [147] F. Raganati, A. Procentese, G. Olivieri, P. Götz, P. Salatino, and A. Marzocchella, "Kinetic study of butanol production from various sugars by clostridium acetobutylicum using a dynamic model," *Biochemical Engineering Journal*, vol. 99, pp. 156–166, 2015.
- [148] P. Krouwel, W. Groot, and N. Kossen, "Continuous ibe fermentation by immobilized growing clostridium beijerinckii cells in a stirred-tank fermentor," *Biotechnology and Bioengineering*, vol. 25, no. 1, pp. 281–299, 1983.
- [149] G. Schoutens, P. Van Beelen, and K. Luyben, "A simple model for the continuous production of butanol by immobilized clostridia: I: Clostridium beijerinckii on glucose," *The Chemical Engineering Journal*, vol. 32, no. 3, pp. B43–B50, 1986.

- [150] G. Schoutens and N. F. Kossen, "A simple model for the continuous production of butanol by immobilized clostridia: II: *Clostridium* species dsm 2152 on glucose and whey permeate," *The Chemical Engineering Journal*, vol. 32, no. 3, pp. B51–B56, 1986.
- [151] A. Mulchandani and B. Volesky, "Modelling of the acetone-butanol fermentation with cell retention," *The Canadian Journal of Chemical Engineering*, vol. 64, no. 4, pp. 625–631, 1986.
- [152] A. Jarzȳbski, G. Goma, and P. Soucaille, "Modelling of continuous acetobutylic fermentation," *Bioprocess Engineering*, vol. 7, no. 8, pp. 357–361, 1992.
- [153] S. Haus, S. Jabbari, T. Millat, H. Janssen, R.-J. Fischer, H. Bahl, J. R. King, and O. Wolkenhauer, "A systems biology approach to investigate the effect of ph-induced gene regulation on solvent production by *clostridium acetobutylicum* in continuous culture," *BMC Systems Biology*, vol. 5, no. 1, p. 10, 2011.
- [154] G. J. Thorn, J. R. King, and S. Jabbari, "ph-induced gene regulation of solvent production by *clostridium acetobutylicum* in continuous culture: parameter estimation and sporulation modelling," *Mathematical Biosciences*, vol. 241, no. 2, pp. 149–166, 2013.
- [155] T. Millat, H. Janssen, G. J. Thorn, J. R. King, H. Bahl, R.-J. Fischer, and O. Wolkenhauer, "A shift in the dominant phenotype governs the ph-induced metabolic switch of *clostridium acetobutylicum* in phosphate-limited continuous cultures," *Applied Microbiology and Biotechnology*, vol. 97, no. 14, pp. 6451–6466, 2013.
- [156] T. Millat, H. Janssen, H. Bahl, R. Fischer, and O. Wolkenhauer, "Integrative modelling of ph-dependent enzyme activity and transcriptomic regulation of the acetone–butanol–ethanol fermentation of *clostridium acetobutylicum* in continuous culture," *Microbial Biotechnology*, vol. 6, no. 5, pp. 526–539, 2013.
- [157] C. Park, M. R. Okos, and P. C. Wankat, "Acetone–butanol–ethanol (abe) fermentation in an immobilized cell trickle bed reactor," *Biotechnology and Bioengineering*, vol. 34, no. 1, pp. 18–29, 1989.
- [158] ———, "Characterization of an immobilized cell, trickle bed reactor during long term butanol (abe) fermentation," *Biotechnology and Bioengineering*, vol. 36, no. 2, pp. 207–217, 1990.
- [159] C. H. Park, M. R. Okos, and P. C. Wankat, "Acetone-butanol-ethanol (abe) fermentation and simultaneous separation in a trickle bed reactor," *Biotechnology Progress*, vol. 7, no. 2, pp. 185–194, 1991.
- [160] C.-H. Park and C. Q. Geng, "Mathematical modeling of fed-batch butanol fermentation with simultaneous pervaporation," *Korean Journal of Chemical Engineering*, vol. 13, no. 6, pp. 612–619, 1996.

- [161] R. Shukla, W. Kang, and K. Sirkar, "Acetone–butanol–ethanol (abe) production in a novel hollow fiber fermentor–extractor," *Biotechnology and Bioengineering*, vol. 34, no. 9, pp. 1158–1166, 1989.
- [162] Z. Shi, C. Zhang, J. Chen, and Z. Mao, "Performance evaluation of acetone–butanol continuous flash extractive fermentation process," *Bioprocess and Biosystems engineering*, vol. 27, no. 3, pp. 175–183, 2005.
- [163] A. P. Mariano, C. B. B. Costa, D. d. F. de Angelis, F. Maugeri Filho, D. I. P. Atala, M. R. W. Maciel, and R. Maciel Filho, "Optimization strategies based on sequential quadratic programming applied for a fermentation process for butanol production," *Applied Biochemistry and Biotechnology*, vol. 159, no. 2, p. 366, 2009.
- [164] I. Angelidaki, L. Ellegaard, and B. K. Ahring, "A mathematical model for dynamic simulation of anaerobic digestion of complex substrates: focusing on ammonia inhibition," *Biotechnology and Bioengineering*, vol. 42, no. 2, pp. 159–166, 1993.
- [165] N. Kythreotou, G. Florides, and S. A. Tassou, "A review of simple to scientific models for anaerobic digestion," *Renewable Energy*, vol. 71, pp. 701–714, 2014.
- [166] M. L. Shuler and F. Kargi, *Bioprocess Engineering: Basic Concepts*. 2nd. Upper Saddle, 2002.
- [167] C. Grady Jr, L. Harlow, and R. Riesing, "Effects of growth rate and influent substrate concentration on effluent quality from chemostats containing bacteria in pure and mixed culture," *Biotechnology and Bioengineering*, vol. 14, no. 3, pp. 391–410, 1972.
- [168] D. Contois, "Kinetics of bacterial growth: relationship between population density and specific growth rate of continuous cultures," *Microbiology*, vol. 21, no. 1, pp. 40–50, 1959.
- [169] J. Monod, "The growth of bacterial cultures," *Annual Reviews in Microbiology*, vol. 3, no. 1, pp. 371–394, 1949.
- [170] H. Moser, *The dynamics of bacterial populations maintained in the chemostat*, 1958.
- [171] D. Contois, "Kinetics of bacterial growth: relationship between population density and specific growth rate of continuous cultures," *Microbiology*, vol. 21, no. 1, pp. 40–50, 1959.
- [172] G. Tessier, "Croissance des populations bactériennes et quantité d'aliment disponible," *Rev. Sci. Paris*, vol. 3208, pp. 209–214, 1942.
- [173] V. H. Edwards, "The influence of high substrate concentrations on microbial kinetics," *Biotechnology and Bioengineering*, vol. 12, no. 5, pp. 679–712, 1970.
- [174] J. L. Webb, *Enzyme and metabolic inhibitors*, 1963.

- [175] J. F. Andrews, "A mathematical model for the continuous culture of microorganisms utilizing inhibitory substrates," *Biotechnology and Bioengineering*, vol. 10, no. 6, pp. 707–723, 1968.
- [176] J. Haldane, *Enzymes London*. Longmans, Grenn, and Co.(reprinted by MIT press, Cambridge, MA 1965, 1930.
- [177] M. M.-c. Tseng and M. Wayman, "Kinetics of yeast growth: inhibition-threshold substrate concentrations," *Canadian Journal of Microbiology*, vol. 21, no. 7, pp. 994–1003, 1975.
- [178] J. Luong, "Generalization of monod kinetics for analysis of growth data with substrate inhibition," *Biotechnology and Bioengineering*, vol. 29, no. 2, pp. 242–248, 1987.
- [179] C. N. Hinshelwood, *Chemical kinetics of the bacterial cell*. Oxford At The Clarendon Press; London, 1946.
- [180] I. Holzberg, R. Finn, and K. H. Steinkraus, "A kinetic study of the alcoholic fermentation of grape juice," *Biotechnology and Bioengineering*, vol. 9, no. 3, pp. 413–427, 1967.
- [181] S. Aiba, M. Shoda, and M. Nagatani, "Kinetics of product inhibition in alcohol fermentation," *Biotechnology and Bioengineering*, vol. 10, no. 6, pp. 845–864, 1968.
- [182] C. Bazua and C. Wilke, "Ethanol effects on the kinetics of a continuous fermentation with *saccharomyces cerevisiae*," in *Biotechnol. Bioeng. Symp.:(United States)*, vol. 19. Univ. of California, Berkeley, Conference Proceedings.
- [183] K. Han and O. Levenspiel, "Extended monod kinetics for substrate, product, and cell inhibition," *Biotechnology and Bioengineering*, vol. 32, no. 4, pp. 430–447, 1988.
- [184] J. Luong, "Kinetics of ethanol inhibition in alcohol fermentation," *Biotechnology and Bioengineering*, vol. 27, no. 3, pp. 280–285, 1985.
- [185] N. Egamberdiev and N. Ierusalimsky, "Effect of ethanol concentration on a growth rate of *saccharomyces vini* (strain pr-1)," *Mikrobiologia*, vol. 37, no. 4, p. 686, 1968.
- [186] A. Mulchandani and J. Luong, "Microbial inhibition kinetics revisited," *Enzyme and Microbial Technology*, vol. 11, no. 2, pp. 66–73, 1989.
- [187] G. Okpokwasili and C. Nweke, "Microbial growth and substrate utilization kinetics," *African Journal of Biotechnology*, vol. 5, no. 4, pp. 305–317, 2006.
- [188] R. Megee Iii, J. Drake, A. Fredrickson, and H. Tsuchiya, "Studies in intermicrobial symbiosis. *saccharomyces cerevisiae* and *lactobacillus casei*," *Canadian Journal of Microbiology*, vol. 18, no. 11, pp. 1733–1742, 1972.

- [189] I. H. Segel, *Enzyme kinetics: behavior and analysis of rapid equilibrium and steady state enzyme systems*. Wiley, 1975.
- [190] W. H. Bell, "Bacterial utilization of algal extracellular products. 1. the kinetic approach," *Limnology and Oceanography*, vol. 25, no. 6, pp. 1007–1020, 1980.
- [191] H. Yoon, G. Klinzing, and H. Blanch, "Competition for mixed substrates by microbial populations," *Biotechnology and Bioengineering*, vol. 19, no. 8, pp. 1193–1210, 1977.
- [192] E. L. Gaden Jr, "Fermentation process kinetics," *Journal of Biochemical Microbiological Technology and Engineering*, vol. 1, no. 4, pp. 413–429, 1959.
- [193] [Online]. Available: <http://arohatgi.info/WebPlotDigitizer>
- [194] J. W. Tukey, "Exploratory data," *Analysis (Addison Wesley, Reading, MA)*, 1977.
- [195] H. Yu, F. Khan, and V. Garaniya, "A sparse pca for nonlinear fault diagnosis and robust feature discovery of industrial processes," *AIChE Journal*, vol. 62, no. 5, pp. 1494–1513, 2016.
- [196] C. Croux and C. Dehon, "Influence functions of the spearman and kendall correlation measures," *Statistical methods & applications*, vol. 19, no. 4, pp. 497–515, 2010.
- [197] B. H. Kim, P. Bellows, R. Datta, and J. Zeikus, "Control of carbon and electron flow in clostridium acetobutylicum fermentations: utilization of carbon monoxide to inhibit hydrogen production and to enhance butanol yields," *Applied and Environmental Microbiology*, vol. 48, no. 4, pp. 764–770, 1984.
- [198] C. Birgen, S. Markussen, A. Wentzel, and H. A. Preisig, "Response surface methodology for understanding glucose and xylose utilization by clostridium beijerinckii ncimb 8052," *Chemical Engineering Transactions*, vol. 65, pp. 61–66, 2018.
- [199] D. Schäpper, M. N. H. Z. Alam, N. Szita, A. E. Lantz, and K. V. Gernaey, "Application of microbioreactors in fermentation process development: a review," *Analytical and Bioanalytical Chemistry*, vol. 395, no. 3, pp. 679–695, 2009.
- [200] D. Weuster-Botz, D. Hekmat, R. Puskeiler, and E. Franco-Lara, *Enabling technologies: fermentation and downstream processing*. Springer, 2006, pp. 205–247.
- [201] C. Blesken, T. Olfers, A. Grimm, and N. Frische, "The microfluidic bioreactor for a new era of bioprocess development," *Engineering in Life Sciences*, vol. 16, no. 2, pp. 190–193, 2016.
- [202] W. Zhang, Z. Liu, Z. Liu, and F. Li, "Butanol production from corncob residue using clostridium beijerinckii ncimb 8052," *Letters in Applied Microbiology*, vol. 55, no. 3, pp. 240–246, 2012.

- [203] M. Kunze, S. Roth, E. Gartz, and J. Büchs, "Pitfalls in optical on-line monitoring for high-throughput screening of microbial systems," *Microbial Cell Factories*, vol. 13, no. 1, p. 53, 2014.
- [204] S. Wewetzer, M. Kunze, T. Ladner, B. Luchterhand, S. Roth, N. Rahmen, R. Kloß, A. C. e Silva, L. Regestein, and J. Büchs, "Parallel use of shake flask and microtiter plate online measuring devices (ramos and biolector) reduces the number of experiments in laboratory-scale stirred tank bioreactors," *Journal of Biological Engineering*, vol. 9, no. 1, p. 9, 2015.
- [205] P. Patakova, D. Maxa, M. Rychtera, M. Linhova, P. Fribert, Z. Muzikova, J. Lipovsky, L. Paulova, M. Pospisil, and G. Sebor, *Perspectives of biobutanol production and use*. InTech, 2011.
- [206] W.-L. Chang, "Acetone-butanol-ethanol fermentation by engineered clostridium beijerinckii and clostridium tyrobutyricum," Thesis, The Ohio State University, 2010.
- [207] M. Ferone, F. Raganati, G. Olivieri, P. Salatino, and A. Marzocchella, "Succinic acid production from hexoses and pentoses by fermentation of actinobacillus succinogenes," *Chemical Engineering Transactions*, vol. 49, 2016.
- [208] G. Hanrahan and K. Lu, "Application of factorial and response surface methodology in modern experimental design and optimization," *Critical Reviews in Analytical Chemistry*, vol. 36, no. 3-4, pp. 141–151, 2006.
- [209] H. I. Velázquez-Sánchez and R. Aguilar-López, "Novel kinetic model for the simulation analysis of the butanol productivity of clostridium acetobutylicum atcc 824 under different reactor configurations," *Chinese Journal of Chemical Engineering*, vol. 26, no. 4, pp. 812–821, 2018.
- [210] V. H. G. Díaz and M. J. Willis, "Kinetic modelling and simulation of batch, continuous and cell-recycling fermentations for acetone-butanol-ethanol production using clostridium saccharoperbutylacetonicum n1-4," *Biochemical Engineering Journal*, vol. 137, pp. 30–39, 2018.
- [211] C. Birgen and H. A. Preisig, *Dynamic Modeling of Butanol Production from Lignocellulosic Sugars*. Elsevier, 2018, vol. 43, pp. 1547–1552.
- [212] M.-H. Eom, B. Kim, H. Jang, S.-H. Lee, W. Kim, Y.-A. Shin, and J. H. Lee, "Dynamic modeling of a fermentation process with ex situ butanol recovery (esbr) for continuous biobutanol production," *Energy and Fuels*, vol. 29, no. 11, pp. 7254–7265, 2015.
- [213] C. Birgen, S. Markussen, A. Wentzel, H. Preisig, and B. Wittgens, "Modeling the growth of clostridium beijerinckii ncimb 8052 on lignocellulosic sugars," *Chemical Engineering Transactions*, vol. 65, pp. 289–294, 2018.
- [214] A. Hirsch and E. Grinsted, "543. methods for the growth and enumeration of anaerobic spore-formers from cheese, with observations on the effect of nisin," *Journal of Dairy Research*, vol. 21, no. 1, pp. 101–110, 1954.

-
- [215] W. J. Sandoval-Espinola, M. Chinn, and J. M. Bruno-Barcena, "Inoculum optimization of clostridium beijerinckii for reproducible growth," *FEMS Microbiology Letters*, vol. 362, no. 19, 2015.
- [216] M. Hollander, D. A. Wolfe, and E. Chicken, *Nonparametric statistical methods*. John Wiley & Sons, 2013, vol. 751.